



2007  
2

This is to certify that the  
thesis entitled

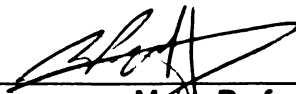
FURTHER CHARACTERIZATION OF THE RETINOPATHY,  
GLOBE-ENLARGED (*rge*) CHICKEN

presented by

GILLIAN CURTIS SHAW

has been accepted towards fulfillment  
of the requirements for the

M.S. degree in Comparative Medicine and  
Integrative Biology



Major Professor's Signature

5/15/07

Date

MSU is an affirmative-action, equal-opportunity employer

LIBRARY  
Michigan State  
University

**PLACE IN RETURN BOX** to remove this checkout from your record.  
**TO AVOID FINES** return on or before date due.  
**MAY BE RECALLED** with earlier due date if requested.

DATE DUE	DATE DUE	DATE DUE

**FURTHER CHARACTERIZATION OF THE RETINOPATHY,  
GLOBE ENLARGED (*rge*) CHICKEN**

By

Gillian Curtis Shaw

A THESIS

Submitted to  
Michigan State University  
in partial fulfillment of the requirements  
for the degree of

MASTER OF SCIENCE

Comparative Medicine and Integrative Biology

2007



## ABSTRACT

### FURTHER CHARACTERIZATION OF THE RETINOPATHY, GLOBE ENLARGED (*rge*) CHICKEN

By

Gillian Curtis Shaw

Previous work has shown that retinopathy, globe enlarged (*rge*) affected chicks eventually become functionally blind and subsequently develop globe enlargement. Electroretinographic (ERG) abnormalities include increased thresholds, a “supernormal b-wave” in response to brighter flashes, a lack of oscillatory potentials and ERG responses that are present long after functional blindness. Screening of several positional candidate genes was performed; however, another research group identified the causative mutation in GNB3, the  $\beta$  subunit of a heterotrimeric G-protein involved in phototransduction in cone photoreceptors. Pharmacological dissection of the *rge* ERG using aspartate, APB and PDA demonstrated decreased cone sensitivity but also suggested abnormalities of the inner retinal ON and OFF pathways. GNB3 has not definitively been shown to be involved in inner retinal pathways, however these ERG results suggest it may play a role in such pathways. Preliminary immunohistochemistry identified GNB3 immunoreactivity in cone cell bodies, outer plexiform layer synaptic terminals and a population of cells in the inner nuclear and ganglion cell layers in normal chicken retina. These data suggest GNB3 may also be important in inner retinal signaling. Further studies are necessary to explore this hypothesis.

## ACKNOWLEDGEMENTS

I would like to acknowledge all of the people who not only facilitated my getting involved with the Comparative Ophthalmology Laboratory but also who helped me as I tackled the work for this project. Dr. John Baker deserves a big thank you because he facilitated the establishment of the NIH T-32 program at Michigan State University for veterinary students to take a year from vet school and work toward a Master's degree. Without this program, I never would have pursued a Master's degree. Dr. Vilma Yusbasiyan-Gurkan, the director of the Comparative Medicine and Integrative Biology program, was very supportive as I made my way through the course of this Master's project. And I never would have gotten involved with the lab had it not been for my friend, Lexi Mentzer, who first introduced me to the lab and its various goings-on.

The folks in the Comparative Ophthalmology Laboratory were instrumental in my successful completion of this project, and without their help I never would have made it. Michelle Curcio patiently taught me how to do most of the molecular work included in this project. She didn't even seem to mind when I asked her how to dilute PCR primers for the 97<sup>th</sup> time! Janice Forcier was an ever-present companion in the dark and expert chicken wrangler, anesthetist and artificial inseminator. Who would have thought doing ERGs at 2am would have been so MUCH FUN! Naline Tuntivanich was also a patient teacher who willingly shared all of her vast ERG knowledge and expertise with me. She always had a kind word and helpful advice for the various stumbling blocks I encountered.

I would also like to thank Fabiano Montiani-Ferreira whose *rge* chicken torch I continued to carry after he had finished his PhD work. He taught me quite a bit about the

*rge* chicken and helped me along as I was getting started with the *rge* chickens. His PhD thesis was my bible as I worked on this project and I slept with it under my pillow each night. His statistical knowledge and willingness to help was greatly appreciated in the interpretation of my results and the statistical analysis. He has become a good friend and I will always consider him to be a mentor as I move onto new things in life.

My committee members, Drs. Hans Cheng, Matti Kiupel, Pat Venta and Art Weber, also deserve acknowledgement as they helped to guide me through the process of the research and the completion of this Master's project. Special thanks go to Dr. Hans Cheng whose advice and laboratory staff helped immensely with the molecular part of this project.

Lisa Allen and all of the vivarium staff deserve a big thank you for taking care of the precious *rge* chickens and putting up with all of my crazy ideas to improve their husbandry.

My mom and dad, Jane and Darrel Shaw, must be mentioned as I would not be in the position I am today without their love, encouragement and support.

Finally, I would like to thank Simon Petersen-Jones my principal investigator and mentor, who not only took me on as a student but also patiently explained the principles of ERGs and phototransduction at least 800 times throughout the course of this project. I thank him for working around the difficulties I encountered as I completed this dual degree program. He was ever patient as I struggled to understand the pathology behind the *rge* chicken while also working towards my DVM. I find it unbelievable how far I've come since I joined the lab in 2004 and I couldn't have done it without Simon's encouragement and support. MUCH THANKS TO ALL!

## TABLE OF CONTENTS

LIST OF TABLES.....	vii
---------------------	-----

LIST OF FIGURES.....	viii
----------------------	------

### CHAPTER 1 – INTRODUCTION

1.1. Structure of the chicken globe.....	1
1.2. Structure and function of the retina.....	3
1.3. Chicken retinal structure.....	6
1.4. Signaling within the retina.....	6
1.4.1. Guanine-nucleotide binding proteins.....	6
1.4.2. Visual transduction.....	7
1.4.3. ON and OFF pathways.....	11
1.5. Retinal dystrophy models.....	13
1.6. Electroretinography.....	15
1.6.1. The electroretinogram.....	15
1.6.2. The origins of the ERG waves.....	18
1.6.3. Light adaptation status and the electroretinogram.....	25
1.6.4. Circadian ERGs.....	25
1.6.5. The ERG in disease states.....	27
1.7. The <i>rge</i> chicken .....	27
1.7.1. Original <i>rge</i> characterization.....	27
1.7.2. Globe enlargement.....	28
1.7.3. Lacquer crack lesions.....	31
1.7.4. Retinal changes.....	34
1.7.5. Vision testing.....	40
1.7.6. Electroretinographic characteristics.....	41
1.7.7. Investigation of several candidate genes.....	48
1.8. Hypotheses.....	49
1.9. The scope of this project.....	49

### CHAPTER 2 – INVESTIGATION OF CANDIDATE GENES

2.1. Introduction.....	52
2.1.1. Background information for the chosen genes.....	55
2.2. Materials and Methods.....	58
2.2.1. Design of primers.....	58
2.2.2. DNA isolation.....	62
2.2.3. PCR amplification.....	63
2.2.4. Purification of PCR products for sequencing.....	64
2.2.4.a. Sodium acetate and isopropanol PCR product Purification.....	64
2.2.4.b. Purification of PCR products cut from gel.....	64

2.2.5: Amplification of genes from retinal cDNA.....	66
2.2.5.a. RNA Extraction.....	69
2.2.5.b. cDNA Synthesis.....	70
2.2.6. Analysis of sequencing results.....	72
2.2.7. Investigation of SNPs identified in candidate genes.....	72
2.2.8. Investigation of GNB3.....	72
2.2.8.a. Development of PCR RE test to genotype birds for GNB3 mutation.....	74
2.2.8.b. GNB3 immunoreactivity in the normal chicken retina.....	77
2.2.8.b.i. Chicks.....	77
2.2.8.b.ii. Retina Collection.....	77
2.2.8.b.iii. Fixation, Embedding and Staining.....	78
2.3. Results.....	79
2.4. Discussion.....	90

### CHAPTER 3 – FURTHER ELECTRORETINOGRAPHIC STUDIES OF THE *rge* CHICKEN

3.1. Introduction.....	94
3.2. Materials and Methods.....	96
3.2.1. Chicks.....	96
3.2.2. ERG Recording.....	97
3.2.2.a. Long flash ERG.....	98
3.2.3. Pharmacological dissection of the ERG.....	99
3.2.4. Circadian electroretinograms.....	100
3.2.5. Data analysis.....	101
3.3. Results.....	102
3.3.1. Long flash ERGs.....	102
3.3.2. APB Injection.....	104
3.3.3. PDA Injection.....	108
3.3.4. Aspartate Injection.....	112
3.3.5. Circadian ERGs.....	115
3.4. Discussion.....	122

### CHAPTER 4 – CONCLUSIONS AND FUTURE STUDIES

4.1. Conclusion.....	128
4.2. Future studies.....	135

REFERENCES.....	138
-----------------	-----

## **LIST OF TABLES**

Table 2.1. Genes examined in this investigation.....	54
Table 2.2. Genomic primers used to sequence the candidate genes.....	59-61
Table 2.3. cDNA primers used to sequence the candidate genes.....	67-68
Table 2.4. Sequence analysis results of the twelve genes examined.....	80
Table 2.5. Polymorphisms found during investigation.....	81-83
Table 3.1. Summary of short flash ERG protocol.....	98

## LIST OF FIGURES

Figure 1.1. Histological and gross structural characteristics of the chicken eye.....	2
Figure 1.2. A simple diagram of the organization of the retina.....	4
Figure 1.3. Plastic-embedded retinal section of a normal chicken at 270 days of age.....	5
Figure 1.4. A simplified diagram of the rod phototransduction cascade and visual cycle.....	10
Figure 1.5. Synapses between rods, cones and their associated bipolar cells.....	12
Figure 1.6. The ERG waves.....	17
Figure 1.7. The long flash ERG.....	22
Figure 1.8. Short flash ERG with oscillatory potentials.....	23
Figure 1.9. Commonly measured parameters of the ERG waveform.....	24
Figure 1.10. Gross ophthalmic photographs from representative <i>rge</i> and control birds.....	30
Figure 1.11. Posterior eyecup from a 49-day-old <i>rge</i> bird showing lacquer cracks.....	32
Figure 1.12. Plastic and resin-embedded retinal sections from <i>rge</i> birds demonstrating morphologic details of the lacquer crack lesions.....	33
Figure 1.13. Semithin sections of outer retina.....	35
Figure 1.14. Mislocalization of glycogen deposits.....	37
Figure 1.15. EM images of photoreceptor synaptic terminals.....	39
Figure 1.16. Representative ERG responses from a control and an <i>rge</i> chick.....	44
Figure 1.17. Light and dark adapted mean a-wave amplitudes and implicit times for 7 day old chicks.....	45
Figure 1.18. Light and dark adapted mean b-wave amplitudes and implicit times for 7 day old chicks.....	46
Figure 2.1. Area of interest on chicken chromosome one.....	53

Figure 2.2. Schematic drawing of GNB3 cDNA with primers and mutation.....	73
Figure 2.3. Restriction enzyme test to establish GNB3 status.....	76
Figure 2.4. GNB3 amino acid sequence alignment.....	86
Figure 2.5. Results of the GNB3 RE test.....	87
Figure 2.6. GNB3 immunoreactivity in normal chicken retina.....	89
Figure 2.7. A computational model of chicken ( <i>Gallus gallus</i> ) GNB3 protein.....	92
Figure 3.1. Long flash ERG.....	103
Figure 3.2. Mean long flash ERG wave amplitude comparisons.....	103
Figure 3.3. APB effect on short flash ERG.....	106
Figure 3.4. APB effect on long flash ERG.....	107
Figure 3.5. PDA effect on short flash ERG.....	110
Figure 3.6. PDA effect on long flash ERG.....	111
Figure 3.7. Aspartate effect on short flash ERG.....	113
Figure 3.8. Aspartate effect on long flash ERG.....	114
Figure 3.9. Mean dark-adapted circadian a-wave amplitudes.....	116
Figure 3.10. Mean dark-adapted circadian b-wave amplitudes.....	116
Figure 3.11. Mean light-adapted circadian a-wave amplitudes.....	118
Figure 3.12. Mean light-adapted circadian b-wave amplitudes.....	118
Figure 3.13. Mean dark-adapted circadian a-wave implicit times.....	120
Figure 3.14. Mean dark-adapted circadian b-wave implicit times.....	120
Figure 3.15. Mean light-adapted circadian a-wave implicit times.....	121
Figure 3.16. Mean light-adapted circadian b-wave implicit times.....	121

Figures in this thesis are presented in color.



# **CHAPTER 1**

## **INTRODUCTION**

### **1.1. Structure of the chicken globe**

The chicken eye, like many avian eyes, is proportionately larger than that of mammals and takes up a larger volume of the head. The outermost wall of the globe is made up of the avascular transparent cornea and the fibrous sclera. The sclera contains ossicles (bones) rostrally and a cartilage cup caudally, both of which help to maintain the shape of the eye. The uveal tract, the middle layer consists of the iris, ciliary body and the choroid. The avian pupil, unlike the mammalian pupil, is controlled by striated muscle as opposed to smooth muscle, and is responsible for regulating the amount of light that is allowed to reach the retina. The choroid contains blood vessels responsible for supplying nutrients to and removing wastes from the retina and the retinal pigmented epithelium (RPE), which is associated with the outer segments of the photoreceptors. An important job of the RPE is to remove spent portions of outer segments of the photoreceptors as they are released. The RPE's relationship to the photoreceptor outer segments changes in a circadian rhythm. During the daylight hours, the RPE cells have processes, which are particularly developed in the avian and fish retinas, that envelope the outer segments; at night these processes retract. The innermost layer of the globe is the neurosensory retina. It is responsible for the conversion of light energy into a chemical and then electrical signal (phototransduction), which, when sent to the brain, allows visual perception. A unique feature of the avian eye globe is the pecten, which is a highly vascular and pigmented structure projecting into the vitreous from the back of

the globe (Figure 1.1), whose complete functions have merely been hypothesized. The most widely accepted theory of its function is that it helps to provide nutrients to the retina (Meyer, 1977).

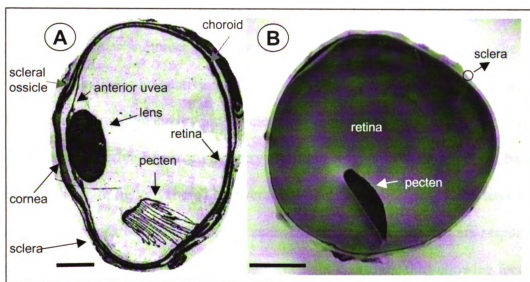


**Figure 1.1.** Histological and gross structural characteristics of the chicken eye. A) Paraffin-embedded cross retinal section of a chicken eye at 7 days of age, the names of the main structures are indicated in the figure. Note the comb-like appearance of the pecten, located anteriorly, overlying the optic nerve head. Stain = hematoxylin/eosin. Bar - 2.5 mm. B) Gross photograph of the posterior eyecup of a 60-day-old chicken eye after removal of the anterior segment, lens and vitreous. The retina is the transparent layer covering the eyecup. Note that the pecten projects into the inferior portion of the posterior chamber. The dorsal part of the pecten is always tilted to the temporal aspect of the eye. Thus, B shows a retinal cup from a right eye. Bar - 5 mm. Figure used with permission from Montiani-Ferreira PhD Thesis 2004.

## **1.2. Structure and function of the retina**

The retina lines the back of the eye globe. It is positioned between the vitreous humor and the choroid. The layers of the retina from the outer to inner retina are as follows: retinal pigmented epithelium (RPE), photoreceptors, outer limiting membrane (OLM), outer nuclear layer (ONL), outer plexiform layer (OPL), inner nuclear layer (INL), inner plexiform layer (IPL), ganglion cell layer (GCL), nerve fiber layer (NFL) and inner limiting membrane (ILM) (Figures 1.2 and 1.3). The photoreceptor layer is composed of the inner and outer segments (IS and OS) of the rods and cones. The outer segments contain the photoactive pigments and phototransduction proteins that are capable of converting light energy into an electrical signal.

Rods are capable of perceiving very low light levels but their responses become saturated with bright lights. There are several different types of cones, which have lower sensitivities than rods but do not become saturated as easily as rods and are responsible for perceiving a broader range of wavelengths of light than rods, thus allowing for color vision. The outer and inner limiting membranes are, in fact, not membranes but are made up of the endfeet of Müller glial cells and appear as dense lines at the light microscopic level. The outer nuclear layer contains the cell bodies of the rods and cones. The innermost part of the photoreceptors, the rod spherules and cone pedicles, make the synaptic connections with the second order neurons (bipolar cells and horizontal cells) in the outer plexiform layer.

The bipolar cells stretch from the outer nuclear layer to the inner plexiform layer, whereas the horizontal cells relay information laterally in the outer plexiform layer (typically from rods to cones or from cones to cones). The bipolar cells communicate

with the ganglion and amacrine cells in the inner plexiform layer. The inner nuclear layer contains the cell bodies of the amacrine, ganglion and Müller cells. Finally, the axons of the ganglion cells make up the nerve fiber layer, which ultimately makes up the optic nerve. The Müller cells are the primary glial cell of the retina and span the retina from the outer nuclear layer to the nerve fiber layer.

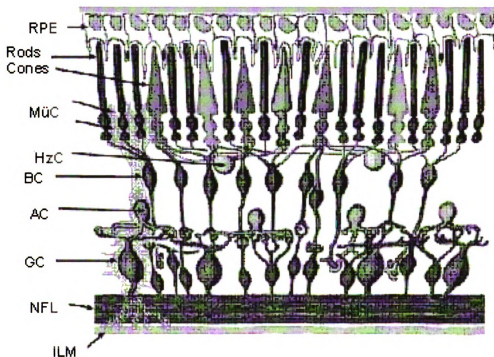


**Figure 1.2.** A simple diagram of the organization of the retina. Key: RPE – retinal pigment epithelium; MüC – Müller cell; HzC – horizontal cell; BC – bipolar cell; AC – amacrine cell; GC – ganglion cell; NFL – nerve fiber layer; ILM – inner limiting membrane. (Source [www.webvision.med.utah.edu](http://www.webvision.med.utah.edu))

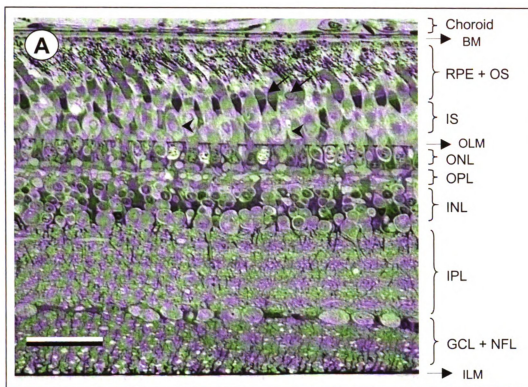


**Figure 1.3.** Plastic-embedded section of a normal chicken retina at 270 days of age. The oil droplets, present in some of the cone photoreceptor inner segments can be seen adjacent to the RPE (arrows). The hyperboloid and the paraboloid (arrowheads) with their characteristic metachromatic appearance in toluidine blue can also be seen. Stain – toluidine blue; Bar – 20  $\mu$ m. Key: BM – Bruch's Membrane; RPE+OS – Retinal Pigment Epithelium + Outer Segment; IS – Inner Segment; OLM – Outer Limiting Membrane; ONL – Outer Nuclear Layer; OPL – Outer Plexiform Layer; INL – Inner Nuclear Layer; IPL – Inner Plexiform Layer; GCL+NFL – Ganglion Cell Layer + Nerve Fiber Layer; ILM – Inner Limiting Membrane. Figure used with permission from Montiani-Ferreira PhD Thesis 2004.

### **1.3. Chicken retinal structure**

Chickens, like most other avian species, fish, reptiles and amphibians, have a cone-dominant retina, whereas nearly all mammals, including humans, have rod-dominant retinas. They possess two types of cones, single and double cones, which exist as either a single cell (single) or tightly associated accessory and principal cell (double). It has been shown that the accessory and principal cells of the double cones are electrically coupled (Smith et al., 1985). Their cones are unique in that they possess oil droplets in the inner segment (ellipsoid) that act as filters through which light must pass before reaching the visual pigment (Bowmaker et al., 1997), a feature only found in birds and some reptiles. There are several different types of cones categorized both by the type of oil droplets and the visual pigment they contain. The oil droplets and visual pigments are characterized by the wavelength of light to which they are most sensitive. There are four different cone pigments with maximal absorbance wavelengths of 415, 460, 505 and 562nm (Fager and Fager, 1981; Yen and Fager, 1984; Yoshizawa T & Fukada Y, 1993). The various types of cones are accompanied by oil droplets of different colors, which help to narrow the spectral sensitivities of the photopigments (Bowmaker et al., 1997).

### **1.4. Signaling within the retina**

#### **1.4.1. Guanine-nucleotide binding proteins**

Guanine nucleotide binding proteins (G-proteins) are involved in many cell signaling cascades in many tissues of the body. They play various roles in regulating the activity of enzymes, ion channels and vesicular transport through their interaction with G protein-coupled receptors (GPCRs) (Neer, 1995; Krapivinsky et al., 1995; Helms, 1995).

Despite their great array of “jobs” they all share the same heterotrimeric structure. The  $\alpha$  subunit is responsible for binding GTP and converting it to GDP and together the  $\beta$  and  $\gamma$  subunits act as a single unit. When activated, the  $\alpha$  subunit exchanges GDP for GTP, dissociates from the  $\beta\gamma$  dimer and goes on to stimulate other pathways. In some systems, such as phototransduction, the  $\alpha$ -GTP complex is active, while in other instances the  $\beta\gamma$  subunit is active. An example of the  $\beta\gamma$  dimer directly initiating a signaling pathway is a G-protein-activated inwardly rectifying K<sup>+</sup> channels (GIRK2) that is activated by G $\beta$ 1 $\gamma$ 2 when co-expressed in *Xenopus* oocytes (Kofuji et al., 1995). When the GTP is hydrolyzed to GDP, the  $\beta\gamma$  dimer binds to the  $\alpha$  subunit once again to reform the holoenzyme. There are different forms of the three subunits that are found in different cell types in various combinations (Hamm and Gilchrist, 1996).

Of particular significance to this project is the  $\beta$ 3 subunit.  $\beta$  subunits are made up of an alpha helix and 7 repeating WD domains that form “propellers.” The  $\alpha$  and  $\gamma$  subunits bind to the  $\beta$  subunit at opposite sides of the molecule.

#### 1.4.2. Visual transduction

As previously mentioned, phototransduction is the process by which light is converted into a chemical signal and is one of the best characterized cell-signaling cascades involving G-proteins. This visual transduction cascade has been well characterized in rod photoreceptors, but has not yet been fully elucidated in cones, although it is thought to involve a similar process. Figure 1.4 is a simplified schematic of phototransduction in rods.

In rods, a photon of light converts the 11-*cis*-retinal molecule to all-*trans*-retinal, which is then combined with opsin to become the visual pigment rhodopsin, thus “bleaching” rhodopsin. One of the intermediates is metarhodopsin II, which is responsible for activating transducin (Emeis et al., 1982). Metarhodopsin II (Rho\*) interacts with the GDP-bound form of transducin ( $G\alpha\beta\gamma$  trimer) and initiates the exchange of GDP for GTP thus dissociating the now-activated  $\alpha$ -subunit from the  $\beta\gamma$  dimer (Molday, 1998). One Rho\* can interact with many transducin complexes thus amplifying the response.  $G\alpha$ -GTP then interacts with cGMP phosphodiesterase (PDE), a heterotrimer consisting of  $\alpha\beta$  catalytic subunits and two inhibitory  $\gamma$  subunits.  $G\alpha$  interacts with the  $\gamma$  subunits (of PDE) causing the release of the  $\alpha\beta$  subunits. The catalytic site of PDE- $\alpha\beta$  is then exposed and lowers the concentration of cGMP in the cytoplasm, which in turn leads to closure of the cGMP-gated ion channels in the cell membrane. This stops the current of  $Na^+$  and  $Ca^{2+}$  ions which steadily flows into the cell in the dark. The closure of the cGMP-gated channels results in hyperpolarization of the cell and a decrease in the release of glutamate from the photoreceptor terminal. To reiterate, when stimulated with light, the photoreceptors *hyperpolarize*, which is unusual amongst excitable cells.

Inactivation of the phototransduction cascade is accomplished by several pathways. Phosphorylation of activated rhodopsin by rhodopsin kinase (RK) reduces the enzymatic activity of activated rhodopsin and generates an affinity of rhodopsin to bind to arrestin (Arr) (Alloway and Dolph, 1999). Arrestin binding to rhodopsin prevents future transducin activation. Hydrolysis of  $T\alpha$ -GTP into  $T\alpha$ -GDP results in deactivation of PDE (Vuong and Chabre, 1991) by releasing PDE $\gamma$  molecules, which can then rebind



to the PDE $\alpha\beta$  complex. In the mean time, T $\alpha$ -GDP is deactivated by rebinding to the T $\beta\gamma$  complex. A decrease of intracellular Ca<sup>2+</sup> due to closure of cGMP-gated channels mediates recoverin (RC), a Ca<sup>2+</sup>-binding protein, to relieve inhibition of guanylate cyclase (GC) (Venkataraman et al., 2003). Activated guanylate cyclase synthesizes cGMP, and is activated by guanylate cyclase activating protein (GCAP) (Palczewski et al., 1994). Because activated GC re-synthesizes cGMP, an elevation of cGMP concentration results in a re-opening of some of the cGMP-gated ion channels, which consecutively increases the inward cation flow responsible for the dark current, leading to rod depolarization and an increase in glutamate release.

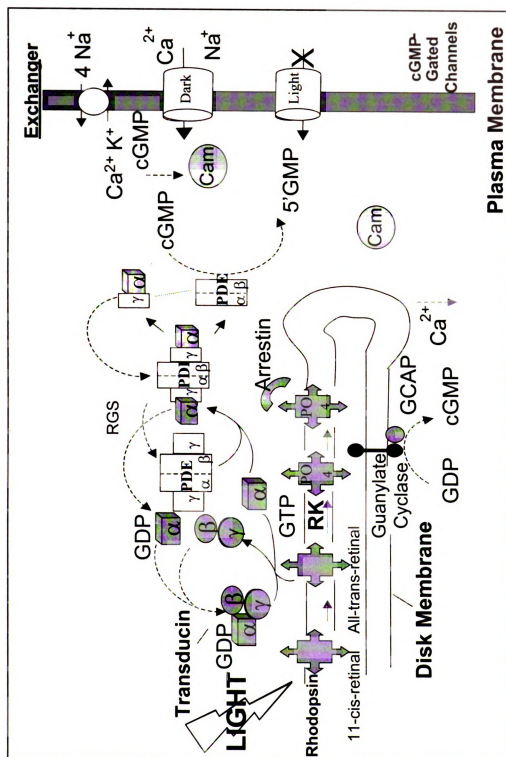


**Figure 1.4.** Diagram of rod phototransduction cascade. Key: GCAP - Guanylate Cyclase Activating Protein; PDE - cGMP Phosphodiesterase;  $\alpha$ ,  $\beta$  and  $\gamma$  - subunits of transducin; RK - Rhodopsin Kinase; RGS - Regulator of G-protein Signaling; Cam - Calmodulin.

### 1.4.3. ON and OFF pathways

The photoreceptors synapse in various ways with several different types of cells including ON-center (rods and cones) and OFF-center (cones only) bipolar cells. When the photoreceptors are stimulated with light, they hyperpolarize reducing glutamate release at the synaptic terminal. This affects the ON and OFF bipolar cells in opposite ways; ON-center bipolar cells respond by depolarizing and OFF-center bipolar cells respond by hyperpolarizing (Dowling and Werblin, 1969; Werblin, 1991). Thus ON bipolar cells are often referred to as depolarizing bipolar cells (DBC) and OFF bipolar cells are referred to as hyperpolarizing bipolar cells (HBC) (Figure 1.5).

The type of synapse between the photoreceptors and the bipolar cells is associated with the type of bipolar cell. Synapses between photoreceptors and bipolar cells that are characterized as invaginating ribbon-type synapses are associated with ON bipolar cells and create a sign-inverting synapse (i.e. when photoreceptors hyperpolarize, ON bipolar cells depolarize). Both rods and cones synapse with bipolar cells with this type of ribbon-synapse, meaning there are rod ON bipolar cells and cone ON bipolar cells. These synaptic connections are made through metabotropic glutamate receptors, specifically mGluR6 receptors, which signal through a G-protein coupled cascade (Nawy and Jahr, 1990; Nawy, 1999).

Cones (but not rods) also synapse with OFF bipolar cells with a basal junction connection and create a sign-preserving synapse because they depolarize when the photoreceptors depolarize in response to light. These synaptic connections are made through ionotropic glutamate receptors (iGluR) (Slaughter and Miller, 1983).

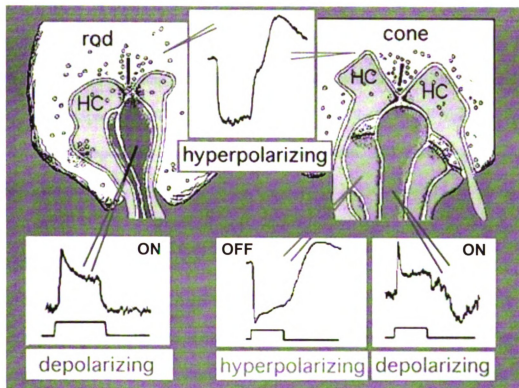


**Figure 1.5.** Synapses between rods, cones and their associated bipolar cells. Rod photoreceptors only synapse with an invaginating synapse with ON bipolar cells creating a sign inverting response – rod ON bipolar cells depolarize in response to rod hyperpolarization. Cones synapse with both basal (OFF bipolar cells) and invaginating synapses (ON bipolar cells). Cone ON bipolar cells are also sign inverting in that they depolarize in response to cone hyperpolarization, whereas cone OFF bipolar cells have sign preserving responses in that they hyperpolarize in response to cone hyperpolarization. HC – Horizontal Cell (Source: [www.webvision.med.utah.edu](http://www.webvision.med.utah.edu))

ON and OFF bipolar cells form single excitatory synapses with specific ganglion cells in the inner plexiform layer in a highly stratified configuration (Raviola and Raviola, 1982). ON cells synapse in layers closer to the ganglion cell layer, while OFF cells synapse in layers closer to the inner nuclear layer (Gouras, 1971; Famiglietti, Jr. and Kolb, 1976; Nelson et al., 1978); therefore, ON bipolar cells synapse with ON ganglion cells and OFF bipolar cells synapse with OFF ganglion cells. Similar to the ON/OFF bipolar cells, ON ganglion cells depolarize in response to stimulation and OFF ganglion cells hyperpolarize.

### **1.5. Retinal dystrophy models**

There are hundreds of animal models of genetic retinal dystrophies, in species from *Drosophila* to dogs to primates. Some of them are naturally occurring (spontaneous), while some of them have had various mutations induced intentionally (knock out). There are currently many mutant mice and several mutant dogs that are being used to study retinal diseases. One example is the RPE65 mutant dog from the Briard breed, a model of Leber's Congenital Amaurosis Type II, in which there is a failure of formation of 11-*cis* retinal in the RPE meaning there is a lack of visual pigment formation. The lack of visual pigment formation has a severe effect on vision. There is an accumulation of all *trans* retinyl esters that leads to a slowly progressive degeneration of the retina (Narfström et al., 1989; Veske et al., 1999; Narfström et al., 2003). Another example is the retinal degeneration (*rd1*) mouse, a model of retinitis pigmentosa, in which a nonsense mutation of the beta-subunit of cGMP phosphodiesterase leads to an accumulation of cGMP and eventually photoreceptor degeneration (Pittler and Baehr,

1991). Both of these models have been used in gene therapy trials (Acland et al., 2005; Pang et al., 2006).

There are also several naturally occurring chicken models of retinal diseases including blindness, enlarged-globe (*beg*), delayed amelanotic (DAM), retinal dysplasia and degeneration (*rdd*) and retinal degeneration (*rd*). The *rdd* chicken was discovered in 1979 in Scotland and further described in the early 1980's (Randall and McLachlan, 1979; Wilson MA, 1982; Randall et al., 1983). Affected chicks have reduced vision at hatch and eventually become blind by 15 weeks of age. Histopathological changes of this model include severe retinal dystrophy involving thinning of the RPE and of all layers of the retina, and near complete loss of the outer nuclear layer and photoreceptors. This genetic abnormality has been shown to be a sex-linked recessive trait, the disease interval of which is homologous to human chromosomes 9 and 5 (Burt et al., 2003).

The blindness, enlarged globe (*beg*) chick was characterized in the early 1980's as having vision abnormalities at hatch, abnormal coordination and eventually developing globe enlargement and blindness (Pollock et al., 1982). No further research has been published regarding the *beg* chicken. Another chicken model of a retinopathy is the delayed amelanotic (DAM) chicken, which suffers a gradual depigmentation due to defective melanocytes and involves the feathers and the choroid and thus the retinal pigmented epithelium (Boissy et al., 1983). The disrupted retinal pigmented epithelium is unable to maintain contact with the outer segments of the photoreceptors and eventually leads to retinal detachment (Fite et al., 1985). Additionally, the abnormal RPE cells are no longer able to phagocytize photoreceptor outer segments, which leads to

impaired function of the photoreceptors and eventually the entire retina (Lahiri and Bailey, 1993).

The retinal degeneration (*rd*) chick is blind at hatch but has a morphologically normal retina indicating normal retinal development. The photoreceptors begin deteriorating at 2-3 weeks of age until eventually very few intact photoreceptors remain at 6 months and the photoreceptor cell bodies are replaced by Müller cell processes (Ulshafer et al., 1984; Ulshafer and Allen, 1985). The causative mutation is a null mutation in the guanylate cyclase 1 gene (GC1), which encodes the enzyme involved in cGMP synthesis. Without GC1, the abnormally low amount of cGMP may lead to permanent closure of the cGMP-gated cation channels located in the photoreceptor cell membrane and elimination of the dark current and chronic hyperpolarization of the photoreceptors (Semple-Rowland et al., 1998). The *rd* chicken is considered a model of Leber's Congenital Amaurosis Type I.

## **1.6. Electrophysiology**

### **1.6.1. The electroretinogram**

When stimulated with light, the cells of the retina react in various ways and produce electrical currents. This electrical activity is detectable at the cornea's surface and the recording of the electrical response is called an electroretinogram (ERG). This allows the retina to be evaluated using a minimally invasive method. The electroretinogram represents the summation of the responses from the entire retina and most of its cell types, some of which have opposing responses. The ERG generally

consists of an initial corneal negative a-wave followed by a corneal positive b-wave, and under certain circumstances a c-wave and a d-wave.

Some of the earliest work with electroretinography was done by Einthoven and Jolly in 1908. They found when the retina was stimulated with light, three waves appeared at various times after stimulation. They named the initial negative wave the a-wave, the second positive wave the b-wave and the last, slower positive wave the c-wave (Figure 1.6) (Einthoven and Jolly, 1908). These wave designations have been used since then. In 1933, Ragnar Granit recorded electroretinograms from an anesthetized cat and found as the anesthesia deepened, the electroretinogram changed. He named the waves P-I, P-II and P-III for the order in which they disappeared as ether anesthesia deepened (Figure 1.6). P-I is a slow cornea positive wave and disappeared first. P-II has an initial fast and sharp positive wave, which then drops to an intermediate potential until the light stimulus is terminated. P-III is a negative wave that appears before the other two and was the most resistant to anesthesia. P-III has been shown to have two components, a fast component and a slow component (Granit, 1933). Since then, Granit's three waves have been associated with Einthoven and Jolly's waves as follows: the a-wave is the fast component of P-III, the b-wave consists of P-II and the slow component of P-III, and the c-wave is P-I.



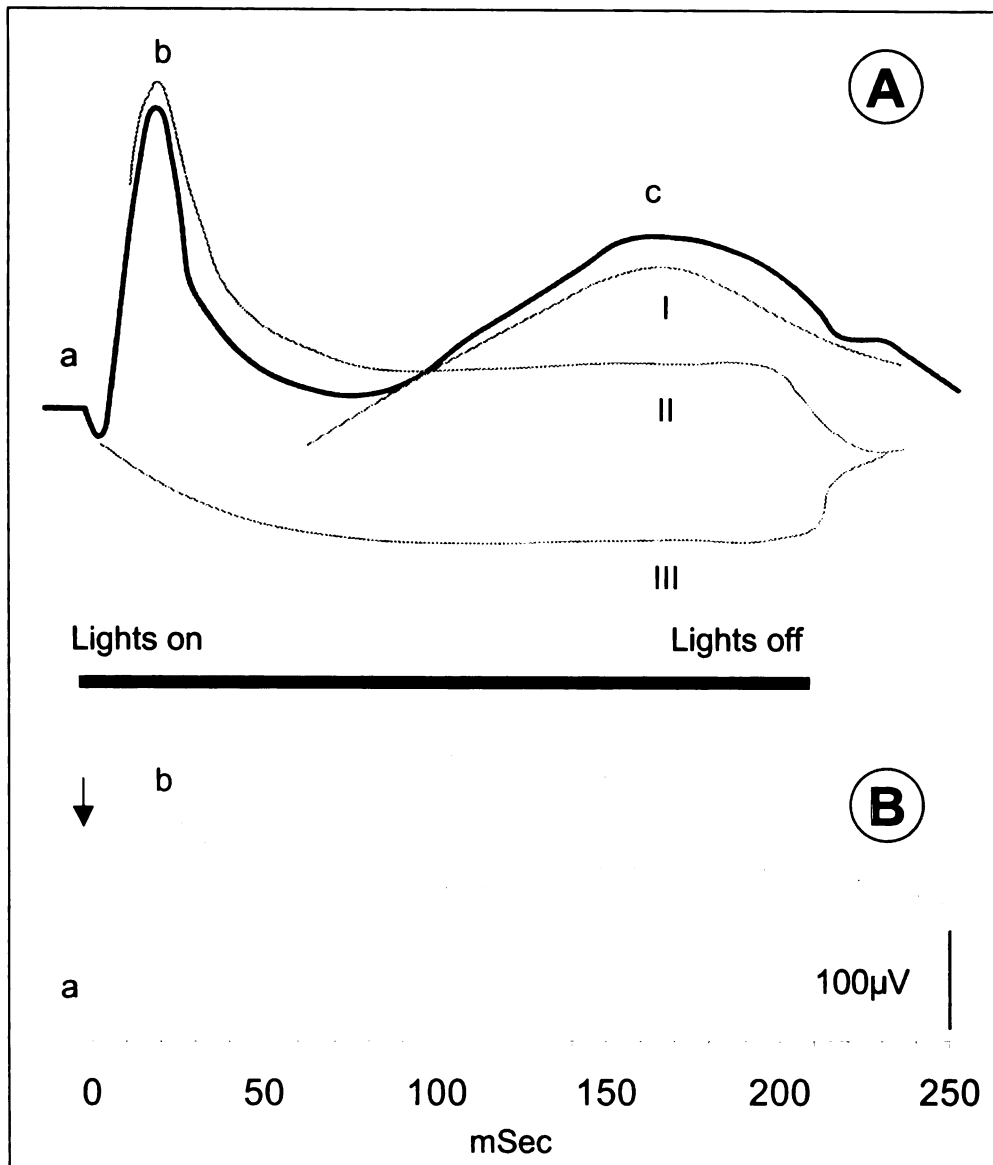


**Figure 1.6.** The ERG waves. A) Diagrammatic representation of the Granit waveforms (I, II and III) which make up the electroretinogram (ERG). Note the superimposed representation of a-, b- and c-waves correlating with the waveforms III, II and I, respectively. B) An actual ERG from a 90 day old chicken. The arrow indicates the timepoint at which the eye was stimulated by a brief flash of light. Note the chicken ERG has the same basic components of a mammalian ERG. The a- and b-waves are marked. Time scales are not equal for A and B. Figure used with permission from Montiani-Ferreira PhD Thesis 2004.

### 1.6.2. The origins of the ERG waves

Much work has been done since the birth of electroretinography to elucidate the origins of the waves of the electroretinogram. Two methods have been used historically; recording of responses with electrodes placed within various layers of the retina and dissociated cells, and pharmacological dissection using agonists and antagonists to alter the response of certain cell types. More recently, knockout models of various essential retinal components have furthered the elucidation of ERG waveform origins.

The a-wave, the first to appear after light stimulation, corresponds with the leading edge of Granit's P-III (the fast component) and has since been found to largely originate from the photoreceptors. When stimulated with light the phototransduction cascade leads to the closure of the cation channels and the hyperpolarization of the photoreceptors, which results in the corneal negative a-wave. The a-wave is visible until the corneal positive b-wave appears. Intraretinal recording revealed that the a-wave is the "light current" from the photoreceptors and is due to the loss of the dark current as cGMP-gated channels close; thus, the a-wave represents the photoreceptors' response to light stimulation (Penn and Hagins, 1969; Sillman et al., 1969). Furthermore, when 2-amino-4-phosphonobutyric acid (APB – a glutamate agonist, also known as L-AP4) is applied, the response of some second order neurons is prevented and the a-wave is the only wave remaining (Slaughter and Miller, 1981; Slaughter and Miller, 1983; Stockton and Slaughter, 1989). Evidence that the a-wave, particularly the cone response, also contains post-receptor contributions was elucidated when N-methyl-D-aspartic acid (NMDA – a glutamate receptor antagonist that decreases the response of third order

retinal neurons) was found to decrease the amplitude of the a-wave (Robson and Frishman, 1996).

The b-wave has been the subject of much debate among electrophysiologists. The results of many studies have shown that the b-wave corresponds to P-II and the slower component of P-III and that it originates from both the bipolar cells and possibly from the Müller cells. The hyperpolarization of the photoreceptors in response to light decreases the amount of neurotransmitter (glutamate) that is released onto the second order bipolar cells, which in turn either depolarize (ON bipolar cells) or hyperpolarize (OFF bipolar cells), which in turn alters the extracellular potassium concentration thus affecting Müller cells. One study using APB, which selectively blocks the response of ON bipolar cells, demonstrated that the b-wave was eliminated after application of APB (Gurevich and Slaughter, 1993). Another study has shown that the b-wave is the summation of the response from both the ON (depolarizing) and OFF (hyperpolarizing) bipolar cells, which create opposite electrical potentials in response to light (Sieving et al., 1994). They coined the phrase the “push-pull model” of the electroretinogram in reference to the competing responses of the bipolar cells in response to light.

Barium, an ion that completely blocks the potassium permeability of Müller cells, has also been used to study the b-wave (Newman, 1989; Reichelt and Pannicke, 1993; Linn et al., 1998). The Müller cells’ involvement in the b-wave was disproved when barium ions were injected intravitreally; the b-wave was augmented instead of being eliminated, which is what would be expected if Müller cells contributed positively to the b-wave (Lei and Perlman, 1999). Other research indicates that third order neurons also contribute to the b-wave because drugs that enhance or decrease the response of third

order neurons also respectively enhance or decrease the b-wave (Awatramani et al., 2001).

The c-wave's origin does not appear to be quite as convoluted as that of the b-wave. It has been shown to originate from the retinal pigmented epithelium (RPE). Several methods have been used to come to this conclusion. Intracellular recordings from the RPE in response to light stimulation had an identical shape and time course as the c-wave of the ERG (Steinberg et al., 1970). Additionally, when the retina is separated from the RPE, light stimulation produces a- and b-waves, but not the c-wave (Pepperberg et al., 1978). The c-wave is dependent on the potassium concentration changes induced by the photoreceptors upon light stimulation (Oakley and Green, 1976; Oakley, 1977). So, although the c-wave originates from the RPE, the photoreceptors must be functional in order to produce the wave.

The d-wave becomes apparent only when the length of the light stimulus is 100ms or greater (*i.e.* a long flash) because it appears at the off set of the light stimulus (Figure 1.7). When the stimulus is shorter, the b-wave and the d-wave are overlapped. Current source density analysis showed that the d-wave originates from the hyperpolarizing (OFF) bipolar cell (Xu and Karwoski, 1994). Pharmacologic dissection using *cis* 2,3-piperidine-dicarboxylic acid (PDA – a glutamate antagonist) suppresses the light responses of OFF bipolar cells and eliminates the d-wave of the ERG, suggesting the d-wave originates from the transmission between photoreceptors and OFF-center bipolar cells (Stockton and Slaughter, 1989). Other research suggests that third order neurons (amacrine and ganglion cells) also contribute to the d-wave. Baclofen, a drug that enhances the light responses of third order neurons, enhanced the d-wave, whereas drugs

that decrease the response of third order neurons decreased the d-wave (Awatramani et al., 2001).

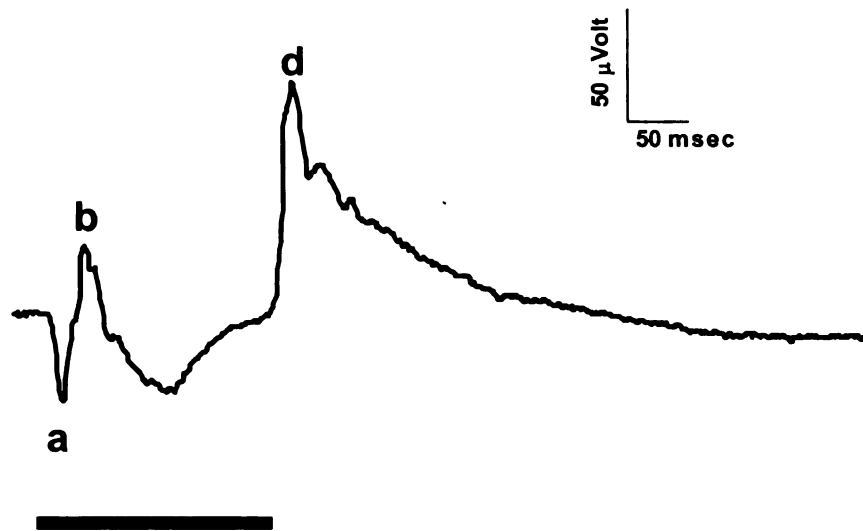


**Figure 1.7.** The long flash ERG. Representative ERG from a normal chicken in response to a prolonged flash of light (150 msec). The a-, b- and d-waves are labeled. Heavy black line indicates length of flash. Notice the d-wave appears at lights-off.

Another relevant component of the ERG is the oscillatory potentials (OPs). These are small amplitude “wavelets” that appear on the rising edge of the b-wave when a bright light is used as a stimulus (Figure 1.8). In order to evaluate them more closely, a band-pass filter can be used to isolate the OPs. The exact cellular origin of OPs has yet to be determined, but some information has been gathered. Intraretinal recordings reveal that the amplitude is the greatest when the electrode is in the inner retina, specifically the inner plexiform layer (Brown, 1968; Ogden, 1973). It is thought the OPs are generated by extracellular electrical currents created by negative feedback pathways between amacrine, ganglion and bipolar cells (Wachtmeister and Dowling, 1978). OP amplitudes are decreased in conditions causing retinal ischemia and because of this, their amplitudes have been used to evaluate diabetic retinopathy, a condition characterized by localized retinal ischemia (Frost-Larsen et al., 1980; Simonsen, 1980; Bresnick and Palta, 1987; Asi and Perlman, 1992; Kizawa et al., 2006).

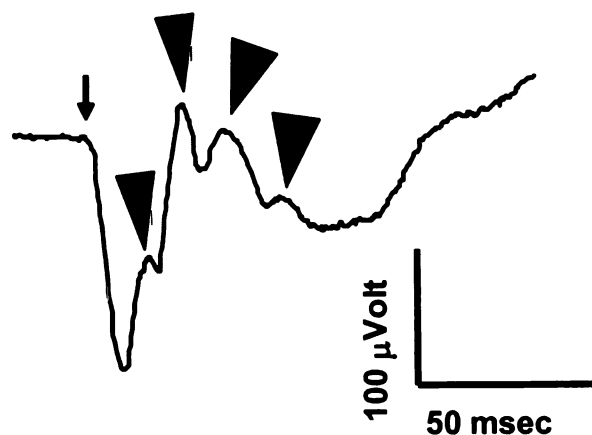


**Figure 1.8.** Short flash ERG with oscillatory potentials. Representative short flash ERG from a normal chicken. The OP's are marked with large black arrow heads. The small arrow indicates the brief light stimulus.

When studying electroretinograms, several parameters are used to evaluate the waveforms (Figure 1.9). The amplitude, which is measured in microvolts ( $\mu\text{V}$ ), of the a-wave is measured from the baseline to the trough (peak) of the a-wave. The b-wave amplitude is measured from the trough of the a-wave to the peak of the b-wave. The implicit time is the amount of time from stimulus onset to the peak of the wave and is measured in milliseconds (msec). The latency of a wave is the amount of time from stimulus onset to the *beginning* of the wave and is also measured in milliseconds.

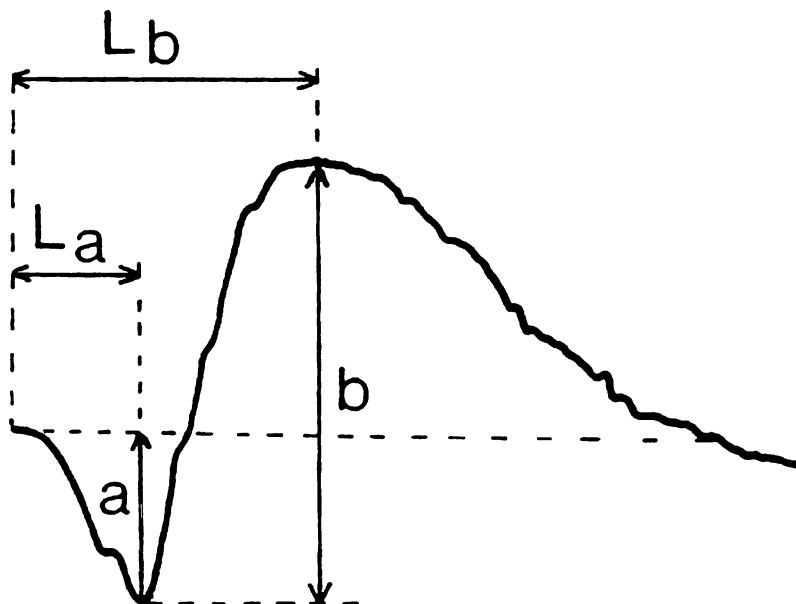


**Figure 1.9.** Commonly measured parameters of the ERG waveform. A-wave amplitudes are measured from baseline to the trough. B-wave amplitudes are measured from the trough of the a-wave to the peak. Implicit times (denoted  $L_a$  and  $L_b$ ) are measured from light stimulus to the peak of the wave. (Source: [www.webvision.med.utah.edu](http://www.webvision.med.utah.edu))



### 1.6.3. Light adaptation status and the electroretinogram

Because ERG waveforms reflect the responses of the photoreceptors, the receptors that are active under the stimulus conditions are those that ultimately shape the ERG waveform; therefore when the stimulus intensity is low and/or the retina is “dark-adapted,” the rod response dominates whereas when the stimulus intensity is bright but the retina is dark-adapted, the response is a mixed rod/cone response. Lighting conditions that elicit a mixed rod/cone response are called mesopic. An ERG performed when a subject is light adapted is termed a photopic ERG and when dark adapted, a scotopic ERG. Photopic ERGs are performed after a subject has been light adapted to a “rod-saturating” background light, which means the rods are incapable of responding to a light stimulus. In addition to stimulus intensity and the light/dark adaptation status, the ERG is also affected by the proportion of rods and cones in a retina; some species have a cone dominant retina (chicken, ground squirrel), whereas some have a rod dominant retina (humans, dogs, rats and mice).

### 1.6.4. Circadian ERGs

Retinal morphology and function has been shown to exhibit circadian variation in many species. Photoreceptors in chicks and rats shed outer segments in a circadian rhythm – rods shed their outer segments soon after lights on and cones shed theirs soon after lights off (LaVail, 1976; Young, 1978). Retinal and behavioral sensitivity of zebrafish are also circadian in nature in that sensitivity thresholds change throughout the day (Li and Dowling, 1998). In chickens, research using electroretinograms has shown that rod function is greater at night and is reduced during the day (Schaeffel et al., 1991).

This differential activity of photoreceptors is known as the retinal Purkinje Shift, which is characterized by rods and cones being active at opposite times of day (rods active at night, cones active during the day) or in different light adaptation (rods after dark adaptation and cones after light adaptation). Further research has shown that b-wave amplitude is rhythmic – the amplitude is larger in the afternoon and that exogenous melatonin administered during the day reduced the b-wave amplitude (Lu et al., 1995). The human's visual threshold is significantly increased 1.5 hours after lights-on, which corresponds with the time that rods are maximally shedding their outer segments (Birch et al., 1984).

Other research has shown that chick's and pigeon's a- and b-wave amplitudes were larger, implicit times were shorter and sensitivity was lower during the day time. Short implicit times and lower sensitivity are considered to be specific to the behavior of cones (McGoogan and Cassone, 1999; Wu et al., 2000). This was attributed to the avian retina being cone-dominant and thus a larger number of photoreceptors were able to respond during the day (when the cones were active) than at night (when only rods were active) (McGoogan et al., 2000). Melatonin is one substance that has been implicated in the circadian rhythm of the ERG and visual system in that when exogenous melatonin is administered, the rhythmicity of a- and b-wave parameters are abolished (Peters and Cassone, 2005). Research has shown that melatonin is manufactured in and released from both the pineal gland and in the retina (Takahashi et al., 1980; Zawilska and Wawrocka, 1993; Bernard et al., 1997). The work of another research laboratory contradicts that of McGoogan and Cassone's in that they found that quail's b-waves are larger at night than during the day (Manglapus et al., 1998). This laboratory implicates dopamine as being a

key regulator in the circadian rhythms of the retina because when retinal dopamine (D2) receptors were blocked during the day the b-wave amplitude is increased (Manglapus et al., 1999).

#### 1.6.5. The ERG in disease states

Because the components of the ERG waveform are created by the various cell types under varying conditions, alterations in the ERG waveform found with specific diseases may offer a clue as to which cells are affected. ERG waves can be normal, reduced in amplitude, supernormal (increased amplitude), absent, or have an abnormal shape or implicit time. Generally speaking, diseases that affect photoreceptors will have reduced a- and b-wave amplitudes. Specifically, diseases affecting rods will present with smaller a- and b-wave amplitudes under scotopic conditions, whereas those that affect cones will cause smaller amplitudes under photopic conditions. Conditions that only affect second order neurons or the transmission of signals from the photoreceptors to the second order neurons will present with normal a-waves and abnormal b-waves. If third order neurons are affected preferentially, the OPs and possibly the b- and d-waves will be affected.

### 1.7. The *rge* chicken

#### 1.7.1. Original *rge* characterization

The focus of this thesis is the retinopathy, globe-enlarged (*rge*) chicken and much work has already been done to characterize its phenotype. The *rge* chicken was identified in commercial flocks in the United Kingdom in the early 1980's. Affected

birds were detectable by 3 weeks of age but became obvious at 8 weeks of age when poultry house equipment was moved as the affected birds appeared lost when their normal counterparts scattered. Affected birds were unable to peck at food particles, although they were able to respond to large moving objects and to bright lights. The birds also exhibited the bizarre behavior of pecking at the air. They had a reduced pupillary reflex, which corresponded to the severity of their functional visual impairment. Fundus examination revealed prominent choroidal vasculature and linear white lesions in the retina. Older birds often developed cataracts. Histopathology revealed an overall thinning of the retina, a reduction in the number of photoreceptor outer segments and nuclei, a thinner inner nuclear layer and a reduced number of ganglion cells (Curtis et al., 1987; Curtis et al., 1988).

The condition was considered autosomal recessive as heterozygous individuals were indistinguishable from homozygous normal individuals. Test matings between an affected and a carrier suggested that there might be a degree of reduced embryonic survival as ratios were not 1:1 as expected (Inglehearn et al., 2003).

#### 1.7.2. Globe enlargement

In addition to the visual impairment and histological abnormalities, the affected birds invariably develop enlarged globes without an increase in intraocular pressure as they get older (non-glaucomatous) (Figure 1.10). This resulted in increased exposure of the sclera at the medial canthi of affected birds. The enlarged globes also had a loss of the normal corneal curvature and appeared flatter (Figure 1.10). Both the axial length and the weight of affected eyes were greater than unaffected birds of the same age. The

anterior chamber of affected birds became very shallow and the anterior surface of the lens was almost in contact with the posterior corneal surface. The vitreal chamber of affected birds gradually became significantly larger and the pecten appeared atrophied as they aged (Montiani-Ferreira et al., 2003; Inglehearn et al., 2003). These changes are considered to be secondary in response to the visual deficits as alterations in globe size have been experimentally linked to induced visual stimulus deprivations (Hodos and Kuenzel, 1984).

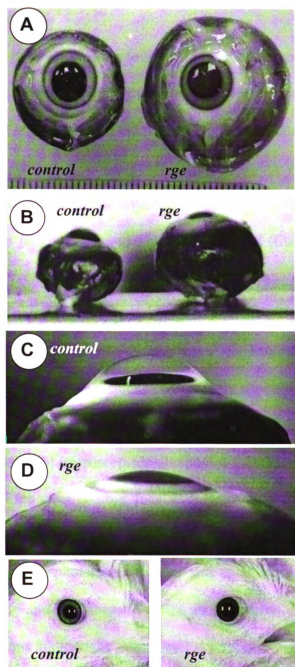


**Figure 1.10.** Gross ophthalmic photographs from representative *rge* and control birds. **A)** Appearance of freshly enucleated eye globes of a control and an affected chick, at 180 days of age. Note the difference in radial diameter of the globes. **B)** Freshly enucleated eye globes of a control and an *rge* chick, at 270 days of age. Note the difference in axial length of the globes. Profile view of the cornea and anterior chamber of a control (**C**) and an *rge* chick (**D**), at 180 days of age. Note the flatter cornea and very shallow anterior chamber of the *rge* eye. **E)** Detail of the eye position inside the orbit of a control and an *rge* bird at 45 days of age. Note the mild lateral strabismus causing greater exposure of the sclera at the medial canthus in the *rge* chick. Figure used with permission from Montiani-Ferreira PhD Thesis 2004.

### 1.7.3. Lacquer crack lesions

Many affected birds develop white linear lesions in the fundus located close to the pecten (Figure 1.11). Histopathologic examination of these lesions revealed focal and severe thinning of the retina in which the photoreceptor inner and outer segments, outer nuclear, outer plexiform and retinal pigment epithelial layers were totally absent, the inner nuclear layer was present but disorganized and the inner retinal layers (nerve fiber, ganglion cell and inner plexiform layers) were mostly normal (Curtis et al., 1988). These lesions have since been characterized as lacquer crack lesions, which are also associated with complications of severe human myopia (Klein and Curtin, 1975; Klein and Green, 1988; Czepita D., 2002). They have also been experimentally induced in form deprivation myopia in chicks and in chicks continuously exposed to light; two situations in which globe enlargement is a resulting feature (Li et al., 1995; Hirata and Negi, 1998).

A more detailed light microscopic evaluation of these lesions revealed mild focal fibrosis at the level of the inner choroid, focal absence of the retinal pigment epithelium, and an accumulation of eosinophilic hyaline material in the subretinal space. Additionally, the overlying photoreceptor inner and outer segments were disorganized and there was thinning and displacement of the inner and outer nuclear layers (Figure 1.12). Semithin sections additionally demonstrated a rupture in Bruch's membrane (the basement membrane of the RPE located between the RPE and the choroid) with scar formation and deposition of collagen fibers (Figure 1.12). These changes were hypothesized to be a result of the abnormal globe enlargement causing the retina to stretch and then break (Montiani-Ferreira et al., 2004).

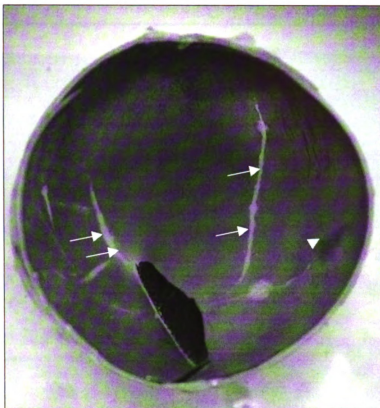


**Figure 1.11.** Posterior eyecup from a 49-day-old *rge* bird showing lacquer cracks. The lacquer crack lesions appear as multiple white to gray linear lesions (white arrows), extending from the pecten to the periphery. Additionally, an area of subretinal hemorrhage (white arrowheads) is present. Figure used with permission from Montiani-Ferreira PhD Thesis 2004.



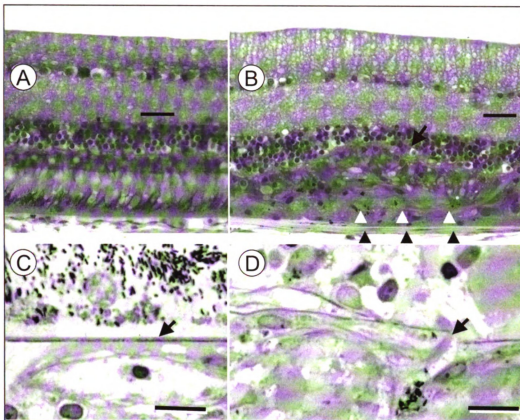


**Figure 1.12.** Plastic and resin-embedded retinal sections from *rge* birds demonstrating morphologic details of the lacquer crack lesions. A) Eye of an *rge* bird at 49 days of age. Cross section through a region of retina adjacent to the lesion shown in B. The retinal architecture is relatively normal with a normal retinal pigment epithelium layer and normal photoreceptor-retinal pigment epithelium interface. However, there is a mild dilation of the photoreceptor inner and outer segments, which is typical of early stage changes observed in the *rge* phenotype. B) Cross section through one of the lesions shown in Figure 1.10 from the central retina. Note the mild focal fibrosis at the level of the inner choroid (black arrowheads) and the absence of retinal pigment epithelium (white arrowheads). There is an accumulation of eosinophilic material in the subretinal space. The overlying photoreceptor inner and outer segments are disorganized and there is thinning and displacement of the outer and inner nuclear layers (black arrow). Stained with H&E. Size bar = 150  $\mu$ m. C & D) Eye of an *rge* bird at 336 days of age. C) This shows the region adjacent to the lesion that is shown in D. Bruch's membrane is intact (arrow) and is lined by the RPE layer on one side and the choriocapillaris on the choroidal side. D) Details of a linear lesion showing an absence of the normal retinal pigment epithelium layer, rupture of Bruch's membrane (arrow), scar formation with deposition of collagen fibers and the abnormal presence of retinal pigment epithelium cell melanosomes on the choroidal side of Bruch's membrane. Stained with toluidine blue. Size bar = 20  $\mu$ m. Figure used with permission from Montiani-Ferreira PhD Thesis 2004.

#### 1.7.4. Retinal changes

A more detailed examination using light microscopy, electron microscopy and immunohistochemistry provided a more complete description of the progression of the pathological changes affecting the *rge* retina. This study showed that at hatch, the *rge* retinas were the same thickness as age-matched control retinas, but they then gradually became thinner as time progressed with all layers except the RPE gradually becoming significantly thinner than controls (Montiani-Ferreira et al., 2005) (Figure 1.13).

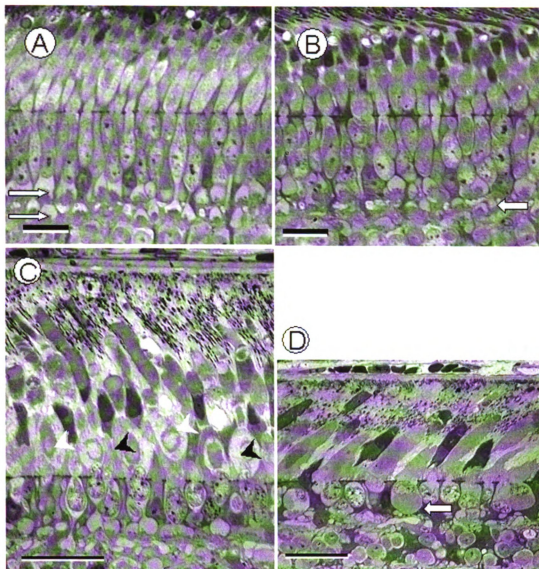


**Figure 1.13.** Semithin sections of outer retina. Sections from control (A & C) and *rge* birds (B & D) at one day (A & B) and 270 days (C & D) of age. A. Control retina has a well organized two-layered arrangement of photoreceptor synaptic termini in the ONL (arrows). B. The mutant retina has dilated photoreceptor cell bodies and disorganization of the OPL architecture (white arrow). Bars for A & B = 10  $\mu$ m. C. Control retina at 270 days has glycogen deposits only in the ISs (external to the outer limiting membrane). These are associated with the rod hyperboloid (white arrowheads) and with the cone accessory cell paraboloid (black arrowheads). D. The mutant retina at 270 days of age is thinned with shortened photoreceptors. Larger glycogen deposits are present and were quite often displaced internal to the outer limiting membrane of the accessory cells of the double cones (arrow). Bars for C & D = 20  $\mu$ m. Adapted from Montiani-Ferreira et al (2005).

The earliest changes found in *rge* retinas were found in the outer plexiform layer and included a disorganization of the photoreceptor synaptic terminal organization and abnormal location of the endoplasmic reticulum (ER) of the photoreceptors (Figure 1.14). The bilayered arrangement of the rod spherules and cone pedicles in control birds was not present in *rge* retinas from an early age. This disorganization became more severe as the birds aged. There also appeared to be fewer synaptic ribbons in the synaptic terminals of photoreceptors from affected retinas although the number of synaptic ribbons in the inner plexiform appeared to be similar to that of control retinas. The endoplasmic reticulum of the photoreceptors was frequently found in the cell bodies rather than in its normal location in the inner segments. Accumulations of glycogen were found in the perinuclear region of the photoreceptors associated with the abnormally located ER (Figure 1.14). No evidence of apoptosis was found using TUNEL staining, caspase 3 staining or morphological criteria (Montiani-Ferreira et al., 2005).

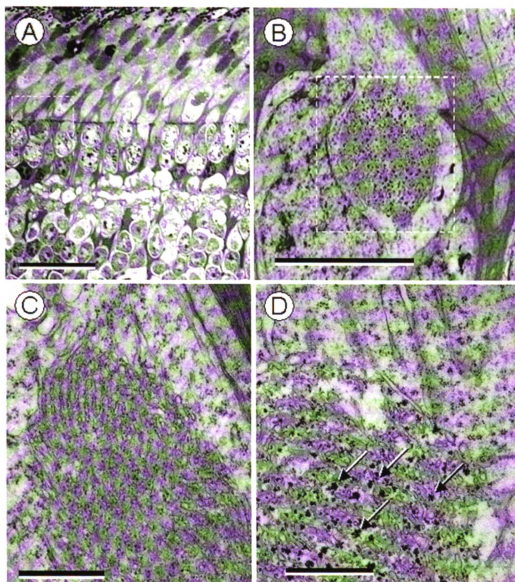


**Figure 1.14.** Mislocalization of glycogen deposits. Semi-thin (A) and ultra-thin (B, C & D) sections of *rge* (A, B & D) and control (C) retina at 7 days of age. **A.** Semi-thin section showing the detail of a large glycogen deposit (dashed white square) in the perinuclear cytoplasm. Note the disrupted OPL. Bar = 20  $\mu\text{m}$ . **B.** Ultrastructural detail of a deposit in the perinuclear cytoplasm of an accessory cell of double cone of a GNB3 mutant bird where it is possible to observe the abnormal accumulation of glycogen (dashed white square). Bar = 5  $\mu\text{m}$ . **C.** Control retina showing evenly-arranged SER in the IS (paraboloid). Small glycogen granules can be seen among the cisterns. Bar = 1  $\mu\text{m}$ . **D.** Higher magnification of section in B to show abnormal glycogen accumulation associated with ER. Bar = 1  $\mu\text{m}$ . Adapted from Montiani-Ferreira et al (2005).

Ultrastructural analysis showed further abnormalities in the photoreceptor terminals. At seven days of age, the photoreceptor pedicles and spherules were increased in size and frequently contained numerous small vesicles and multivesicular bodies. Dense glial cell processes were found between the photoreceptors at 7 days of age and their presence became more prominent as the birds aged (Figure 1.15). The morphological abnormalities in the synaptic terminals of photoreceptors suggest abnormal physiological (specifically synaptic) function and may contribute to the vision loss in the *rge* birds (Montiani-Ferreira et al., 2005).



**Figure 1.15.** EM images of photoreceptor synaptic terminals. **A.** Synaptic terminal of a cone pedicle from a normal control chick at 7 days of age. **B.** A typical example of a synaptic terminal of a cone pedicle of a *rge* chick at 7 days of age. The cytoplasm is less densely stained. Note the disruption in the architecture of the synaptic terminals (small black arrows). Also note the presence of electron dense glial bodies separating the photoreceptors (white arrowheads) and multivesicular bodies (black arrowheads). **C.** Higher power detail of a *rge* chick retinal section at 7 days of age demonstrating one of the sets of numerous flattened (tubuliform) vesicles (white arrow) in a cone pedicle. Size bars = 1 μm. Adapted from Montiani-Ferreira et al (2005).

Immunohistochemical staining using a panel of antibodies showed numerous differences between *rge* and control retinas. Tyrosine hydroxylase (TH) staining revealed the morphology and distribution of amacrine cells were similar between affected and control retinas but in older *rge* birds, there was an increased density of TH positive dendrites. Staining with antibodies against opsin and rhodopsin (found in rods) revealed an increased amount of rhodopsin immunoreactivity was present in the inner segments of *rge* retinas compared to controls. In sections from older *rge* birds, the rods appeared swollen with loss of the normal architectural organization and rhodopsin immunoreactivity was mislocalized to the outer nuclear layer and outer plexiform layer. Mislocalization of opsin is a common finding in retinal dystrophy models (Gao et al., 2002; Nishimura et al., 2004; Rohrer et al., 2005; Beltran et al., 2006). A panel of antibodies to various glial cell and phagocyte components revealed that *rge* retinas contained many activated glial and microglial cells and that phagocytosis was occurring. Staining for synaptic vesicle protein 2 (found in synaptic vesicles) confirmed the disorganization of the OPL found ultrastructurally in that *rge* retinas lacked the normal organized stratification of the OPL (Montiani-Ferreira et al., 2005).

#### 1.7.5. Vision testing

In addition to functional testing like the ability to evade capture and peck at food particles (somewhat subjective), the functional vision of the *rge* birds was also evaluated using an optokinetic device to more objectively characterize the loss of vision as they aged. This device consisted of a drum lined with black and white bars of varying widths that revolved around the chicken being tested. A positive result consisted of the chicken



following the bars as they moved from side to side. The *rge* chicks showed decreased acuity, which was worse in dim lighting. Intriguingly, some chicks had positive responses to the optokinetic device only when wide stripes were used (indicating reduced visual acuity) long after they were no longer able to peck at food particles (Montiani-Ferreira et al., 2003).

#### 1.7.6. Electroretinographical characteristics

The *rge* chicken has been evaluated electroretinographically using short flash electroretinography. Initial electroretinographic work done in the UK reported the ERG waveform of the affected chicks had reduced amplitudes (Curtis et al., 1988), but upon further examination at MSU, this was found to be incorrect for bright stimuli in the younger birds. Preliminary studies have shown that young affected birds have an elevated response threshold (require brighter stimulus intensities to elicit a response), similar photopic and scotopic waveforms, a decrease in oscillatory potentials and most intriguing, a supernormal b-wave amplitude in response to brighter stimuli (Figure 1.16). In a short flash electroretinography intensity series protocol, the *rge* a-waves showed decreased amplitudes and increased latencies to all flash intensities. The b-waves of the *rge* chicks demonstrated higher thresholds, but in response to brighter flashes had greater amplitudes when compared to control chicks, thus it was termed a “supernormal” b-wave. Figures 1.17 and 1.18 contain compiled a- and b- wave amplitudes and latencies in 7 day old *rge* and control birds. There was also evidence that the rod photoreceptors were affected early on in the disease, which correlated with the results of the optokinetic testing in which the *rge* birds had decreased visual acuity in dim light. The ERG

responses of affected birds slowly deteriorate over time but this slow decline does not correspond to functional vision loss; ERG responses are still recordable months after the birds no longer have functional vision. This is unusual among the other chicken retinal dystrophy models and models in other species in which ERG responses are extinguished concurrently with vision loss (Montiani-Ferreira et al., 2007).

**Figure 1.16.** Representative ERG responses from a control and an *rge* chick. Responses from a control (A and B) and an *rge* mutant (C and D) chick at 7 days post hatch under dark-adapted (A and C) and light-adapted (B and D) conditions. Note that due to the cone-dominated retina that the dark-adapted and light-adapted ERG tracings of the normal chick are similar at the higher intensities. Also there is a diminution of the b-wave with increasing stimulus intensity due to a photopic hill effect. The ERG responses of the *rge* chick are quite different from the control. As with normal chicks dark- and light-adapted responses are similar (although the light-adapted amplitudes are slightly lower). However, the response thresholds are elevated compared to the control. The shape of the ERG is quite abnormal: the a-wave tends to have a greater implicit time at the higher flash intensities; the b-wave is smoother than in normal chicks, due to a lack of oscillatory potentials; and the b-wave amplitude is greater than that of the control (“supernormal”) at the higher flash intensities. Flash intensities for each panel (from top to bottom) were: -2.4, -2.0, -1.42, -1.19, -0.79, -0.39, 0.00, 0.39, 0.85, 1.4, 2.3 & 2.9 log cdS/m<sup>2</sup>. x-axis = time (mSec). Figure used with permission from Montiani-Ferriera PhD Thesis 2004.

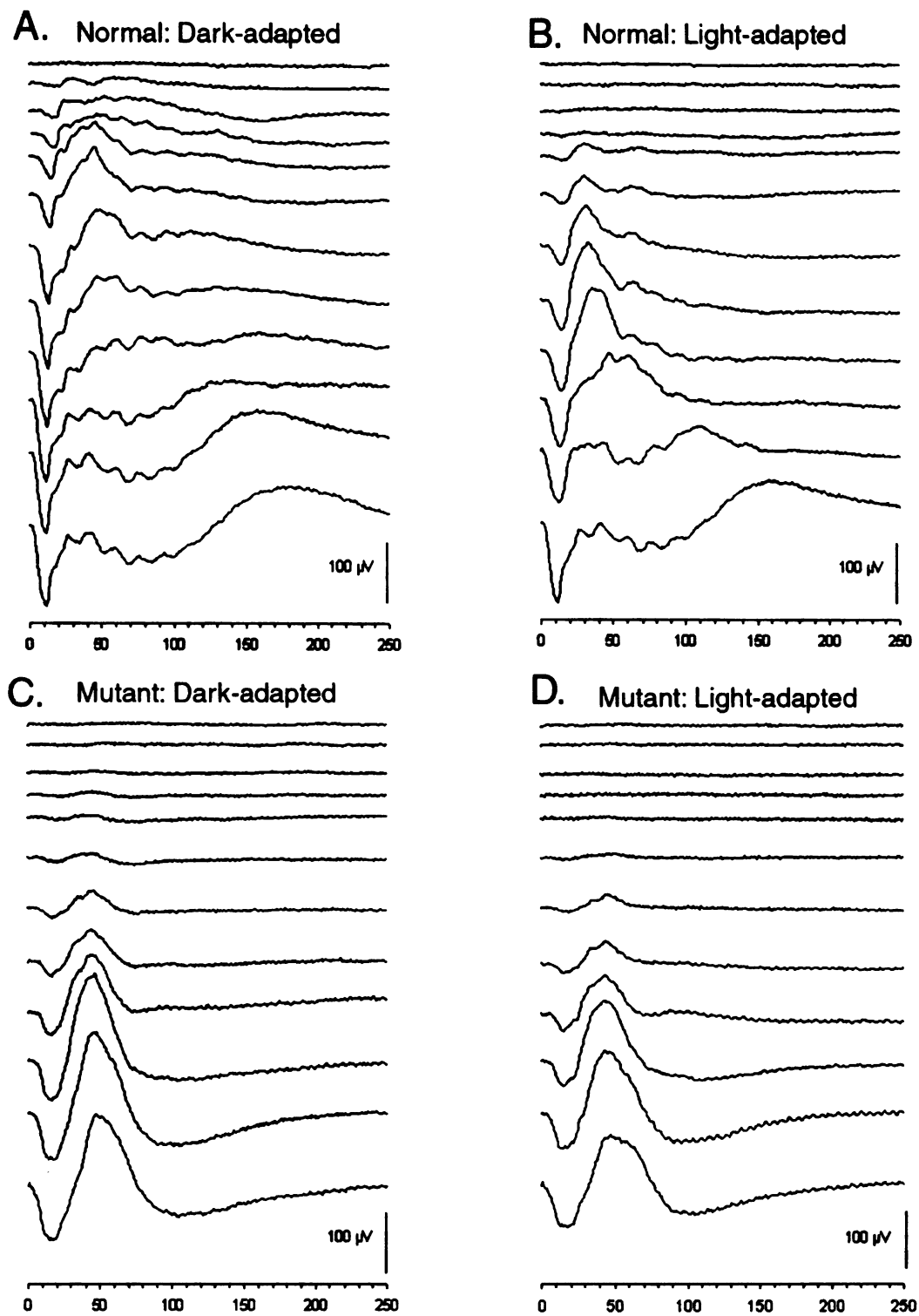


**Figure 1.16.** Representative ERG responses from a control and an *rge* chick.  
Figure legend on facing page.

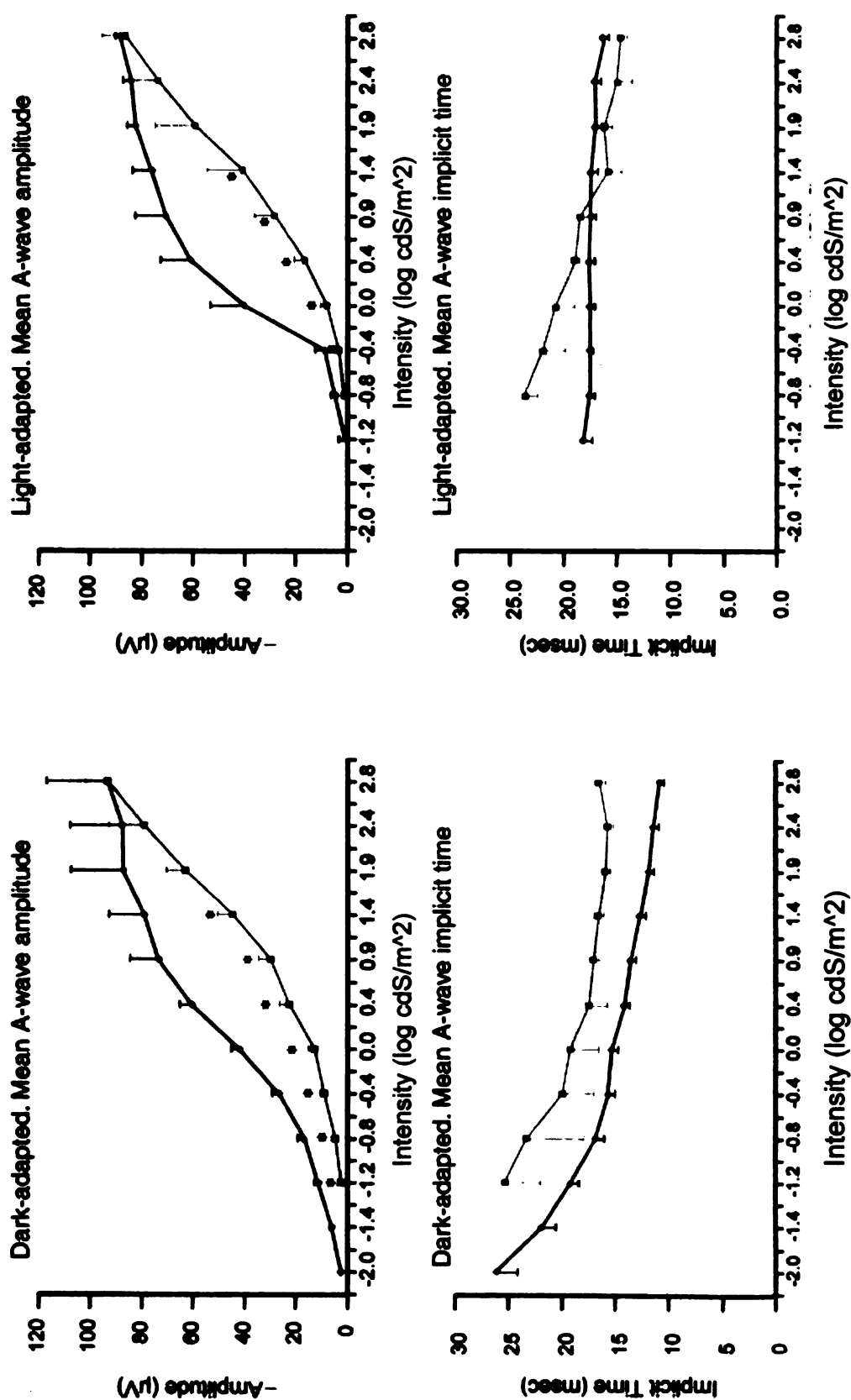


**Figure 1.17.** Light and dark adapted mean a-wave amplitudes and implicit times for 7 day old chicks. Control birds are represented by the black lines and affected birds are represented by the red lines. Error bars represent standard error of the mean. N=7 control and seven *rge* birds. Asterisk (\*) indicates that the amplitude of the *rge* birds was significantly different from the control birds. A  $P < 0.05$  was considered significant.

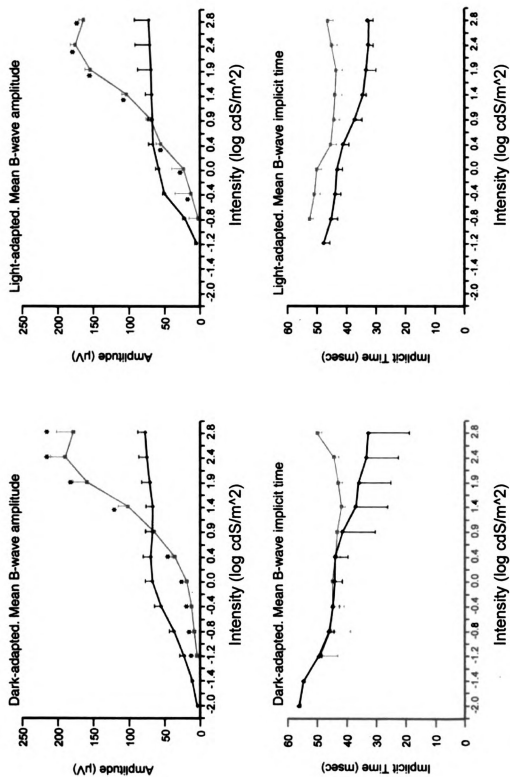


**Figure 1.18.** Light and dark adapted mean b-wave amplitudes and implicit times for 7 day old chicks. Control birds are represented by the black lines and affected birds are represented by the red lines. Error bars represent standard error of the mean. N=7 control and seven *rge* birds. Asterisk (\*) indicates that the amplitude of the *rge* birds was significantly different from the control birds. A  $P < 0.05$  was considered significant.

The supernormal b-wave is an unusual, but not unique, feature of the *rge* chick phenotype. This ERG abnormality has been reported in humans who have the enhanced S-cone syndrome (ESCS). The ERGs of these patients are described as having delayed b-waves that were supernormal in amplitude to brighter flashes but lower in amplitude and markedly delayed in response to weaker flashes (Gouras et al., 1983; Jacobson et al., 1990). The causative mutation appears in the *NR2E3* gene, which is a nuclear receptor that is responsible for determining photoreceptor cell fate, and causes an abnormally large number of S-cones to be formed in the retina and a reduction in rod photoreceptors (Haider et al., 2000; Haider et al., 2001). These S-cones are sensitive to short wavelengths of light. Therefore, these patients have enhanced responses to short wavelengths of light (i.e. blue) (Hood et al., 1995; Haider et al., 2000). This pathogenesis was excluded for the *rge* chicken by doing ERGs with different wavelengths of light. None of the *rge* responses of colored light flashes showed increased amplitudes compared to controls. Additionally, histopathology did not show obvious differences in rod to cone ratios (Montiani-Ferreira, 2004).

Another technique used previously with the *rge* chicks is pharmacological dissection of the electroretinogram. This technique involves injecting a pharmacological agent into the vitreous and performing pre- and post-injection electroretinograms. If the agent is known to affect only certain receptors, then its effect on the ERG can provide information as to what receptor/cell types are contributing to the various ERG components. This is potentially useful when one is trying to elucidate which cell types are being affected by retinal disease. Several agents were used previously to dissect the

*rge* ERG. APB (0.1 mM) was previously used and eliminated the b-wave of the control birds leaving only the a-wave, but did not affect the ERG of the *rge* chicks. PDA (5 mM) was also previously used to dissect the ERG. It truncated the a-wave (smaller amplitude and smaller slope of second half of a-wave) and increased the implicit time of the b-wave of the control birds, but did not affect the *rge* ERG (Montiani-Ferreira, 2004).

#### 1.7.7. Investigation of several candidate genes

In order to rule out the guanylate cyclase gene mutation that is responsible for the *rd* chicken phenotype, an RT-PCR was performed using primers specific to the guanylate cyclase gene. Products were obtained from this RT-PCR indicating that the *rge* mutation is different from the *rd* mutation (Montiani-Ferreira, 2004). Previous work has been done to find the causative gene responsible for the *rge* phenotype. A multipoint linkage analysis was used to map the gene to chicken chromosome 1. It was further localized to between *ADL0314* and *MCW0112*, an interval of 243cM, and represents 99% confidence limits. This region contains between 100 and 200 genes. Within that interval the gene was most closely linked to *LEI0071*. This position on chicken chromosome 1 shows homology with several regions in the human genome: 12p13, 22q13, 7q35 and 21q22 (Inglehearn et al., 2003). Inglehearn's group also examined and excluded several genes known to contain mutations causing human retinal disease: ABCA4, mutated in Stargardt macular dystrophy in humans (Allikmets et al., 1997); IMPDH1, the gene underlying the RP10 retinal dystrophy in humans (Bowne et al., 2002); and TIMP3, a gene mutated in humans with Sorsby's Fundus Dystrophy (Weber et al., 1994).



The interval was further refined by Hans Cheng's laboratory at the USDA Avian Disease and Oncology Laboratory in East Lansing, MI using different microsatellites to perform a linkage analysis. An additional microsatellite marker (*MCW0318* at ~80.5MB) was found to cosegregate with the *rge* gene (Hans Cheng, personal communication 2003). Additionally, it was concluded that human 12p11-13 exhibits the highest amount of conservation for that map region. One additional gene was sequenced and analyzed for mutations. *Vamp1*, also known as synaptobrevin, codes for a protein that is part of the SNARE protein complex (Sherry et al., 2001; Yang et al., 2002; Sherry et al., 2003). The gene was sequenced and no differences between the *rge* and control birds were found, making it unlikely to be responsible for the *rge* phenotype (Montiani-Ferreira, 2004).

### 1.8. Hypotheses

Based on the previous findings of the retinopathy, globe-enlarged chicken, the premise of this research was based on two basic hypotheses. One is that the gene responsible for the phenotype codes for a retinally expressed protein that is located on chicken chromosome one. The second is that both the rod and cone pathways of the retina are affected and specifically that the inner retina has abnormal function.

### 1.9. The scope of this project

The ERG work that had been done previously demonstrated that the *rge* chicks have several unique features (supernormal b-wave and persistence of ERG waveforms long after functional blindness), which warranted a more detailed analysis. Several

techniques were used to further evaluate the *rge* chick including additional pharmacological dissection using specific agonists and antagonists of various cells' responses in the retina, long flash ERG to separate the ON from the OFF responses and circadian ERGs to determine if *rge* chicks' retinas have normal circadian rhythms. The results of these more detailed tests will provide information about how specific cell types in the retina are functioning, which will hopefully aid in determining which cells in the *rge* retina are most affected, and thus could help to narrow the search for the causative gene.

Additionally, a positional candidate gene approach was used to select and sequence potential genes that could be responsible for the *rge* phenotype. The region between 78 and 82 MB on chicken chromosome 1 was evaluated and candidate genes were chosen. The first draft of the chicken genome was published in 2004 and greatly facilitated the molecular work (International Chicken Genome Sequencing Consortium 2004). Nevertheless, toward the end of the research period for this project, the Molecular Vision Group, a competing laboratory in the UK led by Chris Inglehearn, discovered the causative gene. The *rge* phenotype was found to be caused by an in-frame three base-pair deletion in a highly conserved region of GNB3, which is part of a guanine nucleotide binding protein found in the retina (Tummala et al., 2006). An aspartate amino acid residue is deleted in the affected birds. It is predicted that this amino acid deletion alters the tertiary structure of the GNB3 protein by abolishing  $\beta$  sheets in propellers 1 and 5 of the GNB protein. It was also hypothesized that this mutation would create an unstable protein susceptible to premature proteolysis. This was supported by

finding a 70% reduction in GNB3 protein immunoreactivity in retinas from affected birds compared to controls (Tummala et al., 2006).

GNB3 encodes the  $\beta$  subunit of cone-transducin, which is part of the heterotrimeric guanine nucleotide binding protein involved in phototransduction in cones. Transducin is coupled to phosphodiesterase (Peng et al., 1992), which means it is essential for phototransduction. Thus GNB3 plays an important role in regulating the response of the cone photoreceptors to light stimulation.

In light of Tummala et al's findings, immunohistochemistry was performed to localize GNB3 expression in the retina of normal chickens.

## CHAPTER 2

### INVESTIGATIONS OF CANDIDATE GENES

#### 2.1. Introduction

Previous work had mapped the *rge* locus to chromosome 1 (Inglehearn et al., 2003) in a region syntenic to human chromosomes 12p13 and 7q35. Microsatellite marker (MCW0318 at ~80.5MB on chicken chromosome one) was shown to co-segregate with the *rge* locus using the *rge* flock maintained at MSU (H. Cheng, personal communication, 2003). Using this mapping information, genes were selected using a positional candidate gene approach. Twelve genes flanking MCW0318 were chosen, directly sequenced and analyzed for polymorphisms (Figure 2.1 and Table 2.1).

Positional candidate genes were selected for their known expression in the eye or central nervous system, known involvement with retinal or neuronal function or dysfunction and cell signaling function. Table 2.1 shows a complete list of the genes, their locations on chicken chromosome one and in the human genome and a summary of their known functions. The chicken genome (initially the February 2004 assembly) located on the University of California Santa Cruz's Genome Browser website was used to identify genes that mapped to the region flanking MCW0318.

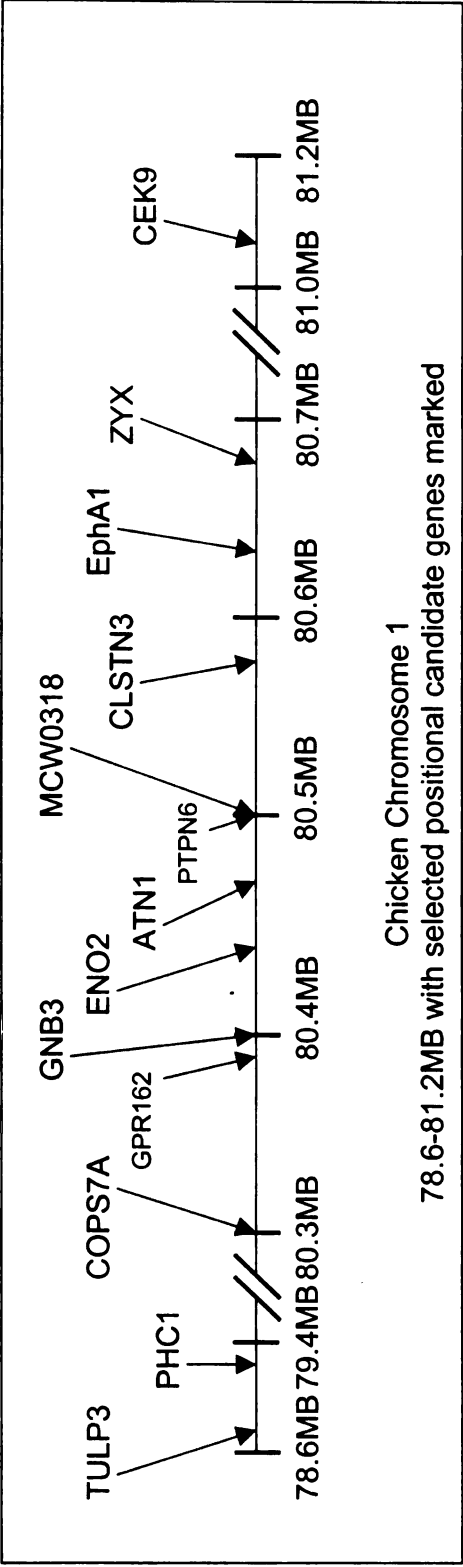


**Figure 2.1.** Area of interest on chicken chromosome one. This is an illustration of the locations of the 12 genes from chicken chromosome one that were investigated for this project. The microsatellite marker, MCW0318, is located roughly in the middle of the interval and is actually found within the PTPN6 gene. Note distances are not drawn to scale. Information obtained from the chicken genome v2.1 (May 2006), as displayed on the UCSC Genome Browser (<http://genome.ucsc.edu/>). Abbreviations as follows: TULP3 – Tubby-like protein 3; PHC1 – polyhomeotic like-1 protein; COPS7A – COP9 signalosome complex subunit 7a; GPR162 – G protein-coupled receptor 162 isoform 2; GNB3 – guanine nucleotide binding protein beta subunit 3; ENO2 – enolase 2; ATN1 – atrophin 1; PTPN6 – protein tyrosine phosphatase non-receptor type 6; CLSTN3 – calsynenin 3; EphA1 – ephrin receptor EphA1; ZYX – zyxin; CEK9 – chicken embryo kinase 9.

Gene	Name	Location	Function
TULP3	tubby like protein 3	78,730,993-78,743,271 (chr12: 2,870,331-2,918,930)	role in maintenance and function of neuronal cells during post-differentiation and development (TULPs implicated in retinitis pigmentosa)
PHC1	polyhomeotic-like 1 protein	79,288,028-79,307,972 (chr12: 8,958,583-8,985,325)	regulator of Hox genes
COPS7A	COP9 signalosome complex subunit 7a	80,303,031-80,306,162 (chr12: 6,703,482-6,711,289)	regulator of the ubiquitin (Ub) conjugation pathway, and phosphorylation of many proteins
GPR162	G protein-coupled receptor 162 isoform 2	80,383,860-80,387,594 (chr12: 6,801,224-6,806,844)	G protein coupled receptor of unknown function
GNB3	guanine nucleotide binding protein beta subunit 3	80,406,295-80,410,396 (chr12: 6,819,636-6,826,817)	G protein beta subunit, cone beta-transducin important in cone phototransduction
Eno2	enolase 2 (gamma neuronal)	80,444,835-80,454,069 (chr12: 6,893,875-6,903,120)	an enzyme of the glycolytic pathway catalyzing the dehydration reaction of 2-phosphoglycerate
ATN1	atrophin 1	80,475,851-80,482,670 (chr12: 6,913,353-6,921,743)	involved in neurodegenerative disease
PTPN6	protein tyrosine phosphatase, non-receptor type 6	80,498,126-80,507,549 (chr12: 6,930,763-6,940,740)	hematopoietic cell development, implicated in "moth eaten" mouse phenotype, which (among other problems) has a retinopathy
CLSTN3	calyculin 3	80,570,723-80,583,166 (chr12: 7,174,237-7,201,985)	postsynaptic membrane protein that is expressed at the highest levels in GABAergic neurons
EphA1	ephrin A1	80,635,033-80,664,753 (chr7: 142,798,328-142,816,107)	ephrin receptors and their ligands are associated with mediating developmental events, particularly in the nervous system and specifically the retina
ZYX	zyxin	80,670,676-80,682,092 (chr7: 142,788,482-142,798,324)	regulator of actin polymerization
CEK9/ EphB6	chicken embryo kinase 9, ephrin receptor B6	81,087,980-81,143,381 (chr7: 142,262,914-142,278,967)	tyrosine kinase involved in regulating cell adhesion and migration

**Table 2.1.** Genes examined in this investigation. The table includes their commonly used abbreviations, their full name, locations on chicken chromosome one and in the human genome (in parentheses) and a brief description of their functions. See text for references to function explanations. MCW0318 is located within the PTPN6 gene. Numbering is as used on UCSC Genome Browser website ([www.genome.ucsc.edu/index.html](http://www.genome.ucsc.edu/index.html)) chicken genome v2.1 (May 2006), human genome (NCBI Build 36.1, March 2006).

### 2.1.1. Background information for the chosen genes

TULP3 (Tubby-like protein 3) is a member of the tubby multigene family, which also contains TUB (tubby), TULP1 and TULP2. It is a small gene family that plays an important role in maintenance and function of neuronal cells during development and post-differentiation (Ikeda et al., 2002). Additionally, tubby-like proteins might function as heterotrimeric-G-protein-responsive intracellular signaling factors (Carroll et al., 2004). TULP1 mutations cause some forms of retinitis pigmentosa in humans and the gene is abundantly expressed in the retina (Heikenwalder et al., 2001). An expressed sequence tag (EST) for TULP3 (EST DR429568) was isolated from whole eye mRNA extracts, supporting its possible role in the retina. At the time it was chosen, its exact chromosomal location in the chicken was unknown, however it was known that it mapped to chromosome one of chicken and was on the syntenic region of chromosome 12 of human. At the time this dissertation was written, its location had been assigned (see Table 2.1 for details).

PHC1 (polyhomeotic-like 1) is a member of the polycomb group (PcG) of gene products, which form multimeric protein complexes and contribute to anterior-posterior specification via the transcriptional regulation of Hox cluster genes (Isono et al., 2005). This gene was selected in an attempt to establish a left-hand boundary for the *rge* interval.

COPS7A (COP9 complex subunit 7a) is a subunit of the COP9 signalosome, which is a multiprotein complex of the ubiquitin-proteasome pathway necessary in eukaryotic development (Schwechheimer, 2004). It is widely expressed in many organs

in the chicken including the cerebrum, cerebellum and hypothalamus/pineal gland (EST BU274813, CD215816, BU345751). It has many functions and is associated with both a target for kinase activity and also associates with and coordinates activity of kinases (Harari-Steinberg and Chamovitz, 2004).

GPR162 (G protein-coupled receptor 162 isoform 2) is a recently characterized protein in the Rhodopsin family of G protein-coupled receptors. It is found in many human tissues including in the brain and eye (EST DA356952.1, BM665884.1) and orthologues have been found in other species including chicken (Gloriam et al., 2005).

Enolase is an enzyme of the glycolytic pathway catalyzing the dehydration reaction of 2-phosphoglycerate (Pias et al., 2005). ENO2 (gamma neuronal enolase 2) is found in the interval of interest on chicken chromosome one and was thus chosen. Additionally, auto-antibodies to alpha-enolase have been associated with an acquired retinopathy (Magrys et al., 2007). Messenger RNA for ENO2 was found in extracts in whole chicken eye (EST DR427176).

ATN1 (atrophin 1) is a gene that is associated with dentatorubral pallidoluysian atrophy, which is a rare neurodegenerative disorder characterized by cerebellar ataxia, myoclonic epilepsy, choreoathetosis, and dementia. The disease is reportedly caused by the expansion of a trinucleotide repeat within this gene, and the number of repeats has been correlated with the severity of the disease (Ikeuchi et al., 1995). The protein is expressed in human brain and eye (EST CD671073.1, AA985328.1).

A deficiency of PTPN6 (protein tyrosine phosphatase non-receptor type 6) is a phosphatase that has been associated with the "viable motheaten" phenotype of mice. This phenotype is associated with immune dysfunction, hyperproliferation of myeloid



cells, regenerative anemia and retinal degeneration. This protein is expressed in murine and human hematopoietic cells (Lyons et al., 2006).

The calsynenin protein family has been localized in the postsynaptic membrane of excitatory central nervous system (CNS) synapses. CLSTN 3 (calsynenin 3) has been found expressed at the highest levels in GABAergic neurons of the nervous system (Hintsch et al., 2002). Its expression has been documented in chicken eyes (EST DR424960).

Ephrins and ephrin related receptors are receptors in the protein-tyrosine kinase family, which have been implicated in mediating developmental events, particularly in the nervous system and specifically the retina (Mann et al., 2004). Both EphA1 (ephrin receptor EphA1) and CEK9 (chicken embryo kinase 9, or ephrin receptor B6) are receptors whose genes are found in the interval of interest on chicken chromosome one. Additionally, expression of CEK9 has been found in both the cerebrum and cerebellum of chicken (EST BU272681, BU353591).

Zyxin is a zinc-binding phosphoprotein that concentrates at focal adhesions and along the actin cytoskeleton (Hoffman et al., 2006). It has been associated with actin assembly at the tip of nerve growth cones during filopodial protrusion (Jay, 2000). It has been found in the chicken central nervous system (EST BU273767.1).

GNB3 is the beta subunit of the guanine-nucleotide binding protein (beta-transducin) of cone photoreceptors. It is an important signaling protein of cone phototransduction (Peng et al., 1992). During screening of the selected positional candidate genes another research group discovered a mutation in the gene coding for GNB3 that is responsible for the *rge* chick phenotype (Tummala et al., 2006). At that

point, further screening of candidate genes was stopped. We then developed a PCR restriction enzyme test to allow rapid genotyping of birds within our *rge* flock. We also obtained an antibody to GNB3 and used it to localize GNB3 expression within the normal chicken retina.

## **2.2. Materials and methods**

The published chicken genome was used to select candidate genes using a positional candidate approach from the regions flanking the microsatellite marker MCW0318 (~80.5MB) and twelve genes were chosen. Refer to Table 2.1 for the genes, their unabbreviated names, locations and functions. The strategy used was to screen each gene by sequencing the coding region and intron/exon boundaries and analyze the sequences for polymorphism.

### **2.2.1 Design of primers**

The published sequence of each gene was obtained from the University of California Santa Cruz's genome browser ([www.genome.ucsc.edu/index.html](http://www.genome.ucsc.edu/index.html)). Intronic primers were designed using Integrated DNA Technology's PrimerQuest program (based on the Primer 3 program, located at <http://www.idtdna.com/Scitools/Applications/Primerquest/>) to amplify each exon and intron/exon boundary of each gene. Primers were purchased from Integrated DNA Technology (Coralville, IA) and were generally 24 bp in length and had melting temperatures between 55 and 60°C. See Table 2.2 for a list of the genomic primers and their locations on chicken chromosome one.

Table 2.2. Legend follows table (see below)					
Gene	Exon #	Forward Primer	Reverse Primer	Product Size (bp)	Position in Genome
TULP3	1	GGAGTCTCTGGTCTGATGTTGGTT	TCTGGAACAAATTTCAGTCTCCCTGCT	506	78736109-78736614
TULP3	2	AGCTCAGAAAAGTGATATAGCACAGA	CTCTCCGCCCATCATGTTCTCTTT	493	78738293-78738785
TULP3	3	CAAGAGGTCTGTATCACACTAAGGC	GGATTACAAGCAGAGGAGTCTTGAAA	405	78740269-78740673
TULP3	4	GGCACTGACTCTCTGGCA	CACAGCAACACAGGTGACCATCTA	314	78743020-78743333
PHC1	4	ATTGGCAGGGACTATCTGGGTGTT	TAGAAGCTGTGTTTCCCTGGCTGA	567	79294840-79295406
PHC1	8	CTTCAGTGTCTCCATGGGCTGTTT	AGGAGCATGGACTTGGGAAAACAGA	811	79299002-79299812
PHC1	9,10	ACCTCAGTGTCTCGCAGTGCTTT	ACACAGTGCATCTTTCCTCGCTA	1096	79301777-79302872
PHC1	11	TAGCGAGGGAAGATGCACGTGTGT	AGGCGAGGAAGAAAAGTCAAGTCCA	511	79302849-79303359
COPS7A	4,5	CATTATTACCTTGGACTGCCACCC	CCTGAATACACATAAGGCAGTGGC	742	80304585-80305327
COPS7A	6	GTGCAGCTCTTGATCTGAAGCACA	GGGCTCTCAACACTGTGGCTTATTT	825	80305427-80306251
GPR162	1	ACTCACATCCTCATGGCAGCAGTA	TGGCTGGTGGATGGAAGATGGA	775	80383973-80384747
GPR162	2	CTGTGTCTCTTGTGTTGTGCCTT	TGCTGTGTCTTTTCGCTACGGTTTG	1511	80385194-80386704
GPR162	3	CAAAACCGTAGCGAAAGACACAGCA	ATGGAGAAGGAGGCAGGCAATGAA	571	80386681-80387251
GPR162	4	GAGACAGCATCAGAAAACATTTCAGTGCC	TGCTGCCTCCCAGATACACTAACA	506	80387787-80388292
ENO2	1	AGAACAGGAGGGAAGCTCCCAT	TCAGCCTAACGTAGCTGCAGTTCT	851	80447452-80448302
ENO2	2,3	AGACAGATGCATGAGGGCTTTTCCT	AGCAGCACTACATCTGTCAACCCCA	611	80448704-80449314
ENO2	4	TGAGATGGACGGCACAGAGAACA	TTACAGAAGCTGGCCCAACGACTTT	597	80450274-80450870
ENO2	5	AGTCCCTCTCCAGTTGTTTGCCACT	AAACTTTCCCTAGGAAGGCCCTGT	619	80451199-80451817
ENO2	6,7	ATCAGACTCACGTTGGCTCCTTCT	TTACAGCAGCTGCCACTCTAATACC	762	80451769-80452530
ENO2	8,9	GGTATTAGAGTGGCAGCTGCTGAA	TACTTTACCTCTGCACCTTGCCCT	469	80452506-80452974
ENO2	10	AGGCAAGGTGCAGAGGTGAAAGTA	AGAGTGATTCCGATGCCCAACAAGA	533	80452932-80453464
ATN1	1,2	TTCTTGTCTCCCTTTTCAGTGCCCA	TGGTCTGTGTCTGTGATTCCCAA	634	80475725-80476358
ATN1	3	ATGGTCTGCAACAGAGATGGTGGT	TGAGGTGGCAGAGCTATCAAGCAA	336	80476521-80476856
ATN1	4	GGCAGCAAGAGAACTGCCAAATGA	AGCATGGGTGGAAGTGGAAAGAAGA	607	80477307-80477913
ATN1	10,11,12	GCTGCAGGTATCCTGATGCTGTTT	AGGATAGGAGGTCCCAATGACCACA	909	80479762-80480670
ATN1	13,14	GGGCCACACTGCTTTCACATGAAAT	TGGAGCCACGCACATATAGGAAAA	909	80481328-80482236
ATN1	15	AGCTTGATGGGTTAGAAGTGCAGC	ACCTTTCAGGTCCATCACTGGTGT	434	80482449-80482882

<b>Table 2.2. Continued</b>					
PTPN6	1	ACCAAGGTTATCCATGCTGTTGCC	ACCATGGAAGTGCAGCAAAACCATC	494	80498565-80499058
PTPN6	2	TGCAGTTCATGGTAGGAGGTGAT	AAGCTGAAAGCTCAATGCAAGGG	786	80499045-80499830
PTPN6	3,4	TGGATCTCACTTGGTGCTTTCCCA	TCTTAGACACACCTCGTCTGCTT	719	80501601-80502319
PTPN6	5,6	TTCTGCAGGCTTCCATCCACTAA	AGTAGGTGGTCACTCAGAGGAACA	924	80502566-80503489
PTPN6	7	GCACCATCCAATTATCCATCCCTG	TGATGCTTTCCTCCTTCCCTCCCT	638	80503193-80503830
PTPN6	10,11	TGCCTTCTGCCTGTCTCCACTTA	GCAGCTGTTTCATCACAGCCACAAA	766	80504419-80505184
PTPN6	12	GCCTATTCTGGTGCAATGCAGGT	TCAGGGAAGGCGAAAGCCACATTA	580	80504975-80505554
PTPN6	13	TGGTCTATGGCAGCTGCTGATTCT	GTGGTTCAACAAGAGGGTTGCACTT	607	80505491-80506097
PTPN6	14	TTGGTGCCTCCAGAAATGTGTTGC	TAAACCAAGCCAGCAGGTGGAAGA	661	80506131-80506791
CLSTN3	2	CTCTTCCCAGTCTCTCTTAGCCTT	CTGGAACAAAGGTTTAGAGGCGA	405	80570569-80570973
CLSTN3	3	AGTGGTAATGAGGGAGAAAGGAG	GTAAGGCATCACTCAGACTCAGCA	1142	80571670-80572811
CLSTN3	4,5	AGGTGGTGTATGGCTCCTAATCA	GGACAGAGTAGATTGACATAAAGGG	780	80572993-80573772
CLSTN3	7,8	TAGAAAGGCATTGTCCCTGAAGGTG	CTGGCTCTCCCTTCACTTCCATTT	622	80575424-80576045
CLSTN3	9	GCTGCCTAAGTTTCAAAAGGATGC	TGGATGGACAAGATCAAGGAGCTG	516	80576724-80577239
CLSTN3	10,11	CTGTTGCTGTGCTGTTGCTTTGCTC	TCCCTAGGACCTTAGGAAAACCACT	832	80577736-80578567
CLSTN3	12	GTGAAATGTTGGTGGAACTTGGG	AATACCCAACTGACCCCTGTCTTG	684	80578774-80579457
CLSTN3	14,15	TTAACAGGGCACTTTCCCTTCCAC	ACAGTTTGACCCATACTGCAGACC	790	80580861-80581650
CLSTN3	16,17	AGTAAGAAGGAATCACCTGTGCCC	ATCACTGCTGTCACTCATCGTCCCTC	574	80582766180583339
EphA1	1	TCTCCACCCACTTGCCTTGATCTT	ATACAAGCAGACCAGGCTGTTTCC	358	35264486-35264843
EphA1	2	TCTTCTCTCCAGCCATGCTTTCTGA	TCCCGAATCCACTCCTTTGTGTCT	656	80634867-80635522
EphA1	3	TAACAGTGGCAGGGAGAGTGGAA	ATCAGAGAGGGCACTTAGGGCAAA	820	80646116-80646935
EphA1	4	TGGAAGCAGGAGTTTCATAGCCAGT	ATGAAGCCCAAGAAGGAGTGGAGA	835	80648221-80649055
EphA1	5,6	ACTACTCCATCTTGTCTCTGCCACT	GTGGATTCAATAGCTCTTGTGGGT	984	80653512-80654495
EphA1	7,8	TGTGGAAGAGAAAGGTGTGGCAGT	CCCTGATGACAAGGAATGCAGGAA	679	80655023-80655701
EphA1	9	TCAAAATCTGGTCACTCTGCTGCCT	ACTGCAACATGCTGGTCTTCCCTCT	375	80658500-80658874
EphA1	10	AGAAAGAGCTCTGCACCTACCCAGA	AGGGCAAAGCTACAGAAGCAGAGA	381	80659283-80659663
EphA1	11,12	TCTCTGCTTCTGTAGCTTTGGCCT	TTTCCCAACATAGCCTCCCTGACA	594	80659640-80660233
EphA1	13	TGTCAGGGAGGCTATGTTGGGAAA	ACTGCCAAAGACAGCACTCTGGAT	631	80660210-80660840
EphA1	14	ATCCAGAGTGTGCTCTTTGGCAGT	GCTCACAGCAAGGCTGTCTTCAAA	900	80660817-80661716

Table 2.2. Continued					
EphA1	15	GGCATCAGTATCTTACACCCACAGCA	CCCAAGTCAAAAGCTTGGCCACATT	580	80661808-80662387
EphA1	16	GCCCTGAATGGCAAAATGGAGCTAA	CTGCTCACAGAACATTCAGCCGT	573	80662429-80663001
EphA1	17	TCTCCTTCGGTGTGTGACACTT	TGCTCTCTTTCGCTCTGATAGGAGT	761	80662843-80663603
EphA1	18	AGTCACAAAGGTGGGAGAAATCCAGT	ACTCTAGAGCAGAGGTCCCAACAT	1316	80664443-80665758
ZYX	1	TGTGAGCCATTGCTCTGATCCAGT	AGGCAATGGTGGAGATTTGGTCCT	522	80671416-80671937
ZYX	2	TACCATCCTCAGTGTCTCACCTGT	CAGGAAGCATTTGGACAAATGCCCT	715	80672203-80672917
ZYX	3	AGTGCTTCACCTGCTTCAAGTGTG	ACAGCACTGTCTCATCTTTCCCA	747	80672492-80673238
ZYX	4,5	TGTTGAGAGGCAGAACTAGGGACA	ACAGGTGAAGCACTGAGGATGGTA	848	80672894-80673741
ZYX	6	TCTTACCATTGTGGGTCTGGGACA	TGTCCCTAGTTCTGCCTCTCAACA	762	80673718-80674479
ZYX	7	ACGTGGAGCAGCAGGAGTAAGAAA	ACTTATGCTGGTGCATAGGGTGGT	864	80675650-80676513
ZYX	8	TTAGTTGCCGTTCCCTCCTTCCCTGT	CCATCAGGGTGAATGTTCCCTGCAA	780	80677997-80678776
CEK9	1	TATCAAGTTCTGTCCACGCCCTCCT	GTCTTGCTGTTCTTTGGCCTCAGCA	954	81087879-81088832
CEK9	2	AGTCCATGCTGTGCTGTTCTCTCT	AGTGTGGCTGATTTCTACACAACCC	542	81092919-81093460
CEK9	3	CATCGTTCTACTGGCATCTGACCT	CCCAAGGTCCCTCAACTCATCAA	828	81094199-81095026
CEK9	4	AGTGCCCTTAGGCCAGTTTCCTTT	ACAGACAGCTTGCAAAAGCAGAAAG	531	81097901-81098431
CEK9	5	TCACAGGAGAGGGACTGCATTGTT	AGAAATTTGGTCCACTTCAGGCCAC	728	81099652-81100379
CEK9	6	AGGAAGGAAAGCACTGGAGAAAGCA	TCTACACTGCTCTTCTAGTGACCC	642	81101934-81102575
CEK9	7	TCCTCTCCTCCTCTTCTCCTCTTT	TACACTCTGCTCCTGCTGAAAAGGT	495	81102935-81103429
CEK9	8	AGCGAGGGAGTGACTTAACCCCTTT	AGCTGGGAAATGCAGATGGACAGA	439	81104374-81104812
CEK9	9,10	AGGTATTAGGTGCCATCGGAGAGA	TGCTGTCTGACCCAAAGAGCTACA	1073	81109155-81110227
CEK9	12	ACACCAGCAGCACGAGTTAAATGC	AAGAGAAGGAAGCCAGGGATGTT	396	81114341-81114736
CEK9	13,14	AGGTCTGTCTTCTATGTCTGGTGC	AGTTTCCAACTGCATTCCTGGCTC	996	81126600-81127595
CEK9	15	GACTGTGCTTACACTTTGCCTGGT	AGTCTTGTGTATTCCAGCCTCCCT	476	81128067-81128542
CEK9	16	AAGAAATGAAGGTGATGGGTGGGA	ATCCCGTGACGTCTGTAGAACAGT	822	81142749-81143570

**Table 2.2.** Genomic primers used to sequence the candidate genes. The table includes the gene, the exon number, the forward and reverse primer, the length of the expected product and the location on chicken chromosome one (based on version 2.1 of the draft chicken genome assembly from May 2006). The primer set for exon 1 of EphA1 maps to 35264486-35264843 using version 2.1 of the draft chicken genome assembly; however, in version 1.0 (February 2004), it mapped just upstream from the primer set for exon 2 of EphA1. Several exons of some of the genes were never sequenced because the work was discontinued when Tummala et al discovered GNB3 was the responsible gene.

### 2.2.2. DNA isolation

The DNA from one affected and one carrier bird was isolated from whole blood using the Puregene DNA purification system (Gentra, Minneapolis, MN) and used in the reactions. Whole blood was collected from the jugular vein of the birds and used to isolate DNA. The exact contents and concentrations of the Puregene kit's solutions were proprietary and not possible to provide.

- 40  $\mu$ L of whole blood added to 6 mL of Cell Lysis solution and vortexed
- 2 mL of Protein Precipitation solution added and vortexed
- Centrifuged for 10 minutes at 2000 x g, supernatant poured into 10 mL of ice cold 100% ethanol and mixed until DNA pellet formed
- Centrifuged for 5 minutes at 2000 x g, supernatant discarded and 10 mL 70% ethanol added to the tube and mixed to wash the DNA pellet
- Centrifuged for one minute at 2000 x g, the supernatant discarded and pellet allowed to dry for 10 minutes
- 500  $\mu$ L of DNA hydration solution added to pellet and DNA allowed to rehydrate over night at room temperature
- DNA concentration established using a NanoDrop (ND-1000 Spectrophotometer, NanoDrop Technologies, Wilmington, DE)
- If needed, the sample was diluted to approximately 100 ng/ $\mu$ L and then it was stored at -20°C until needed.

### 2.2.3. PCR amplification

The polymerase chain reactions (PCRs) were carried out using the *Taq* DNA Polymerase kit (Invitrogen, Carlsbad, CA). Each reaction included the following components:

- 5  $\mu$ L of 10X bovine serum albumin
- 5  $\mu$ L 10X PCR buffer (200 mM Tris-HCl (pH 8.4), 500 mM KCl)
- 5  $\mu$ L 2 mM dNTP's
- 1.5  $\mu$ L of 50mM MgCl
- 1.5  $\mu$ L (15 pmoles) 10X forward primer
- 1.5  $\mu$ L (15 pmoles) 10X reverse primer
- 1  $\mu$ L of template DNA (~100 ng)
- 0.25  $\mu$ L of *Taq* polymerase
- 29.25  $\mu$ L of molecular grade water for a total reaction volume of 50 $\mu$ L

PCR conditions were optimized for each primer set, and in general were close to the following: 94°C for 5 minutes, (94°C for 30 seconds, 57°C for 30 seconds, 72°C for 30 seconds) 35 times, 72°C for 30 seconds and then held at 4°C. 5  $\mu$ L of PCR product was run on a 1% agarose gel with ethidium bromide for visualization in TAE (tris-acetate-EDTA) buffer. Gels were documented with an Eagle Eye System (Stratagene, LaJolla, CA).

#### 2.2.4. Purification of PCR products for sequencing

##### 2.2.4.a. Sodium acetate and isopropanol PCR product purification

If the PCR product was robust and contained one single band, it was purified with isopropanol and sodium acetate.

- 4.5  $\mu\text{L}$  of 3 M sodium acetate added to the remaining PCR product (usually 45  $\mu\text{L}$  remained) and mixed by pipetting
- 31.5  $\mu\text{L}$  of 100% isopropanol added to the tube, mixed and incubated for 5 minutes at room temperature
- Centrifuged at 20,800  $\times g$  for 10 minutes, supernatant discarded and the pellet allowed to dry for 10 minutes
- 40  $\mu\text{L}$  molecular water added to the tube and the pellet allowed to resuspend for 24 hours at room temperature, then stored at  $-20^{\circ}\text{C}$  until needed

##### 2.2.4.b. Purification of PCR products cut from gel

When the PCR resulted in more than one product, the band of the predicted size was cut from the gel and the PCR product was isolated using the QIAquick Gel Extraction Kit (Qiagen, Valencia, CA) as summarized below. The exact contents and concentrations of the Qiagen kit's solutions were proprietary and not possible to provide.

- Band cut from gel under UV illumination, transferred to a 1.5 mL centrifuge tube and weighed
- 3 volumes of Buffer QG to one volume of gel were added to the tube and vortexed



- Tube incubated at 50°C for 10 minutes until the gel slice had dissolved
- The resulting solution was applied to the provided column in a clean microcentrifuge tube and then centrifuged at 20,800 x *g* for one minute
- Flow-through was discarded, an additional 500 µL of Buffer QG applied to the tube, recentrifuged for one minute and the flow-through was discarded
- 750 µL of Buffer PE (wash buffer) applied to the column (provided with the Qiagen kit) and allowed to incubate for three minutes at room temperature.
- Column and tube were spun again for one minute, the flow-through discarded and then centrifuged again for one minute
- Column placed into a clean 1.5 mL microcentrifuge tube, 30-50 µL of molecular grade water was applied to the column and allowed to stand at room temperature for one minute
- Column and tube centrifuged for one minute to elute the PCR product, which was stored at -20°C until needed

The purified products (whether sodium acetate purified or cut from the gel) were then run on a 1% agarose gel with ethidium bromide in TAE buffer again and the concentrations were estimated by comparison to a standardized DNA ladder. The products were then sent to Michigan State University's Genomics Technology Support Facility for direct sequencing using the appropriate primer (from those used to create the PCR product) to separately sequence forward and reverse sequences. The sequences were aligned and analyzed using Sequencher 4.0 (Gene Codes Corporation, Ann Arbor, MI). Differences between the affected and carrier sequences were recorded.

#### 2.2.5. Amplification of genes from retinal cDNA

Reverse transcriptase polymerase chain reaction (RT-PCR) was used with chicken retinal mRNA to confirm expression in the retina and to check for the possibility of alternate splicing. cDNA sequences for each gene were generated using mRNA extracted from wild type retinas (and carrier and affected retinas for GNB3) using a similar protocol for the genomic sequences (as far as primer design – except exonic primers were selected) and RT-PCR. Table 2.3 contains the primer sequences used for the cDNA amplification and sequencing.

**Table 2.3.** Legend follows table (see below)

Gene	Forward Primer	Reverse Primer	Product Size (bp)
PHC1	TCAGCCAAAGCTCTTGGGATTCTGT Chr 1: 79291731-79291754	TGAACCTGATCTGTGTCTGCATGG Chr 1: 79297276-79297296	642
PHC1	ACGCAGTCTGTTCTCCTTGGGAAT Chr 1: 79296115-79296138	TGGTGATGAATGGCAATCTGCTGC Chr 1: 79299311-79299334	830
PHC1	AGACTGTGGGCATGAACCTTACCA Chr 1: 79298837-79298860	TGACTCTGCCTTGCAGCTTATATGC Chr 1: 79302122-79302145	857
PHC1	ATGGCATCAACCTCTGCTTCCCTGT Chr 1: 79306654-79306677	TCTCCTAATGCCACGAGCCTTTGA Chr 1: 79307659-79307682	808
COPS7A	TCTTCCACCTGCTCACCATCTTCG Chr 1: 80303413-80303436	GCCCTTTGGCTTTGGAAGCTTCTTG Chr 1: 80305254-80305278	603
COPS7A	GTTAGCCGAGCCAAACACACAAA Chr 1: 80304784-80304807	TCCAAGCTTCTGTGATGCCCTACA Chr 1: 80305938-80305961	620
GPR162	TATCATTCATCTCTCCACCCTGC Chr 1: 80384229-80384252	TACCATTCTGTGCTTGCCTCGTCT Chr 1: 80388082-80388105	919
GPR162	ACAACAATCTACTGTGGTGGCTGG Chr 1: 80383842-80383865	ACCAAAGCCCAGACCTATCTTGCT Chr 1: 80384315-80384338	497
GNB3	AGATCCTGATTCAAGGTTGCCAC Chr 1: 80406258-80406272	TCTTCTGTGCTGCCCTGCTCAATGT Chr 1: 80408300-80408323	584
GNB3	TGTGCACTCTGGGACATTGAGACA Chr 1: 80408288-80408310	TGTGCTTGGCTGATGATGCTGTG Chr 1: 80410424-80410447	597
ENO2	ACCAGCACTTTCTCAGTCTCTCGT Chr 1: 80444868-80444891	AAGCTGGCAGGAAAGGATGAGAT Chr 1: 80450554-80450574	498
ENO2	ACAAGGCTGGCTACACAGACAAGA Chr 1: 80451899-80451922	TGATGTGGGAAAGAGCTGAAGGGT Chr 1: 80453209-80453232	657
ENO2	AACTGCCTCCTGCTCAAAGTCAAC Chr 1: 80452342-80452365	ACTGCACATGCTTCGGCATAACAAC Chr 1: 80453509-80453532	640
ENO2	ACCCTTCAGCTCTTCCCACATCA Chr 1: 80453209-80453232	TGTTGCTTTGCTGAGCGTTGACTG Chr 1: 80454003-80454026	805
ATN1	AGGTGACTGTAGTAATCCTCCTGGGT Chr 1: 80482104-80482615	AGGTTCAACAAGCACTGGATCGT Chr 1: 80479498-80479521	935
PTPN6	AAGGCACCTCTCCAGAAACAGAGT Chr 1: 80498148-80498171	TGAAGTGCTCCACAAGATCTGCCA Chr 1: 80502806-80502829	847
PTPN6	CCGTCTCAAAGTCAACCACATCAA Chr 1: 80502065-80502088	CGCATTTGGAATGCTCTCCTGCTT Chr 1: 80504949-80504972	859
PTPN6	ATGATAGTGAGGCTGTGCGTGAGA Chr 1: 80504841-80504865	CACACCATCACACACTGGCATA Chr 1: 80507484-80507505	1145
CLSTN3	CCGCTGTTTGCACTGGACAAAGAT Chr 1: 80570804-80570827	AGGCAGCAAGTCAATCTCTCCTGA Chr 1: 80575125-80575148	816
CLSTN3	AGGGCTGGAAACAAGAGGATTGAGT Chr 1: 80574496-80574517	TGTCATGAATGAGGGCAGGGTCAT Chr 1: 80575897-80575920	675
CLSTN3	ACTTCACCTCTGTGTGTGGATGA Chr 1: 80575294-80575317	AAGCGCAGGGAATTCATGTAAGCG Chr 1: 80578308-80578331	688
CLSTN3	TTGGAGAGCCGGAGGTTATTGAA Chr 1: 80577956-80577979	TTCTCTCATAAAGAGCAGCGCCA Chr 1: 80581125-80581148	722
CLSTN3	TATTTCTACACAGGTGGAGGCCAA Chr 1: 80579008-80579031	TTACCTGCTCTGCCCTCACAGTTT Chr 1: 80583285-80583308	777
ZYX	AGACTCTGCCAGTGCAAGTTGGTTA Chr 1: 80671593-80671616	ACAGTGGTCGGACAGCGTAGTTAT Chr 1: 80670711-80670734	905

<b>Table 2.3. Continued</b>			
<b>ZYX</b>	TATGCTCCACGCTGCTCAGTATGT Chr 1: 80672539-80672562	ACTCTGCTTCCACACTCTTACCCA Chr 1: 80671202-80671225	<b>747</b>
<b>ZYX</b>	ACCTCAGCCTCCCAATTTACCTA Chr 1: 80673952-80673975	ACACGCACTGTCTCATCTTTCCCA Chr 1: 80672492-80672515	<b>657</b>
<b>ZYX</b>	ACCCACAGAAGAAATTTGCACCCG Chr 1: 80678473-80678497	TGCAGTGGGTCTACGCATGTCTTT Chr 1: 80673500-80673524	<b>854</b>
<b>CEK9</b>	AGTATCGCAAGTTCACCTCCTCCA Chr 1: 81094865-81094888	AGGTGCTTGTGGTCTGTCCAACT Chr 1: 81088237-81088260	<b>870</b>
<b>CEK9</b>	AATTTGGAGAGGTGTGCTTTGGGC Chr 1: 81099360-81099383	GAGCAGATGGCTTGCGGATCATTT Chr 1: 81094469-81094492	<b>777</b>
<b>CEK9</b>	TGTCATCTGCAAGGAATGCCCAAC Chr 1: 81109684-81109707	AGGAACTCTCGACGCTGTTCATCA Chr 1: 81099272-81099295	<b>924</b>
<b>CEK9</b>	AGTGTCCAGCTGTGGTGAAAGGAT Chr 1: 81127028-81127051	AGGCCAAGACAGTGTGATGCTACT Chr 1: 81104640-81104663	<b>806</b>
<b>CEK9</b>	GCTCTGGCTGGTTTGCTTCTTTCA Chr 1: 81143172-81143195	CAGTTGTGCTTGCCTCTTCAGCAT Chr 1: 81126929-81126952	<b>692</b>

**Table 2.3.** cDNA primers used to sequence candidate genes. The table includes the gene, the forward and reverse primer, the length of the expected product and the location on chicken chromosome one (based on version 2.1 of the draft chicken genome assembly from May 2006).

#### 2.2.5.a. RNA Extraction

Retinas were collected from adult chickens, flash frozen in liquid nitrogen and then stored at  $-80^{\circ}\text{C}$  until needed. The RNeasy Mini-Kit (Qiagen, Valencia, CA) was used to isolate the RNA from the tissues. All reusable materials (mortar and pestle, spatulas, etc) were washed with RNase Away (Invitrogen Corp., Carlsbad, CA) and baked at  $200^{\circ}\text{C}$  for 24 hours to remove RNases. The exact contents and concentrations of the Qiagen kit's solutions were proprietary and not possible to provide.

- Frozen retina ground under liquid nitrogen in a mortar and pestle and then the powder was transferred to a microcentrifuge tube
- 600  $\mu\text{L}$  Buffer RLT added and the sample was mixed/disrupted using a 22 gauge needle on a 3 mL syringe
- Sample centrifuged at  $16,100 \times g$  for 3 minutes and the supernatant transferred via pipette to a clean tube
- 1 volume of 70% ethanol was added and mixed by pipetting
- Mixture placed on an RNeasy spin column in a clean tube, centrifuged for 15 seconds and the flow-through discarded
- 700  $\mu\text{L}$  of Buffer RW1 added to the column, recentrifuged for 15 seconds to wash the column and then the flow-through discarded
- 500  $\mu\text{L}$  Buffer RPE was added, recentrifuged for 15 seconds to wash the column again and the flow-through was discarded
- An additional 500  $\mu\text{L}$  Buffer RPE was added, column centrifuged for 2 minutes and the flow-through discarded

- Column transferred to a clean tube and then recentrifuged for one minute to remove any remaining Buffer RPE
- Column again transferred to clean microcentrifuge tube, 30  $\mu$ L of RNase-free water was applied to the column and then centrifuged 1 minute to elute the RNA
- RNA stored at -80°C until needed

The RNA was treated to remove DNA using DNase enzyme (Roche Diagnostics Corporation, Indianapolis, IN). Briefly, 1  $\mu$ L of DNase enzyme and 1  $\mu$ L of 10X Reaction Buffer (Roche – contents proprietary) with magnesium chloride was added per 8  $\mu$ L of RNA solution. This solution was incubated at 37°C for one hour and then stored at -80°C until needed.

#### 2.2.5.b. cDNA Synthesis

The DNA-free RNA was then used to create cDNA using the Fermentas First Strand cDNA Kit (Fermentas Inc., Hanover, MD). The exact contents and concentrations of the Fermentas kit's solutions were proprietary and not possible to provide.

- 2  $\mu$ L mRNA (of unknown concentration) combined with 0.5  $\mu$ g of oligo(dT)<sub>18</sub> primer and nuclease free water to reach 11.5  $\mu$ L
- Mixture incubated at 70°C for 5 minutes and then chilled on ice
- 4  $\mu$ L 5X reaction buffer for reverse transcriptase, 2 $\mu$ L dNTP Mix (10mM each), 0.5  $\mu$ L RiboLock™ Ribonuclease Inhibitor (20u), and then DEPC-

treated water to reach 18  $\mu$ L added to the tube and incubated at 37°C for 5 minutes

- 40 units of reverse transcriptase (M-MuLV Reverse Transcriptase) was added to the reaction, it was incubated at 37°C for 60 minutes, then 70°C for 10 minutes and then chilled on ice
- This cDNA was then stored at -20°C until needed

Primers were created as described previously and used to generate products, which were then sequenced and analyzed with Sequencher 4.0. Table 2.3 shows the cDNA primers. The cDNA sequences were used to verify expression in the retina and to check exon boundaries.

#### 2.2.6. Analysis of sequencing results

Using Sequencher 4.0, reading frames were determined and polymorphisms were noted, the majority of which were single nucleotide polymorphisms (SNPs). Nucleotide variations that resulted in amino acid changes were analyzed by comparing the deduced amino acid sequence with that of human or other available species and/or run through SIFT (Sorting Intolerant from Tolerant) (<http://blocks.fhcrc.org/sift/SIFT.html>) and/or Polyphen (<http://www.bork.embl-heidelberg.de/PolyPhen/>) programs. Aligning amino acid sequences across species was accomplished with the CLUSTALW program at the Multiple Sequence Alignment website (<http://align.genome.jp/>).

#### 2.2.7. Investigation of SNPs identified in candidate genes

Birds of known status (30 homozygous affected and 39 obligate carriers) were genotyped for one SNP from each of the genes ENO2, COPS7A and GPR162 using pyrosequencing at the USDA Avian Disease and Oncology Laboratory in Dr. Hans Cheng's lab. This was performed to assess whether the genes were in linkage disequilibrium with the *rge* status, indicating whether it was possible for the gene in question to be a candidate gene.

#### 2.2.8. Investigation of GNB3

GNB3 was also sequenced from retinal cDNA from wild type and affected birds as previously described to confirm Tummala et al's findings. Figure 2.2 is a schematic diagram of the GNB3 cDNA sequence with cDNA primers and mutation marked.



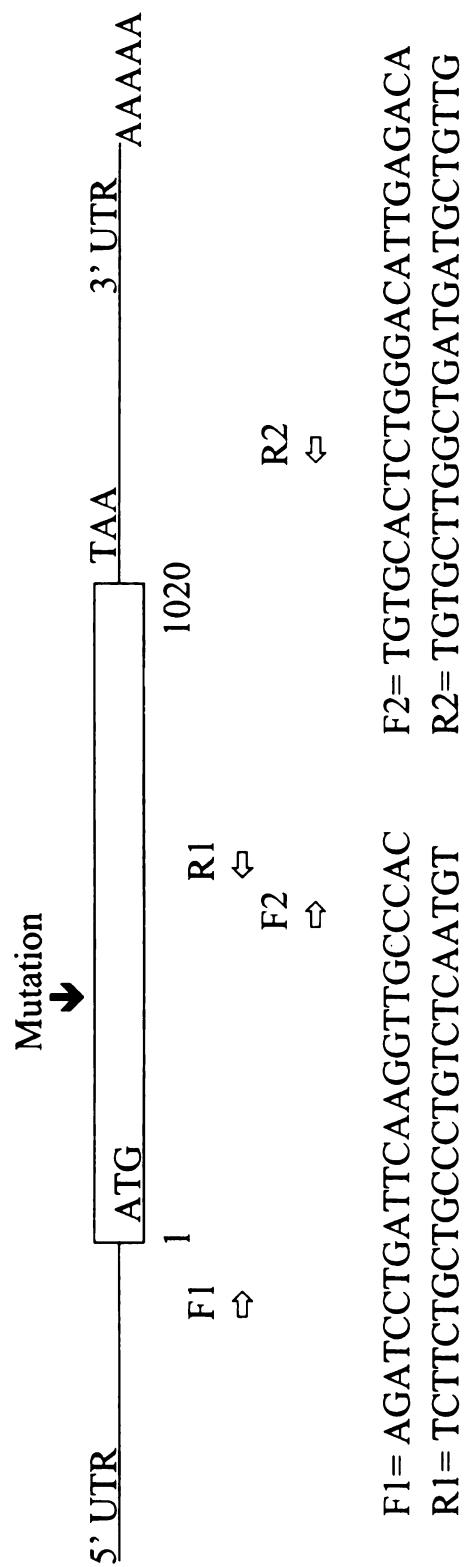


**Figure 2.2.** Schematic drawing of GNB3 cDNA with primers and mutation. The rectangle represents the translated region of GNB3. Abbreviations as follows: UTR – untranslated region; ATG – start codon; TAA – stop codon; F1 – forward primer #1; R1 – reverse primer #1; F2 – forward primer #2; R2 – reverse primer #2; AAAAA – poly-A tail.

#### 2.2.8.a. Development of PCR RE test to genotype birds for GNB3 mutation

A custom made computer program designed to develop mismatch restriction enzyme digest tests (Petersen-Jones 2003 unpublished) was used to create a restriction enzyme test for rapid genotyping of birds for the GNB3 mutation. As there were no restriction enzymes that could naturally be used in differentiating the normal allele from the affected allele, a mismatch primer was made that preserved a restriction enzyme cleavage site at the deletion site in the resulting PCR product from the normal birds, but removed the cleavage site from the affected ones (Figure 2.3). The restriction enzyme HpyIII188 has a restriction site sequence of TCNNGA, and when a PCR was run with a mismatch primer, the product from the normal allele had an HpyIII188 cleavage site associated with the site of interest, while the mutant allele did not because of the deletion. The PCR product was 192 bp for the wild type allele and 189 bp for the *rge* allele. After restriction enzyme digestion of the PCR product, affected birds had a single product of 189 bp, normal birds had two products – one that was 161 bp and another that was 31 bp in length. The carriers had three products (189, 161 and 31 bp).

The PCR with the mismatched primer was run with an annealing temperature of 55°C. A sample of the PCR product was run in a 1% gel to ensure that the PCR amplified the product and that the product was the correct size (192 bp) and then the rest of the PCR product was digested with the HpyIII188 enzyme. For a 20 µL digestion reaction the following components were used:

- 12 µL of PCR product
- 0.25 µL of HpyIII188 enzyme (New England Biolabs, Ipswich, MA)
- 2 µL of 10X NEBuffer 4 (provided with the enzyme, contents proprietary)

- 2  $\mu\text{L}$  10X bovine serum albumin
- 3.75  $\mu\text{L}$  molecular grade water.

These components were mixed and allowed to digest at 37°C for one to two hours. The product of this incubation was run in a 4% agarose gel. The higher percentage gel was required to differentiate the size difference in the bands.

### GENOMIC DNA FROM THE AREA OF INTEREST OF GNB3

Exon 5 CGCGTGAAGGCAACGTCAAAGTGAGCAGGGAAGTCTCAGCTCATACAGgt  
Gagtgttctgcctaccagtggcctgggtgtctctgcttccaaatctcact  
cttctaaccctgctctgtctctcatactcactggttcctgctccccagGT  
Exon 6 TACCTCTCCTGCTGCCGGTT (TCTTGA) TGACAACAGTATTGTGACTAGC  
TCTGGAGATACCACATGgtaagtattatcctctatcttattgacatgagc

**GAT** = deleted codon from affected birds  
(TCTTGA) = Hpy188III cleavage site

### DESIGN OF ASSAY

Exon 5 CGCGTGAAGGCAACGTCAAAGTGAGCAGGGAAGTCTCAGCTCATACAGgt  
gagtgttctgcctaccagtggcctgggtgtctctgcttccaaatctcact  
cttctaaccctgctctgtctctcatactcactggttcctgctccccagGT  
Exon 6 TACCTCTCCTGCTGCCGGTT (TCTTGA) TGaCAACAGTATTGTGACTAGC  
TCTGGAGATACCACATGgtaagtattatcctctatcttattgacatgagc

ACGTCAAAGTGAGCAGGGAAGTCT = forward primer

GcCAACAGTATTGTGACTAGCTCTGGA = mismatch reverse primer

### PCR PRODUCT - WILD TYPE ALLELE

ACGTCAAAGTGAGCAGGGAAGTCTCAGCTCATACAGgtgagtgttctgcc  
Taccagtggcctgggtgtctctgcttccaaatctcactcttctaaccctg  
ctctgtctctcatactcactggttcctgctccccagGTTACCTCTCCTGC  
TGCCGGTT (TCTTGA) TGcCAACAGTATTGTGACTAGCTCTGGA

Hpy188III cleavage site present, so two bands created after digestion (161 bp and 31 bp)

### PCR PRODUCT AFFECTED ALLELE:

ACGTCAAAGTGAGCAGGGAAGTCTCAGCTCATACAGgtgagtgttctgcc  
taccagtggcctgggtgtctctgcttccaaatctcactcttctaaccctg  
ctctgtctctcatactcactggttcctgctccccagGTTACCTCTCCTGC  
TGCCGGTTTCTTGcCAACAGTATTGTGACTAGCTCTGGA

No Hpy188III cleavage site present, so only one band of 189 bp present after digestion

**Figure 2.3.** Restriction enzyme test to establish GNB3 status. This figure shows the restriction enzyme test designed to distinguish normal (+/+) from carrier (*rge*/+) from affected (*rge/rge*) birds. A mismatch reverse primer removes the Hpy188III cleavage site from the affected bird sequence but doesn't affect the site in the normal bird sequence. Thus the PCR products from normal birds have two bands (161 and 31 bp), those of carrier birds have three bands (189, 161, 31 bp) and those of affected birds have only one band (189 bp). UPPERCASE = exonic sequence, lowercase = intronic sequence.

#### 2.2.8.b. GNB3 immunoreactivity in the normal chicken retina

##### 2.2.8.b.i. Chicks

Chicks used in the immunohistochemistry studies were from the *rge* colony of chickens, which is housed under 12 hour light:dark cycles in the vivarium facility at Michigan State University's College of Veterinary Medicine. Fertile eggs were produced in two ways; natural insemination between male and female carriers and artificial insemination between affected roosters and carrier females. The eggs were collected once a day, stored at 50°F in a humidified cooler and incubated in batches. The eggs were hatched in incubators (Hova-Bator, G.Q.F. Manufacturing Co., Savannah, GA). The chicks were typed (control or affected) via electroretinogram or their MCW0318 status was determined (Hans Cheng's Laboratory). All procedures were conducted in accordance with the ARVO Statement for the Use of Animals in Ophthalmic and Vision Research and approved by the Michigan State University All-University Committee on Animal Use and Care.

##### 2.2.8.b.ii. Retina Collection

Immediately following euthanasia using an overdose of pentobarbital (Fatal Plus, Vortech Pharmaceutical, Dearborn, MI), bilateral enucleation was performed. The eyes were hemisected at the equator, the vitreous body removed and the posterior segment of the eye immersed into fixative.

#### 2.2.8.b.iii. Fixation, Embedding and Staining

For IHC analyses, retinal samples were fixed in 4% paraformaldehyde, 3% sucrose in 0.1 M phosphate buffer for 48 hours at 4°C and then dehydrated in ethanol from 65 to 100% concentration, rinsed twice in xylene, and embedded in paraffin blocks prior to sectioning. Five-µm thick sections were cut and mounted on double-gelatinized glass slides and dried at 65°C for 20 minutes. After deparaffination in xylene, sections were rehydrated gradually in ethanol (100% then 95%) and, finally in distilled water.

The sections were incubated in a preheat antigen retrieval buffer (Citrate buffer, DakoCytomation, Carpinteria, CA) for 20 minutes at 97°C. After the section had been cooled to 50°C, it was incubated in 50mM TRIS-buffered saline (TBS; pH 7.6) for 5 minutes, followed by 10 minutes incubation with a protein-blocking agent (DakoCytomation) prior to application of the primary antibody. Goat anti-rabbit secondary antibody from the Labeled Streptavidin-Biotin 2 System and Horseradish Peroxidase (LSAB2 System-HRP, DakoCytomation) was used to reveal primary antibody-positive immunoreactivity. Immunoreaction was visualized with 3,3'-diaminobenzidine substrate (Liquid DAB substrate chromogen system, DakoCytomation), and the sections were counterstained with hematoxylin (Gill III formula<sup>TM</sup>, Surgipath Medical Industries Inc., Richmond, IL) for 10 minutes. The sections were then washed in distilled water, rinsed in tap water for 5 minutes, blued with 0.04% lithium carbonate, washed again in distilled water, dehydrated in 100% and 95% ethanol then in xylene before being coverslipped.

The primary antibody used was a polyclonal anti-GNB3 antibody raised in rabbits against the peptide (ADITLAELVSGLEVV) and affinity purified (Invitrogen

Corporation, Carlsbad, CA) (received as a gift from Dr. Anand Swaroop, University of Michigan) (Yu et al., 2004). Immunostaining was carried out at MSU's Diagnostic Center for Population and Animal Health by the technicians in the Histopathology Laboratory.

### **2.3. Results**

A compilation of the polymorphisms found in the twelve sequenced genes can be found in Table 2.4. The sequencing of each gene in its entirety was not completed because this area of the work stopped once the causal gene and mutation were identified. At the time the molecular work was being completed, the actual number of exons in chicken TULP3 was unknown; however, 4 exons were sequenced. The cDNA sequence of EphA1 was unobtainable after repeated trials using retinal cDNA from an adult chicken and therefore it was assumed that it was not expressed in the adult retina.

A total of 128 polymorphisms were found. The majority of them (126) were single nucleotide polymorphisms (SNPs), with 94 of them being intronic and 32 of them being exonic. Additionally, two insertion/deletions were found. Most of the exonic SNPs were "synonymous" meaning they did not cause an amino acid change because they were in the third codon position (wobble position). However, 5 of the exonic SNPs were "non-synonymous" meaning they caused an amino acid change. One non-SNP polymorphism was an exonic 6 bp deletion in both carrier and affected chickens in CEK9 compared to the published mRNA sequence (U23783.1). A 3 bp deletion in the coding region of the GNB3 gene was found in the affected retinal cDNA (as described by Tummala et al 2006) but not in the wild type transcript.

Gene	# Exons Sequenced 4/4?	# Exonic SNPs	# Intronic SNPs	Other Info
TULP3*		0	0	
PHC1	5/15	1	4	2 intronic SNPs not in linkage disequilibrium
COPS7A	3/6	2	1	
GPR162	4/7	1	7	One amino acid change (Leu to Phe)
GNB3**	Entire coding region sequenced from cDNA	3		3 bp deletion in affected only (aspartic acid residue)
ENO2	10/11	1	14	
ATN1	10/16	4	5	
PTPN6	12/15	1	9	
CLSTN3	14/18	5	14	Two amino acid changes (Gly to Ser and Asp to Gly)
EphA1*	18/18	7	21	One amino acid change (Cys to Tyr)
ZYX	8/8	1	8	
CEK9	15/16	6	11	6 bp indel in both carrier and affected genomic and wild type cDNA (Leu and Pro) and two amino acid changes (Ile to Thr and Gln to Glu)

**Table 2.4.** Sequence analysis results of the twelve genes examined. A total of 132 polymorphisms were found. Not all exons and splice sites were sequenced because work stopped when the GNB3 mutation was identified as the causative mutation of the *rge* phenotype. At the time the molecular work was being completed, the actual number of exons in chicken TULP3 was unknown.

\* Only have genomic sequence      \*\* Only sequenced cDNA not genomic DNA



<b>Table 2.5.</b> Legend follows table (see below)					
<b>Gene</b>	<b>SNP</b>	<b>Affected</b>	<b>Carrier</b>	<b>Exon/Intron</b>	<b>Position</b>
PHC1	c/t	c/c	c/t	Intronic	79294985
PHC1	c/t	c/c	c/t	Intronic	79295134
PHC1	a/g	a/g	g/g	Intronic	79301971
PHC1	c/t	c/t	t/t	Intronic	79302263
PHC1	G/C	G/G	G/C	Exonic	79303210
COPS7a	G/C	C/C	G/C	Exonic	80304771
COPS7a	g/a	a/a	g/a	Intronic	80304924
COPS7a	G/A	A/A	G/A	Exonic	80305939
GPR162	c/t	c/c	c/t	Intronic	80386502
GPR162	t/c	t/t	t/c	Intronic	80386919
GPR162	G/A	G/G	G/A	Exonic	80386959
GPR162	g/a	a/a	g/a	Intronic	80387111
GPR162	c/t	c/c	c/t	Intronic	80387154
GPR162	c/t	c/c	c/t	Intronic	80387167
GPR162	a/g	a/a	a/g	Intronic	80387210
GPR162	C/T	C/C	C/T	Exonic	80388044
GPR162	g/c	c/c	g/c	Intronic	80388162
GNB3	GAT mutation in <i>rge</i> bird			Exonic	80407769- 80407771
GNB3	G/A	A/A	G/A	Exonic	80407596
GNB3	C/T	T/T	C/T	Exonic	80409299
GNB3	T/C	C/C	T/C	Exonic	80410288
Eno2	t/c	t/t	t/c	Intronic	80448998
Eno2	g/a	g/g	g/a	Intronic	80449226
Eno2	t/c	t/t	t/c	Intronic	80450390
Eno2	g/a	g/g	g/a	Intronic	80451299
Eno2	T/C	T/T	T/C	Exonic	80451573
Eno2	a/g	a/a	a/g	Intronic	80451673
Eno2	c/t	c/c	c/t	Intronic	80451708
Eno2	t/g	t/t	t/g	Intronic	80451790
Eno2	a/g	a/a	a/g	Intronic	80451846
Eno2	a/g	a/a	a/g	Intronic	80452093
Eno2	t/a	t/t	t/a	Intronic	80452533
Eno2	t/c	t/t	t/c	Intronic	80452663
Eno2	t/c	t/t	t/c	Intronic	80452967
Eno2	c/t	c/c	c/t	Intronic	80453035
Eno2	t/c	t/t	t/c	Intronic	80453228
ATN1	C/T	C/C	C/T	Exonic	80477586
ATN1	c/t	c/c	c/t	Intronic	80477679
ATN1	g/a	a/a	g/a	Intronic	80477833
ATN1	C/T	C/C	C/T	Exonic	80479960
ATN1	C/T	C/C	C/T	Exonic	80479963
ATN1	G/A	G/G	G/A	Exonic	80480044
ATN1	c/g	g/g	c/g	Intronic	80481707
ATN1	t/a	a/a	t/a	Intronic	80481763
PTPN6	A/G	A/A	A/G	Exonic	80498822
PTPN6	a/g	a/a	a/g	Intronic	80499374

<b>Table 2.5. Continued</b>					
PTPN6	a/g	g/g	a/g	Intronic	80499755
PTPN6	g/a	g/g	g/a	Intronic	80502917
PTPN6	t/c	c/c	t/c	Intronic	80503178
PTPN6	g/t	t/t	g/t	Intronic	80503406
PTPN6	t/a	t/t	t/a	Intronic	80503412
PTPN6	a/g	g/g	a/g	Intronic	80503498
PTPN6	c/a	c/c	c/a	Intronic	80506546
PTPN6	a/t	a/a	a/t	Intronic	80506547
CLSTN3	a/g	a/a*	g/a	Intronic	80570927
CLSTN3	G/C	G/G*	C/G	Exonic	80573569
CLSTN3	A/T	A/A*	T/A	Exonic	80573671
CLSTN3	a/g	a/a*	g/a	Intronic	80576883
CLSTN3	t/a	t/t*	t/a	Intronic	80576896
CLSTN3	c/a	c/c*	c/a	Intronic	80576937
CLSTN3	a/g	a/a*	g/a	Intronic	80576938
CLSTN3	g/t	g/g*	t/g	Intronic	80576954
CLSTN3	c/t	c/c*	t/c	Intronic	80577189
CLSTN3	T/C	C/C	T/C	Exonic	80578867
CLSTN3	a/g	g/g	a/g	Intronic	80579147
CLSTN3	c/g	g/g	c/g	Intronic	80579255
CLSTN3	a/g	g/g	a/g	Intronic	80582879
CLSTN3	G/A	A/A†	G/A	Exonic	80583113
CLSTN3	t/c	c/c	t/c	Intronic	80583181
CLSTN3	c/t	t/t	c/t	Intronic	80583200
CLSTN3	c/t	t/t	c/t	Intronic	80583215
CLSTN3	c/t	t/t	c/t	Intronic	80583233
CLSTN3	A/G	G/G†	A/G	Exonic	80583311
EphA1	g/a	a/a	g/g	Intronic	80635136
EphA1	a/c	c/c	a/c	Intronic	80639103
EphA1	C/T	C/C	C/T	Exonic	80653703
EphA1	G/A	G/G	G/A	Exonic	80653727
EphA1	g/t	g/g	g/g	Intronic	80653799
EphA1	t/c	t/t	t/c	Intronic	80658597
EphA1	g/a	a/a	g/a	Intronic	80658612
EphA1	c/t	t/t	c/t	Intronic	80659402
EphA1	c/t	c/c	c/t	Intronic	80659672
EphA1	c/g	c/c	c/g	Intronic	80659679
EphA1	t/c	t/t	t/c	Intronic	80659710
EphA1	G/A	A/A†	G/A	Exonic	80659816
EphA1	c/t	t/t	c/t	Intronic	80660491
EphA1	g/a	g/g	g/a	Intronic	80660520
EphA1	t/c	c/c	t/c	Intronic	80660948
EphA1	C/T	C/C	C/T	Exonic	80661294
EphA1	a/t	t/t	a/t	Intronic	80661840
EphA1	c/t	t/t	c/t	Intronic	80661844
EphA1	t/c	t/t	t/c	Intronic	80661887
EphA1	t/c	t/t	t/c	Intronic	80661938
EphA1	c/g	c/c	c/g	Intronic	80661941

<b>Table 2.5. Continued</b>					
EphA1	g/c	g/g	g/c	Intronic	80662030
EphA1	C/T	C/C	C/T	Exonic	80662702
EphA1	g/a	a/a	g/a	Intronic	80662915
EphA1	g/c	g/g	g/c	Intronic	80662981
EphA1	a/t	t/t	a/t	Intronic	80663419
EphA1	G/A	G/G	G/A	Exonic	80665007
EphA1	A/G	G/G	A/G	Exonic	80665253
ZYX	a/g	a/a	a/g	Intronic	80676221
ZYX	c/g	c/c	c/g	Intronic	80676108
ZYX	t/c	t/t	t/c	Intronic	80675843
ZYX	C/T	T/T	C/T	Exonic	80674119
ZYX	g/c	g/g	g/c	Intronic	80673643
ZYX	c/t	c/c	c/t	Intronic	80672793
ZYX	a/c	c/c	a/c	Intronic	80672759
ZYX	a/g	a/a	a/g	Intronic	80672658
ZYX	t/c	c/c	t/c	Intronic	80672592
CEK9	t/c	t/t	t/c	Intronic	81143482
CEK9	C/T	C/C	C/T	Exonic	81127231
CEK9	G/A	A/A	G/A	Exonic	81127131
CEK9	CTGCCA indel			Exonic	81114604- 81114609
CEK9	T/C	C/C†	T/C	Exonic	81114581
CEK9	T/C	T/T	T/C	Exonic	81114430
CEK9	c/t	t/t	c/t	Intronic	81109959
CEK9	t/c	c/c	t/c	Intronic	81109905
CEK9	g/a	g/g	g/a	Intronic	81103132
CEK9	c/t	t/t	c/t	Intronic	81102932
CEK9	t/c	t/t	t/c	Intronic	81102282
CEK9	t/g	g/g	t/g	Intronic	81100282
CEK9	C/G	C/C†	C/G	Exonic	81093332
CEK9	c/t	t/t	c/t	Intronic	81093232
CEK9	c/t	t/t	c/t	Intronic	81093159
CEK9	g/a	a/a	g/a	Intronic	81093031
CEK9	g/a	g/g	g/a	Intronic	81093112
CEK9	G/A	A/A	G/A	Exonic	81088082

**Table 2.5.** Polymorphisms found during investigation. \*=affected same as published. †=SNP changes amino acid in affected bird (see text for description of change).

The affected bird was heterozygous for two of the intronic SNPs in PHC1, suggesting a crossover event between the PHC1 locus and the disease locus.

Pyrosequencing revealed that each of the SNPs analyzed from the three genes (ENO2, COPS7A and GPR162) was in linkage disequilibrium with disease status meaning that all of the carriers were heterozygous and all of the affected birds that were tested were homozygous at the locus.

The non-synonymous SNP in EphA1 caused a cysteine to tyrosine amino acid change in the affected bird. The SIFT program described the substitution as “tolerable” and the Polyphen program reported the change as “benign.” In addition to the SIFT and Polyphen results, the amino acid substitution is not in a well-conserved region (across species) suggests the change may not affect protein function.

The first non-synonymous SNP in the CEK9 gene changes an isoleucine residue to a threonine residue in the affected birds. SIFT predicted that this substitution would be “tolerated” and Polyphen predicted the change to be “benign.” This coupled with the fact that it is not a well-conserved region (across species) suggests the amino acid substitution may not affect protein function. The second amino acid changing SNP in CEK9 was a “wild type” SNP meaning the affected sequence was identical to the published genomic and mRNA sequences (NM\_001004387, U23783.1) and the carrier sequence is the one that differed. The wild type and affected sequence coded for a glutamine and the carrier sequence indicated that the homozygous normal bird sequence would code for glutamic acid. The 6 bp indel found in CEK9 was very close to the first SNP (Ile to Thr substitution) and was thus in a region of the gene that is not well conserved. The published mRNA sequence for CEK9 (U23783.1) contained 6 bp (CTGCCA – leucine

and proline residue) whereas both of the carrier and affected DNA samples were “missing” the 6 bp in the genomic sequence, as was the wild type retinal cDNA sample when compared to the published mRNA sequence (U23783.1). The published genomic sequence (NM\_001004387) was also “missing” these 6 bp. The area of the protein sequence that is affected by these insertion/deletions is not well conserved across species, therefore this polymorphism is difficult to evaluate. This evidence suggests that either there is an error in the published mRNA sequence or that it is insignificant.

GNB3's sequence from retinal cDNA confirmed Tummala et al's findings; a 3 bp deletion of the 153<sup>rd</sup> codon in the affected birds was found. Three synonymous exonic SNPs were also found. The 3 bp deletion was in frame and removed an aspartic acid residue. When this deletion was entered in the CLUSTALW program (<http://align.genome.jp/>) and compared with mouse, rat and human GNB3, it became apparent that this amino acid deletion occurred in a highly conserved region across species (Figure 2.4), suggesting that its deletion was potentially significant.

The restriction enzyme test was developed successfully, allowing typing of chicks of unknown status. Figure 2.5 shows a gel with the results of the restriction enzyme test of a normal, a carrier and an affected bird. Note that the 31 bp band is not visible on the gel due to its small size.

```

Mouse_NM_013530_GNB3 MGEMEQLRQEAEQLKKQIADARKACADITLAELVSGLEVVGVRVQMRTRRT
Rat_NM_021858_GNB3  MGEMEQLKQEAEQLKKQIADARKACADITLAELVSGLEVVGVRVQMRTRRT
Human_NM_002075_GNB3 MGEMEQLRQEAEQLKKQIADARKACADVTLAELVSGLEVVGVRVQMRTRRT
RGE_Chicken          MGEMEQMKEAEQLKKQIADARKACADTTLAQIVSGVEVVGRIQMRTRRT
Normal_Chicken_GNB3  MGEMEQMKEAEQLKKQIADARKACADTTLAQIVSGVEVVGRIQMRTRRT
*****:;*****:*****:***:;***:*****:*****

Mouse_NM_013530_GNB3 LRGHLAKIYAMHWATDSKLLVSASQDGKLIVWDTYTTNKVHAIPLRSSWV
Rat_NM_021858_GNB3  LRGHLAKIYAMHWATDSKLLVSASQDGKLIVWDTYTTNKVHAIPLRSSWV
Human_NM_002075_GNB3 LRGHLAKIYAMHWATDSKLLVSASQDGKLIVWDSYTTNKVHAIPLRSSWV
RGE_Chicken          LRGHLAKIYAMHWSTDSKLLVSASQDGKLIVWDTYTTNKVHAIPLRSSWV
Normal_Chicken_GNB3  LRGHLAKIYAMHWSTDSKLLVSASQDGKLIVWDTYTTNKVHAIPLRSSWV
*****:;*****:*****:*****:*****:*****

Mouse_NM_013530_GNB3 MTCAYAPSGNFVACGGLDNMCSIYNLKSREGNVKVSRELSAHTGYLSCCR
Rat_NM_021858_GNB3  MTCAYAPSGNFVACGGLDNMCSIYSLKSREGNVKVSRELSAHTGYLSCCR
Human_NM_002075_GNB3 MTCAYAPSGNFVACGGLDNMCSIYNLKSREGNVKVSRELSAHTGYLSCCR
RGE_Chicken          MTCAYAPSGNFVACGGLDNMCSIYNLKTREGNVKVSRELSAHTGYLSCCR
Normal_Chicken_GNB3  MTCAYAPSGNFVACGGLDNMCSIYNLKTREGNVKVSRELSAHTGYLSCCR
*****:;*****:*****:*****:*****:*****

↓

Mouse_NM_013530_GNB3 FLDDNNIVTSSGDTTCALWDIETGQQKT V FVGHTGDCMSLAVSPDYKLF I
Rat_NM_021858_GNB3  FLDDNNIVTSSGDTTCALWDIETGQQKT V FVGHTGDCMSLAVSPDYKLF I
Human_NM_002075_GNB3 FLDDNNIVTSSGDTTCALWDIETGQQKT V FVGHTGDCMSLAVSPDFNLF I
RGE_Chicken          FL-DNSIVTSSGDTTCALWDIETGQQKT V FLGHTGDCMSLAVSPDFKLF I
Normal_Chicken_GNB3  FLDDNSIVTSSGDTTCALWDIETGQQKT V FLGHTGDCMSLAVSPDFKLF I
** *.*****:;*****:*****:;***

Mouse_NM_013530_GNB3 SGACDASAKLWDVREGTCRQTF TG HESDINAICFFPNGEAICTGSDDASC
Rat_NM_021858_GNB3  SGACDASAKLWDVREGTCRQTF TG HESDINAICFFPNGEAICTGSDDASC
Human_NM_002075_GNB3 SGACDASAKLWDVREGTCRQTF TG HESDINAICFFPNGEAICTGSDDASC
RGE_Chicken          SGACDATAKLWDVREGTCRQTF SG HESDINAICFFPNGEAICTGSDDATC
Normal_Chicken_GNB3  SGACDATAKLWDVREGTCRQTF SG HESDINAICFFPNGEAICTGSDDATC
*****:;*****:*****:*****:*****:*****

Mouse_NM_013530_GNB3 RLFDLRADQELTAYSQESIICGITSVAFSLSGRLLFAGYDDFNCNVWDSL
Rat_NM_021858_GNB3  RLFDLRADQELTAYSHESIICGITSVAFSLSGRLLFAGYDDFNCNVWDSL
Human_NM_002075_GNB3 RLFDLRADQELICFSHESIICGITSVAFSLSGRLLFAGYDDFNCNVWDSM
RGE_Chicken          RLFDLRADQELIVYSHESIICGITSVAFSRSGRLLLAGYDDFNCNIWDSL
Normal_Chicken_GNB3  RLFDLRADQELIVYSHESIICGITSVAFSRSGRLLLAGYDDFNCNIWDSL
*****:;*****:*****:*****:*****:*****

Mouse_NM_013530_GNB3 KCERVGILSGHDNRVSLGVTADGMAVATGSWDSFLKIWN
Rat_NM_021858_GNB3  KCERVGVLSGHDNRVSLGVTADGMAVATGSWDSFLKIWN
Human_NM_002075_GNB3 KSERVGILSGHDNRVSLGVTADGMAVATGSWDSFLKIWN
RGE_Chicken          KAERVGILSGHDNRVSLGVTADGMAVATGSWDSFLKIWN
Normal_Chicken_GNB3  KAERVGILSGHDNRVSLGVTADGMAVATGSWDSFLKIWN
+ + + + +

```

**Figure 2.4.** GNB3 amino acid sequence alignment. This figure shows the amino acid sequence alignment of GNB3 aligned using the CLUSTAL program. The amino acid sequences from mouse, rat and human were obtained from the UCSC Genome Browser and the *rge* chicken sequence was obtained from a translation of sequenced retinal cDNA. This shows how well conserved the protein is between the 4 species. The deleted amino acid is an aspartic acid residue (D – in gray with ↓ above it).

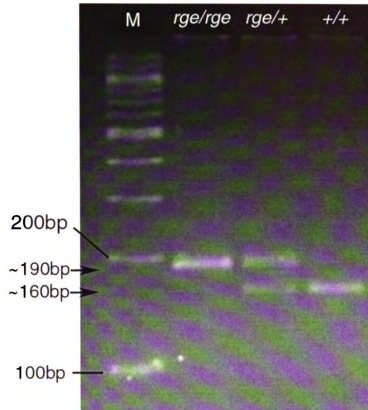


**Figure 2.5.** Results of the GNB3 RE test. This figure shows a 4% agarose gel with the final results of the Hpy188III restriction enzyme test for affected (*rge/rge*), carrier (*rge/+*) and normal (*+/+*) birds. The normal bird has one band 161 bp in length, the carrier has two bands 161 and 192 bp in length and the affected bird has one band 189 bp in length. The 31 bp band is not visualized on the gel. M = molecular ladder (100 bp DNA Ladder N3231S, New England BioLabs, Ipswich, MA)

Immunohistochemistry for GNB3 in the normal chicken retina (Figure 2.6) shows GNB3 immunoreactivity in several retinal locations. The natural pigmentation in the retina (dark brown) must be differentiated from the lighter brown chromogen. In addition to cone outer segments, there is also some immunoreactivity in the region of cone cell bodies and in synaptic terminals in the outer plexiform layer. A population of cells within the inner layer of the inner nuclear layer, (the region where amacrine cells are located) and ganglion cell layer were also immunoreactive.



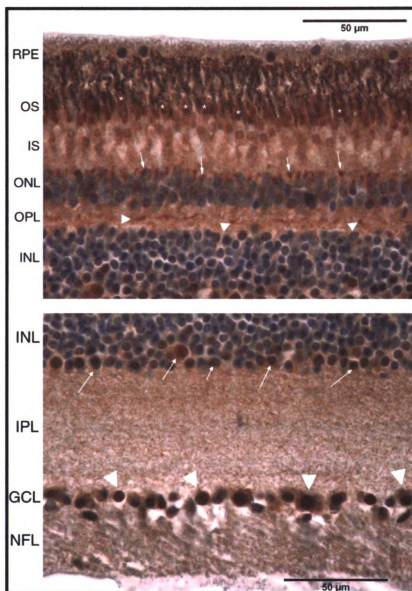


**Figure 2.6.** GNB3 immunoreactivity in normal chicken retina. This photomicrograph displays GNB3 antibody IHC using a rabbit anti-GNB3 polyclonal antibody (Gift from Dr. Anand Swaroop, U of Michigan). The upper image is the outer retina. The brown chromogen used is a slightly lighter brown than the RPE pigmentation but the similarity in color does make the immunoreactivity of cone outer segments (\*) a little more difficult to appreciate. In addition to immunoreactivity of cone outer segments some immunoreactive (IR) structures between the photoreceptor cell bodies can be seen (arrows). IR synaptic termini are present in the OPL (arrowheads). The lower image is the inner retina. A subpopulation of cells in the inner aspect of the INL are IR to this GNB3 antibody (arrows). The cell bodies of the ganglion cell layer are also IR to this GNB3 antibody (arrowheads). Key: RPE = retinal pigment epithelium; OS = photoreceptor outer segments; IS = photoreceptor inner segments; ONL = outer nuclear layer; OPL = outer plexiform layer; INL = inner nuclear layer; GCL = ganglion cell layer; NFL = nerve fiber layer. This figure is presented in color.

## 2.4. Discussion

The majority of polymorphisms found in the positional candidate genes were intronic SNPs, which is expected as introns are not as highly conserved as exons. The majority of exonic SNPs were in the codon's third position (wobble position) and so did not alter the amino acid that was ultimately expressed. Each of the SNPs analyzed with pyrosequencing was in linkage disequilibrium with the disease status, meaning affected birds were homozygous and carriers were heterozygous. This means those three genes (ENO2, COPS7A and GPR162) were considered to be within the disease interval.

The discovery of the SNPs in PHC1 that were heterozygous in the affected and not the carrier means the gene is not in linkage disequilibrium with the *rge* locus. Because of this, PHC1 is in a region that can be considered a left hand boundary for the disease interval. As stated previously the location of TULP3 was unknown at the time the molecular work was being done. Once the updated version of the chicken genome was published, TULP3's location was assigned to an area upstream from PHC1. Consequently, due to PHC1's lack of linkage disequilibrium with the disease status, TULP3 was determined to be located outside of the interval for the *rge* gene locus, although no SNPs were found to confirm this.

The 3 bp deletion in GNB3, which removes an aspartic acid, is present only in the affected chicken sequence. When compared to mouse, rat and human GNB3 amino acid sequences, it is in a conserved region (Figure 2.2). All three of the other species GNB3 amino acid sequences contain the aspartic acid residue that the *rge* chicken is missing, which strongly suggests that this is the *rge* mutation. This region is also conserved across four of the five GNB proteins identified in humans (GNB1: NM\_002074; GNB2:

NM\_002075; and GNB4: NM\_021629). GNB5's amino acid sequence is not well conserved across species.

GNB3 is the beta subunit of a G-binding protein and is made up of an amino-terminal  $\alpha$ -helical segment followed by 7 repeating units called WD repeats that form a propeller structure (Sondek et al., 1996). Each WD-repeat consists of 40-60 amino acid residues bordered by a GH (glycine-histidine) and a WD (tryptophan-aspartic acid). Each propeller is composed of a four-stranded anti-parallel  $\beta$ -sheet (Neer, 1995). The four strands are labeled a, b, c and d. The aspartic acid deletion in the *rge* mutant is positioned in a beta hairpin between the a and b  $\beta$  strands of the third propeller; therefore, the deletion of this amino acid residue could possibly affect the folding of this protein (Figure 2.7). The amino acid deletion was modeled with the "What if" computer program using bovine GNB1 as a close homologue of GNB3, and the results suggested that this deletion abolishes  $\beta$  sheets in propellers 1 and 5 of the GNB protein (Tummala et al., 2006). The CASP5 committee (Critical Assessment of Methods for Protein Structure Prediction) predicted that the mutant GNB3 protein would be unstable and liable to premature proteolysis. This prediction was supported by the finding that there was a 70% reduction in GNB3 protein immunoreactivity in affected retinas when compared to age- and sex-matched normal retinas (Tummala et al., 2006).

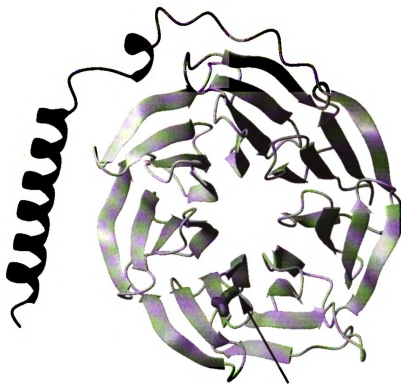


**Figure 2.7.** A computational model of chicken (*Gallus gallus*) GNB3 protein. The protein has a 7 propeller arrangement characteristic of G-protein beta subunits. The side chain of the 153Asp deleted in the *rge* chicken is shown (black arrow). It is in the beta hairpin between the a and b beta strands of the third propeller. Figure created with the help of William J. Wedemeyer.

As previously stated, when it became known that Tummala et al had found the gene and causative mutation, the molecular work was abandoned except for confirming their findings and developing the restriction enzyme test to quickly and accurately test chicks as they hatched.

Additionally, immunohistochemistry was done in paraffin embedded control chicken retina to establish GNB3's locations in the retina. The results obtained are similar to those obtained by other research groups in that GNB3 immunoreactivity is found in cones and in the inner retina (inner nuclear layer) (Peng et al., 1992; Huang et al., 2003). Ganglion cells were also found to have GNB3 immunoreactivity, which has not been reported elsewhere. The moderate amount of background staining that appeared is probably due to this particular antibody's lack of specificity for chicken GNB3. The sequence the antibody was raised against is ADITLAELVSGLEV V (from mouse GNB3) and the corresponding sequence in chicken GNB3 is ADTTLAQIVSGVEVV, which is only a 73% match.

## CHAPTER 3

### FURTHER ELECTRORETINOGRAPHIC STUDIES OF THE *rge* CHICKEN

#### 3.1. Introduction

The retinopathy, globe-enlarged (*rge*) chick has an unusual autosomal recessive retinal dystrophy whose unique electroretinographic features have previously been partially characterized. Previous work has shown that *rge* chicks have a progressive deterioration in vision from hatch such that they are functionally blind by approximately one month of age. Electroretinographic responses of the *rge* chicks are abnormal from hatch with altered b-wave shape and reduced oscillatory potentials (OPs). In the first few weeks of life the *rge* ERGs have supernormal b-wave amplitudes in response to brighter flashes, which is of particular interest. The ERG responses slowly deteriorate with age and surprisingly are maintained for a considerably longer time than functional vision, which is unusual amongst retinopathies (Montiani-Ferreira et al., 2007).

The use of ERG as a diagnostic tool has been further enhanced by greater knowledge of the retinal processes underlying the different components of the ERG, mainly when different techniques, such as the use of drugs (pharmacological dissection) and intracellular recordings, were introduced. Since then, it has commonly been assumed that cells in the distal part of the sensory retina (photoreceptors, bipolar cells and Müller cells), are the main contributors to the ERG, while proximal processes contribute less to the response. The pharmacological dissection approach also has been used to investigate the ERG of animal models of inherited retinal disease.

Several different pharmacological compounds were used in this study in an attempt to determine the origin of the supernormal b-wave:

- APB (2-amino-4-phosphonobutyric acid, also known as L-AP4), a glutamatergic receptor agonist that acts on metabotropic glutamate receptors, has been shown to isolate the OFF-hyperpolarizing responses thus removing the majority of the b-wave of the ERG (Slaughter and Miller, 1981; Stockton and Slaughter, 1989).
- PDA (cis-2,3-piperidinedicarboxylic acid), a glutamatergic receptor antagonist isolates the response of the photoreceptors and ON-depolarizing bipolar cells by blocking transmission from photoreceptors to OFF bipolar cells and horizontal cells and transmission from bipolar cells to third order neurons (Slaughter and Miller, 1983; Stockton and Slaughter, 1989).
- Aspartate blocks all post-receptoral responses; thus, it reveals the PIII response or the fast component of the a-wave, which originates from the photoreceptors (Cervetto and MacNichol, Jr., 1972; Murakami et al., 1975).

In contrast to the standard short flash ERG in which the ON and OFF responses are super-imposed on one another, the long flash ERG allows the separation of the ON responses from the OFF responses due to the length of the flash. It was utilized in this study with the addition of the various previously mentioned pharmacological agents in an attempt to analyze the ON and OFF components of the *rge* chick.

Avian species, chickens included, have been shown to have circadian rhythms in their ERG waveforms, although the literature is contradictory about what differences are seen between day and night and why (Schaeffel et al., 1991; Manglapus et al., 1998; Wu et al., 2000). In order to establish whether the *rge* chicks maintained a circadian rhythm in the face of visual deficits, the effect of circadian rhythm on ERG was also investigated in both control and affected chicks.

### **3.2. Materials and methods**

#### **3.2.1. Chicks**

Chicks used in the ERG studies were from an experimental colony of *rge* chickens, which is housed under 12 hour light:dark cycles in the vivarium facility at Michigan State University's College of Veterinary Medicine. Fertile eggs were produced in two ways; natural insemination between male and female carriers and artificial insemination between affected roosters and carrier females. The eggs were collected once a day, stored at 50°F and incubated in batches. The eggs were hatched in incubators (Hova-Bator, G.Q.F. Manufacturing Co., Savannah, GA). The chicks were typed (control or affected) via electroretinogram or later in the project by restriction enzyme test specific for the phenotype causing mutation. Previous studies have shown that heterozygous birds had no ERG abnormalities when compared to homozygous normal chicks (Montiani-Ferreira et al., 2007); therefore both heterozygous carriers and homozygous normal birds were used as controls. All procedures were conducted in accordance with the ARVO Statement for the Use of Animals in Ophthalmic and Vision



Research and approved by the Michigan State University All-University Committee on Animal Use and Care.

### 3.2.2. ERG recording

All electroretinograms were performed between the hours of 8am and 5pm (except the night time circadian ERGs) to avoid circadian effects on the ERG. For all of the electroretinographic studies, the chicks were dark adapted for one hour and then anesthetized with isoflurane delivered in 100% oxygen. Body temperature was maintained with a water blanket. The left eye was typically used to record electroretinographic responses. Their pupils were dilated with topical 1% vecuronium bromide (ESI Lederle, Philadelphia, PA). A Burian-Allen bipolar corneal contact lens (Hansen Labs, Coralville, IA) lubricated with 2.5% hydroxypropyl methylcellulose (Goniosol; Alcon Laboratories, Inc., Fort Worth, TX) was used to record the responses. A ground electrode was inserted subcutaneously in the hind limb.

Full-field (Ganzfeld) flash intensity-series and long flash ERGs were recorded with a UTAS-E 3000 Electrophysiology unit (LKC Technologies Inc, Gaithersburg, MD) with the bandpass set between 1 and 500 Hz. The stimulus was delivered by a Ganzfeld unit consisting of a spherical chamber painted with reflective white paint in which the anesthetized chicks were placed with the test eye (and lens) exposed to the interior of the bowl. Short flash series were done with the LKC Ganzfeld, which can produce a wide range of light intensities from discharge of xenon flash tubes. Dark-adapted and light-adapted intensity series were done following the protocol outlined in Table 3.1. After the

dark-adapted series had been recorded, the chicks were light adapted (while anesthetized) to a white background light of 30 cd/m<sup>2</sup> and then the light-adapted series was performed.

<b>Intensity (cdS/m<sup>2</sup>)</b>	<b># Flashes Averaged</b>	<b># Seconds between flashes</b>
-3.19	10	1
-2.80	10	1
-2.60	10	1
-2.0	10	1
-1.6	10	1
-1.19	10	1
-0.80	10	1
-0.40	10	1
0.00	3 (10)	5 (1)
0.39	2 (5)	30 (5)
0.86	2 (5)	45 (10)
1.36	1 (3)	120 (30)
1.90	1 (3)	180 (45)
2.39	1 (2)	240 (60)
2.82	1 (2)	360 (60)

**Table 3.1.** Summary of short flash ERG protocol. Dark-adapted series utilized all of the listed flash intensities whereas light-adapted series only utilized -2.0 cds/m<sup>2</sup> and brighter flashes. Numbers in parentheses were the values used for light-adapted series when they differed from the dark-adapted series.

### 3.2.2.a. Long flash ERG

Long flash ERGs were performed with a customized Ganzfeld stimulator, which can create an adjustable duration of light stimulus with a rod saturating background light (43 cd/m<sup>2</sup>) (Sieving et al., 1994) and recorded with the previously mentioned UTAS-E 3000 electrophysiology unit (LKC Technologies Inc; Gaithersburg, MD). The stimulator can produce longer flashes of light (50-300 msec), and has a maximum intensity of 180 cd/m<sup>2</sup>. The long flash recordings were typically done following the light-adapted series.

Thus, the anesthetized chicks were transferred to the long flash Ganzfeld and were allowed to light adapt to the background light for 10 minutes before recording. Flashes were either 150 or 200 msec in length and the responses to 10 flashes were averaged with 5 seconds between flashes. In order to evaluate the long flash response, 5 control and 5 affected chicks were used to record long flash responses (these were the day-time long flash responses from the circadian ERGs). Pharmacological dissection was also employed in concert with the long flash technique (see section 3.2.3 for details of technique). All ERG waveforms were averaged, stored and displayed by LKC software for further analysis.

### 3.2.3. Pharmacological dissection of the ERG

The pharmacological agents were injected intravitreally to attain the following final vitreal concentrations: APB, 3 mM; PDA, 7 mM; sodium aspartate, 50 mM. These concentrations were selected based on the results of studies in other species. All of the drugs were obtained from Sigma (St. Louis, MO) and the solutions were made by dissolving the compounds in balanced salt solution (Alcon Laboratories, Fort Worth, TX). The drugs were injected into the vitreous body of anesthetized chicks with a 30 gauge needle attached to a Hamilton syringe in a volume of 0.02 mL. The injected eye was not reused for any electroretinography or histopathology.

For the pharmacological dissection, the pre-injection ERG was performed as previously stated. APB and aspartate injection ERGs included dark-adapted and light-adapted series and a long flash response, while the PDA ERGs only included the light-adapted series and the long flash response because PDA only effects cone-driven

pathways. The dark-adapted and light-adapted intensity series were done according to Table 3.1. Following the long flash ERG recording, the pharmacological agent was injected and then the chick was allowed to recover from anesthesia in the dark until the post-injection dark-adapted ERG was begun. The post-injection ERG was repeated one to two hours after the injections of APB, PDA and aspartate to allow diffusion of the agent to the retina, time for it to find its target and exact its effect.

APB injection and ERGs were done with 4 controls, which ranged in age from 14 to 26 days, and 4 affected birds, which ranged in age from 13 to 23 days. PDA injection and ERGs were done with 7 control birds, which ranged in age from 13 to 177 days, and 8 affected birds, which ranged in age from 24 to 50 days. Aspartate injection and ERGs were done with 4 control birds, which ranged in age from 14 to 56 days, and 4 affected birds, which ranged in age from 11 to 26 days.

#### 3.2.4. Circadian electroretinograms

Both daytime and nighttime ERGs were performed to evaluate circadian ERG differences and consisted of dark-adapted and light-adapted series and a long flash response (as outlined above). The daytime ERG was started around 1pm (halfway between lights on in the morning and lights off in the evening), and the nighttime ERG was started around 1am (halfway between lights off in the evening and lights on in the morning). Circadian ERGs were done with 5 control birds and 5 affected birds all of which were between 15 and 22 days of age.

### 3.2.5 Data analysis

Raw data was imported into and analyzed with Microsoft Excel 2003 (Microsoft Corporation, Redmond, WA). Pharmacological dissection ERG waveforms were plotted using Excel and visually analyzed. Peak a- and b-wave amplitudes of circadian and long flash ERGs and d-waves of long flash ERGs and implicit times of circadian ERGs were measured and averaged. A-wave amplitudes were measured from the baseline to the lowest trough of the a-wave and b-wave amplitudes were measured from the trough of the a-wave to the highest peak of the b-wave. A 5  $\mu$ Volt criterion threshold was used, meaning any wave with an amplitude of less than 5  $\mu$ Volt was excluded. Implicit times are measured from the time of light onset to the peak of the wave being analyzed.

Affected and control long flash mean a-, b-, and d-wave amplitudes were compared using a t-test. Several comparisons were made for the circadian ERGs. Circadian implicit times and amplitudes were averaged for each light intensity. As a first step in the statistical analysis a descriptive test that included a skewness of the distribution analysis (PROC MEANS, SAS 2001–version 8.2. SAS Institute Inc., Cary, NC, USA) was run on the implicit time and amplitude data. Kolmogorov-Smirnov test of normality also was performed. The distribution of the data revealed to be right-skewed (around +2) and therefore considered as non-Gaussian. The data was then log-transformed and the mean values were compared between day and night using a paired t-test. Emphasis was placed on day/night differences within the groups (affected and control) because previously published results demonstrated significant differences in the ERG responses between control and affected birds (Montiani-Ferreira et al., 2007).

Results were considered statistically significant when  $P$  values were less than 0.05. The resulting data were back-transformed to be shown on graphs and tables.

### **3.3. Results**

#### **3.3.1. Long flash ERGs**

The long flash ERG of both the control and the affected birds contain the same components: a negative a-wave at lights on followed by a positive b-wave, a return to baseline and then a positive d-wave at lights off. The d-wave of the control birds' long flash ERGs quickly rises to a peak, then, following an initial rapid drop from that peak, it slowly returns to baseline. The wave amplitudes of the *rge* long flash a-, b- and d-waves were greatly reduced compared to control birds ( $P < 0.0001$  for each wave). Figure 3.1 shows representative long flash ERG waveforms from an affected and a control bird. Figure 3.2 shows the mean a-, b- and d-wave amplitudes of both control and affected birds.

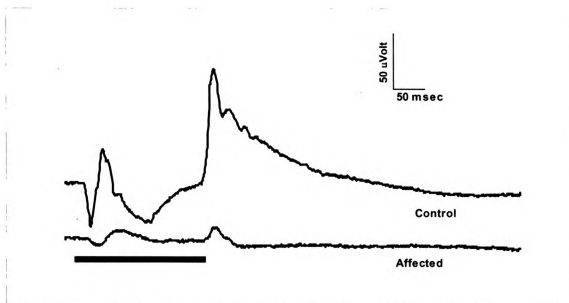


**Figure 3.1.** Long flash ERG. Representative long flash ERG waveforms from a control (top wave) and an affected bird (bottom wave) of comparable ages. Note the markedly attenuated amplitudes of the a-, b- and d-waves of the *rge* chicks. The heavy black bar indicates the length of the flash stimulus (200 msec).

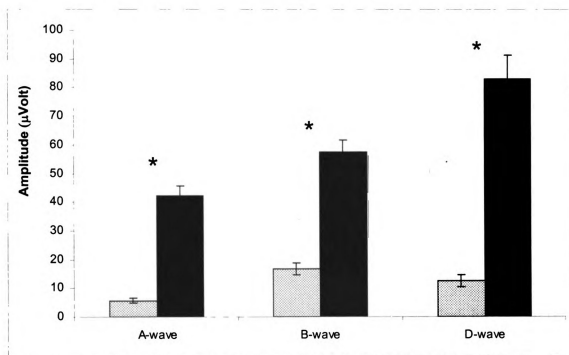


**Figure 3.2.** Mean long flash ERG wave amplitude comparisons. Stippled columns are amplitudes of affected birds, while black columns are amplitudes of control birds. There was a significant difference between affected and control amplitudes for each wave. (\*) indicates a significant difference between affected and controls ( $P < 0.0001$ ).

### 3.3.2. APB Injection

The control chicks' post-APB dark-adapted and light-adapted ERG waveforms were similar in that the b-wave was eliminated, which allowed the a-wave to reach a more negative potential. The peak of the a-wave was followed by a slow return to baseline over the recording time (Figure 3.3 A and B). The return to baseline happened more quickly with the lower intensities than it did at the higher intensities.

APB also eliminated the b-wave of the long flash ERG of the control birds (Figure 3.4 A). It increased the amplitude of the a-wave, which began slowly returning to baseline until lights off. The ON bipolar cell components which are removed by APB are displayed by subtracting the post-injection waveform from the pre-injection waveform (Figure 3.4). In the case of APB injection in the control birds, the subtraction displays the ON response and includes a small negative deflection then a b-wave that does not return to baseline until lights off and a small residual d-wave.

The *rge* chicks' post-APB dark-adapted and light-adapted ERG waveforms were also similar to each other, but differed from those of the control chicks. The APB increased the amplitude of the a-wave and made it wider and had a slight but variable effect on the b-wave (Figure 3.3 C and D). In some birds, the b-wave had a slightly larger amplitude post-injection whereas some birds' b-waves were not altered post-injection.

APB also increased the *rge* a-wave amplitude in the long flash ERG; however, it returned to baseline more rapidly than in the control (Figure 3.4 B). At lights off a positive d-wave was present. The subtraction of the *rge* pre- and post-APB long flash



waveform to reveal the ON bipolar cell response showed a positive going “b-wave” that returned to baseline more rapidly than in the control.

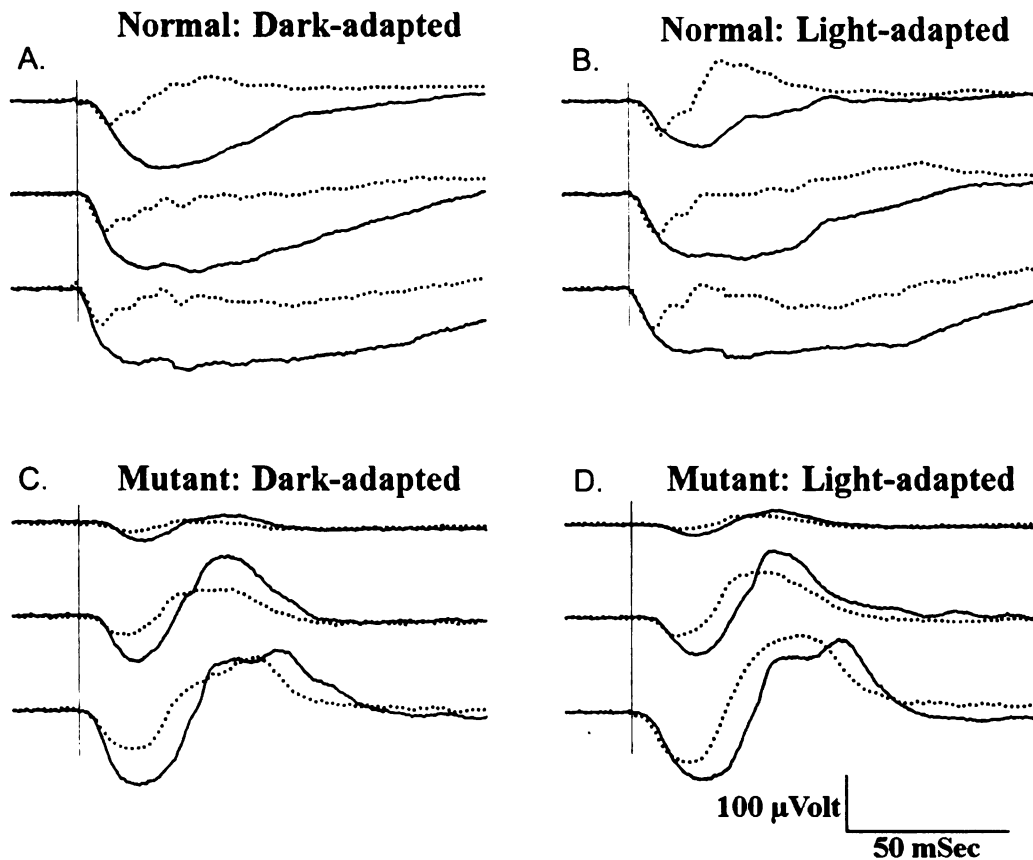


**Figure 3.3.** APB effect on short flash ERG. Representative ERGs showing the effect of intravitreal APB on the ERG of control (A and B) and mutant (*rge*) (C and D) chicks under dark-adapted (A and C) and light-adapted (B and D) conditions. The dotted lines represent the responses prior to intravitreal injection and the solid lines the responses after APB was administered. Note that in the control chick the b-wave is eliminated by APB revealing a portion of the PIII response, whereas in the mutant chick APB has very little effect on the b-wave amplitude but does slightly enhance the a-wave. Flash intensity from top: 0.39, 1.36 and 2.39 log cdS/m<sup>2</sup>. Final concentration of APB was 3 mM.

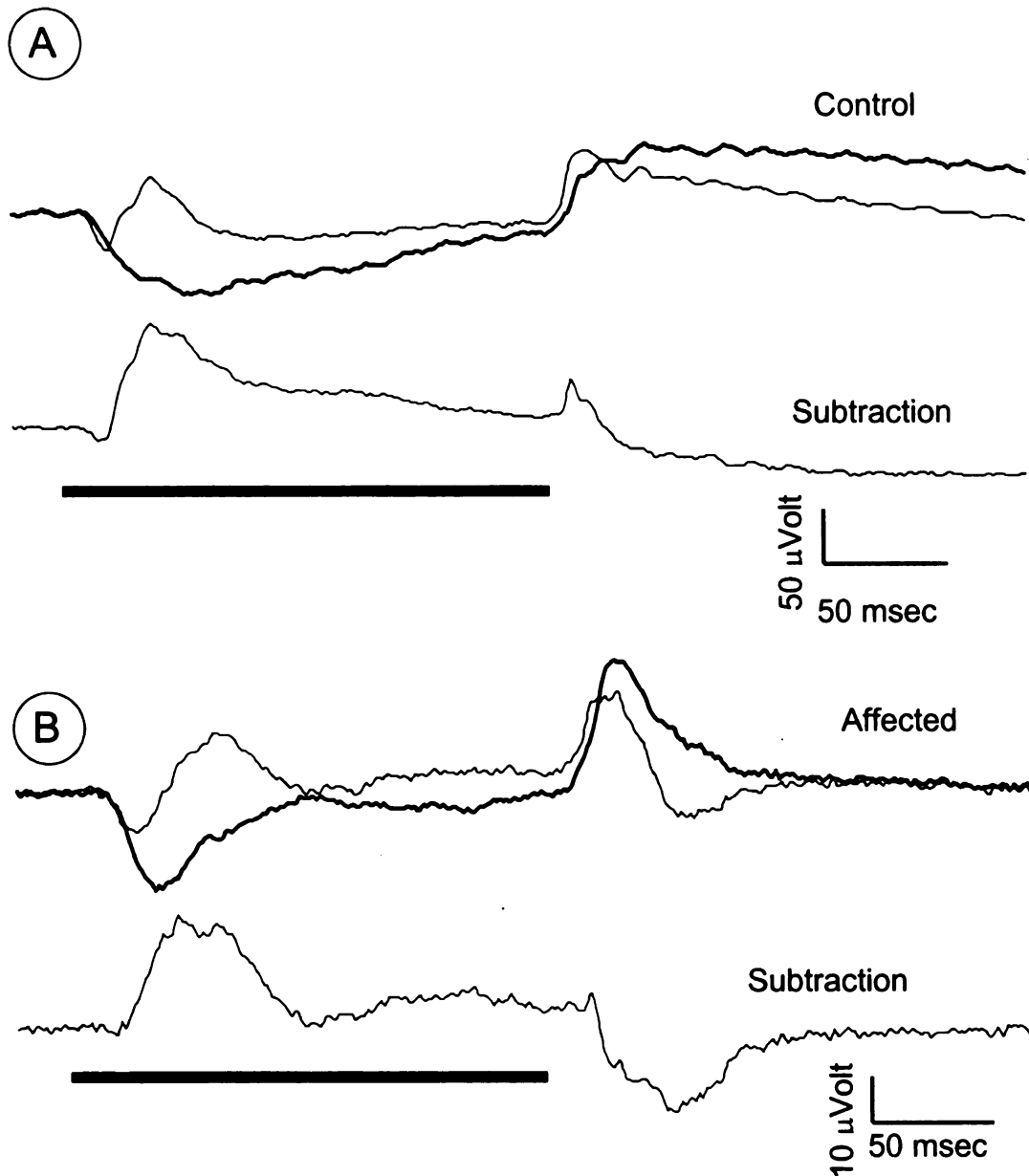


**Figure 3.4.** APB effect on long flash ERG. Representative ERGs showing the effect of intravitreal APB on the long flash ERG of control (A) and affected (B) chicks under light adapted conditions. Heavy black lines represent length of light flash. The thin tracings represent the responses prior to intravitreal injection and the heavier tracings the responses after APB was administered. The tracings labeled "Subtraction" are the pre-injection ERG minus the post-injection ERG and in this case show the response from the ON bipolar cells. Note that the scale for the affected tracings is different from the control tracings. Note that in the control chick the b-wave is eliminated by APB revealing the PIII response, whereas in the mutant chick APB reduces the amplitude of the b-wave but doesn't entirely eliminate it. The effect on the b-wave allows the affected chick's a-wave to reach a larger amplitude than before the injection. Final concentration of APB was 3 mM.

### 3.3.3. PDA injection

PDA blocks a negative component of the control chick ERG resulting in a greatly decreased a-wave amplitude and an increased b-wave amplitude (Figure 3.5 A).

The results of the long flash ERG after PDA injection in control birds is similar to the short flash in that the a-wave is almost completely eliminated and the b-wave amplitude larger. Additionally, the d-wave is almost completely eliminated (Figure 3.6). The components removed by PDA are displayed in the “subtraction” waveform (obtained by subtracting the post-injection waveform from the pre-injection waveform). In the case of PDA injection in the control birds, the subtraction displays the OFF response and includes a negative potential at lights on, which would contribute to the generation of the a-wave and decrease the b-wave amplitude, and a positive wave at lights off, which forms the major portion of the d-wave. In other words, the OFF bipolar cells, the horizontal cells and third order neurons have opposite potentials at lights on (and oppose the b-wave) and a positive response at lights off to form most of the d-wave.

PDA consistently made the slope of the a-wave shallower, increased the a-wave implicit time and decreased the amplitude of the b-wave of the *rge* chicks’ ERGs (Figure 3.5 B).

PDA decreased the *rge* a-wave amplitude, increased the implicit time and delayed the beginning of the downward slope of the a-wave in the long flash (Figure 3.6 B). Although both waves were still present post-PDA injection, the amplitude of both the b- and d-waves was greatly decreased. The subtraction waveform displays the contributions of the OFF bipolar cells, horizontal cells and the third order neurons and in the case of the

*rge* birds includes components of a-, b- and d-waves and is quite different from that of the control birds.

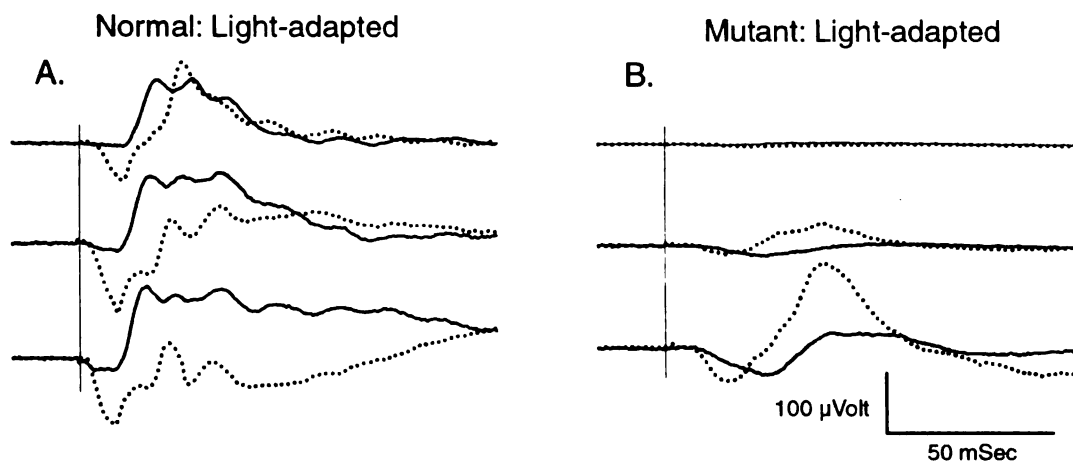


**Figure 3.5.** PDA effect on short flash ERG. Representative ERGs showing the effect of intravitreal PDA on the ERG of control (A) and *rge* (B) chicks under light-adapted conditions. The dotted lines represent the responses prior to intravitreal injection and the solid lines the responses after PDA was administered. A negative component of the control chick ERG is removed resulting in a reduction in a-wave amplitude. The photopic hill effect is also removed. The result in the mutant bird is quite different in that PDA appears to remove a positive component of the b-wave thus reducing the b-wave amplitude. It also results in a delay in the a-wave. Flash intensity from top: 0.39, 1.36 and 2.39 log cdS/m<sup>2</sup>. Final concentration of PDA was 7mM.

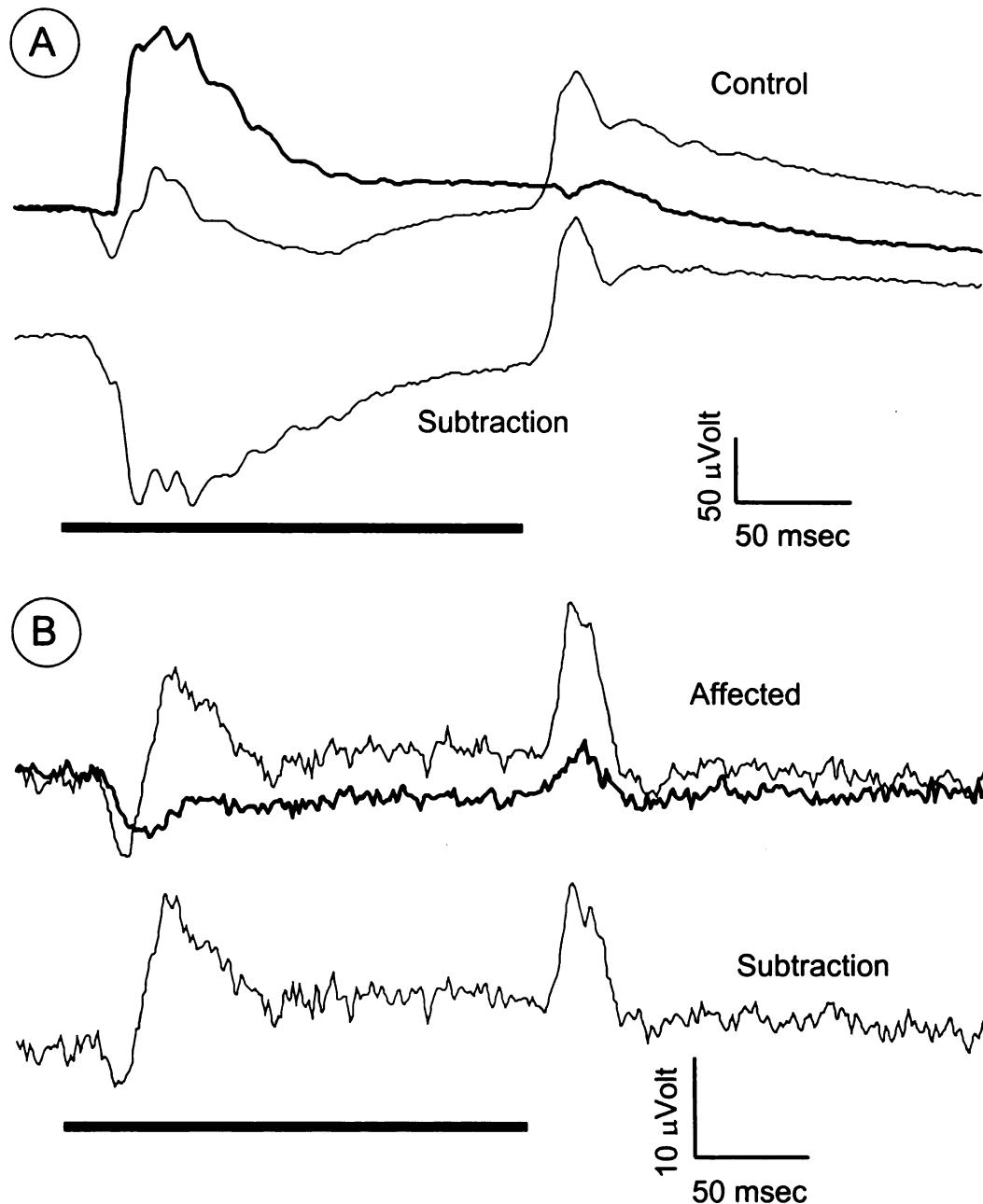


**Figure 3.6.** PDA effect on long flash ERG. Representative ERGs showing the effect of intravitreal PDA on the long flash ERG of control (A) and affected (B) chicks under light adapted conditions. Heavy black lines represent length of light flash. The thin tracings represent the responses prior to intravitreal injection and the heavier tracings the responses after PDA was administered. The tracings labeled "Subtraction" are the pre-injection ERG minus the post-injection ERG and in this case show the response from the OFF bipolar cells and any downstream responses from second and third order neurons. Note that the scale for the affected tracings is different from the control tracings. Note that in the control chick a negative component at lights-on is eliminated, which almost completely eliminated the a-wave and greatly increased the b-wave. Additionally, the d-wave is greatly decreased at lights-off. In the affected chick, PDA greatly reduces the amplitude of all three waves (a-, b- and d-waves) and delays the beginning of the down slope of the a-wave. Final concentration of PDA was 7mM.

#### 3.3.4. Aspartate injection

Aspartate completely eliminated the b-wave of both the control chicks' dark-adapted and light-adapted ERGs, thus revealing the true amplitude of the PIII response (Figure 3.7 A and B).

Aspartate had similar effects on the control chicks' long flash ERG in that it eliminated the b-wave and in doing so greatly increased the a-wave amplitude and implicit time (Figure 3.8 A). At lights off, a d-wave appeared, but it had a longer implicit time and was wider than the pre-injection d-wave, much like the d-wave post-APB injection. As expected, the aspartate subtraction included an immediate negative potential at lights on (which must contribute to the a-wave), a positive potential (which makes up the b-wave), and a positive response at lights off.

Aspartate had the same effect on the *rge* ERG waveforms as it did on the control chicks' ERG waveforms in that it eliminated the b-wave in both the dark-adapted and light-adapted ERGs, thus increasing the a-wave amplitude and implicit time (Figure 3.7 C and D). However, unlike the control birds, the remaining amplitude in the light-adapted series was smaller in amplitude than that of the dark-adapted series.

The post-aspartate long flash of the *rge* chicks was similar in shape to that of the control chicks but lower in amplitude. The b-wave was eliminated thus increasing the a-wave amplitude and implicit time and the d-wave amplitude was decreased and appeared wider (Figure 3.8 B). The subtraction waveform was also similar to the control birds, but lower in amplitude.



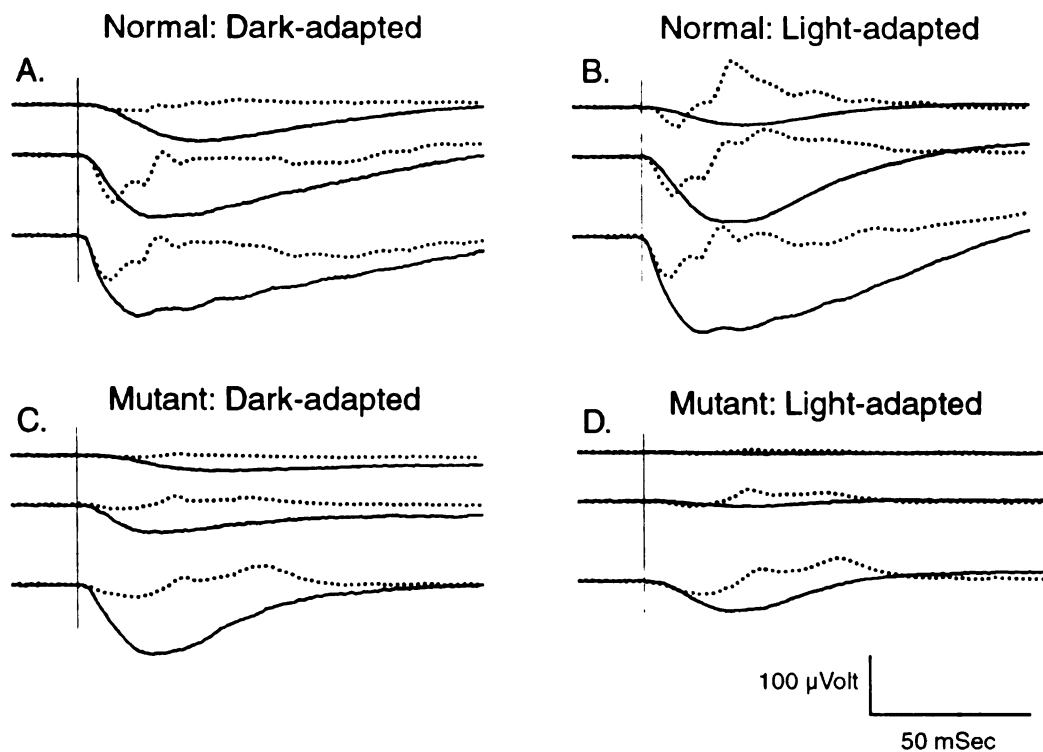


**Figure 3.7.** Aspartate effect on short flash ERG. Representative ERGs showing the effect of intravitreal aspartate on the ERG of control (A and B) and GNB3 mutant (C and D) chicks under dark-adapted (A and C) and light-adapted (B and D) conditions. The dotted lines represent the responses prior to intravitreal injection and the solid lines the responses after aspartate was administered. Aspartate removes the post-receptor responses in both control and GNB3 mutant birds leaving the PIII (photoreceptor) response. Flash intensity from top: 0.39, 1.36 and 2.39 log cdS/m<sup>2</sup>. Final vitreal concentration of aspartate was 50mM.

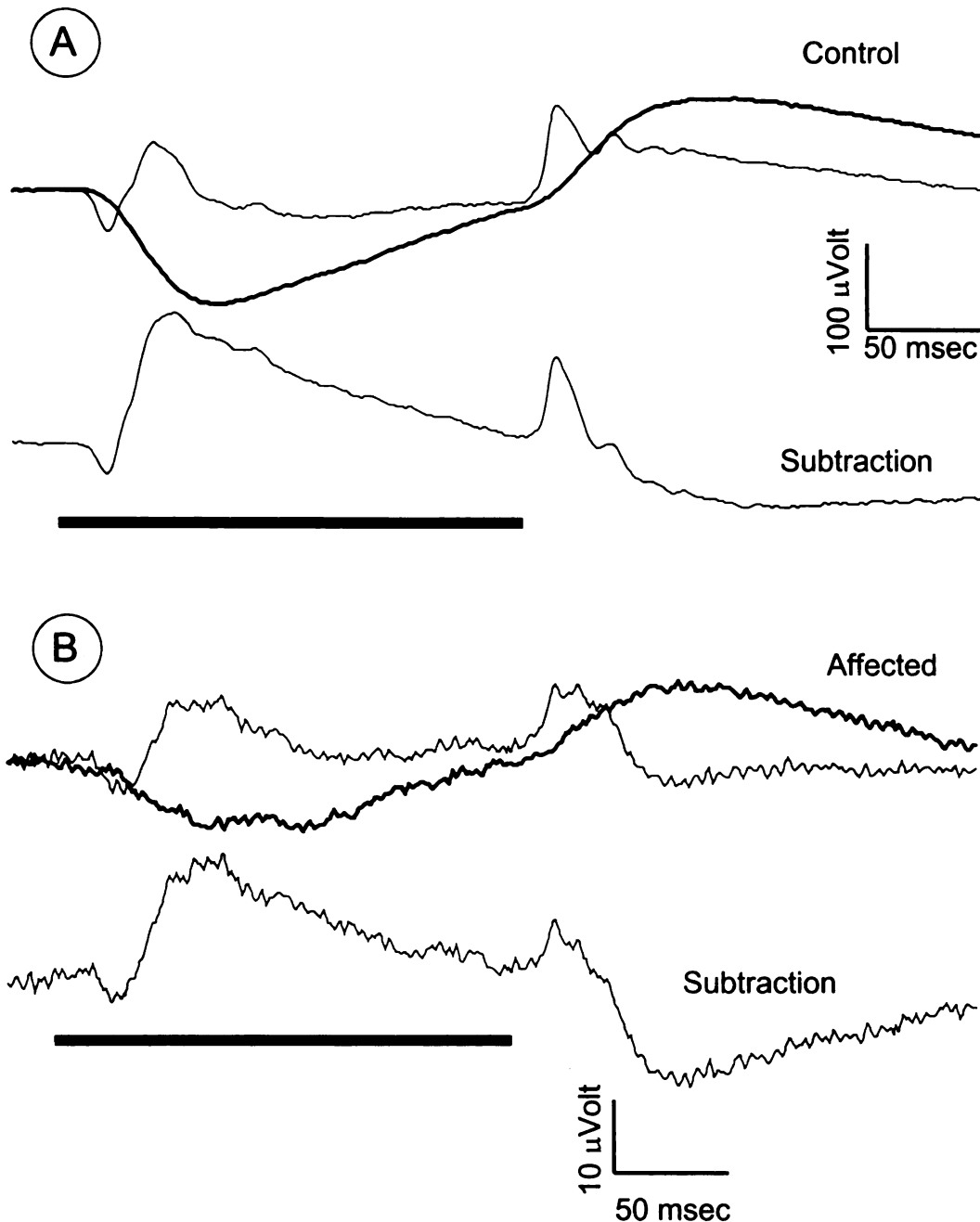
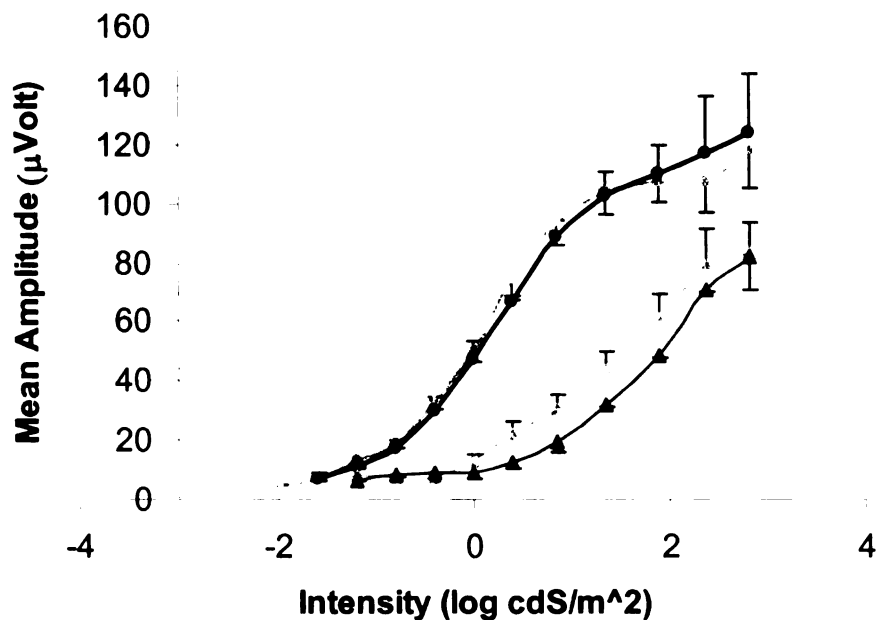


**Figure 3.8.** Aspartate effect on long flash ERG. Representative ERGs showing the effect of intravitreal aspartate on the long flash ERG of control (A) and affected (B) chicks under light adapted conditions. Heavy black lines represent length of light flash. The thin tracings represent the responses prior to intravitreal injection and the heavier tracings the responses after PDA was administered. The tracings labeled "Subtraction" are the pre-injection ERG minus the post-injection ERG and in this case show the photoreceptor response. Note that the scale for the affected tracings is different from the control tracings. In both chicks, the b-waves were eliminated leaving the PIII response, but a component of the d-wave was spared. Final concentration of aspartate was 50mM.

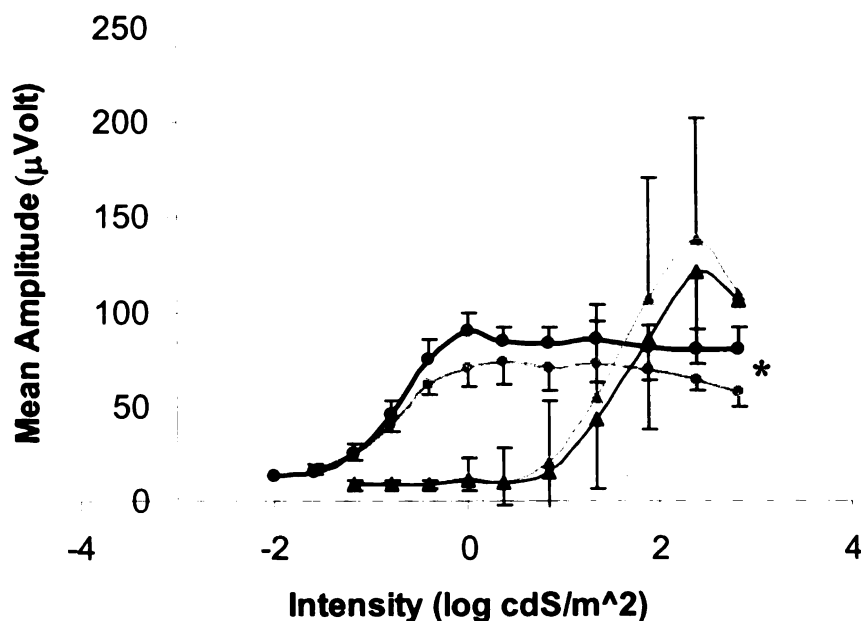
### 3.3.5. Circadian ERGs

Figure 3.9 displays the mean dark-adapted a-wave amplitudes of both control and affected birds during the nighttime and daytime. There were no statistically significant differences between nighttime and daytime amplitudes for either group.

Figure 3.10 contains the averaged dark-adapted b-wave amplitudes of both control and affected birds during the nighttime and daytime. The affected birds' dark-adapted b-wave amplitudes were larger than those of the control birds at the higher intensities (the "supernormal" b-wave) (Figure 3.10), which has been reported previously (Montiani-Ferreira et al., 2007). The control birds' dark-adapted b-wave amplitudes reached a plateau at relatively low light intensities, whereas the affected birds' dark-adapted b-wave amplitudes peaked at a much higher intensity. When the overall day and night dark-adapted b-wave amplitudes were compared they were found to be significantly different ( $P = 0.017$ ).



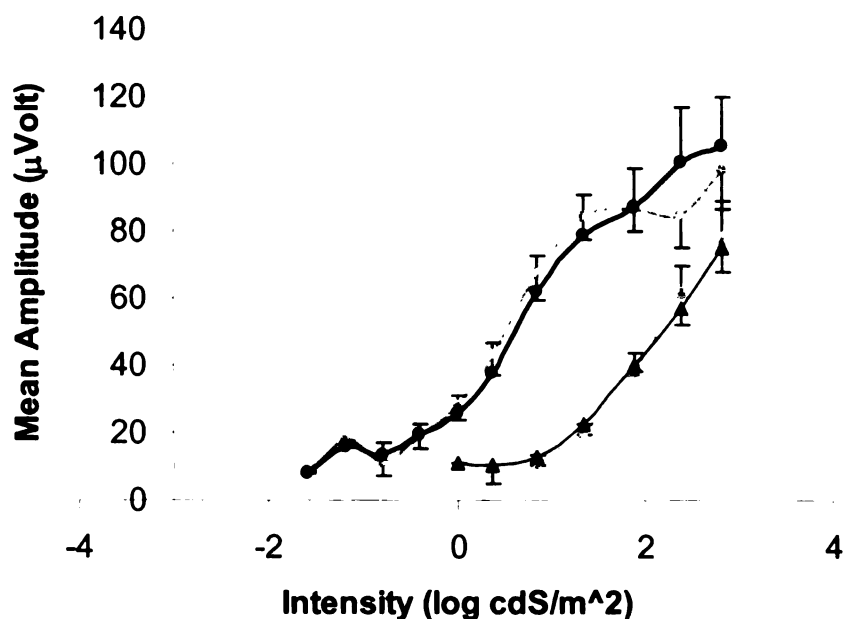
**Figure 3.9.** Mean dark-adapted circadian a-wave amplitudes. Gray tracings indicate daytime amplitudes and black tracings indicate nighttime amplitudes. Heavy tracings with circles are control chicks and those with triangles are affected chicks. Error bars display standard error of the mean. None of the differences between day and night were significant.



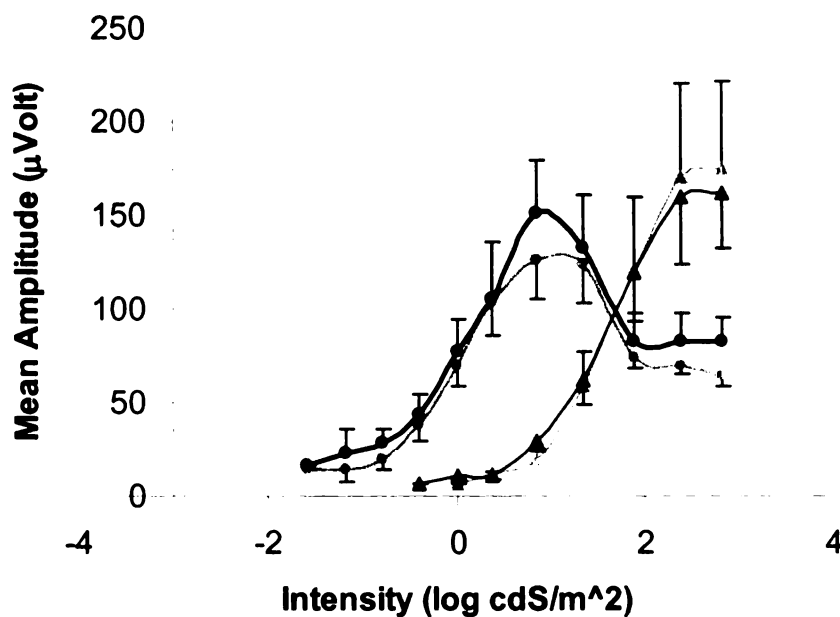
**Figure 3.10.** Mean dark-adapted circadian b-wave amplitudes. Gray tracings indicate daytime amplitudes and black tracings indicate nighttime amplitudes. Heavy tracings with circles are control chicks and those with triangles are affected chicks. Error bars display standard error of the mean. (\* indicates a significant difference between by the overall day and night amplitudes for the control birds only ( $P = 0.017$ )).

Figure 3.11 displays the mean light-adapted a-wave amplitudes of both control and affected birds during the nighttime and daytime. There were no statistically significant differences between nighttime and daytime amplitudes for control or affected birds.

Figure 3.12 displays the mean light-adapted b-wave amplitudes of both control and affected birds at nighttime and daytime. The control birds' b-wave amplitudes exhibit a "photopic hill" in that the highest amplitudes are reached at intermediate intensities after which point the amplitudes decrease. The affected birds' light-adapted b-wave amplitudes are larger than those of control birds at the higher intensities (the "supernormal b-wave") as reported previously (Montiani-Ferreira et al., 2007). Control birds' light-adapted b-wave amplitudes were slightly greater at night than during the daytime, but the differences were not statistically significant. Affected birds' light-adapted b-wave amplitudes were similar at night and during the day with no statistically significant differences.



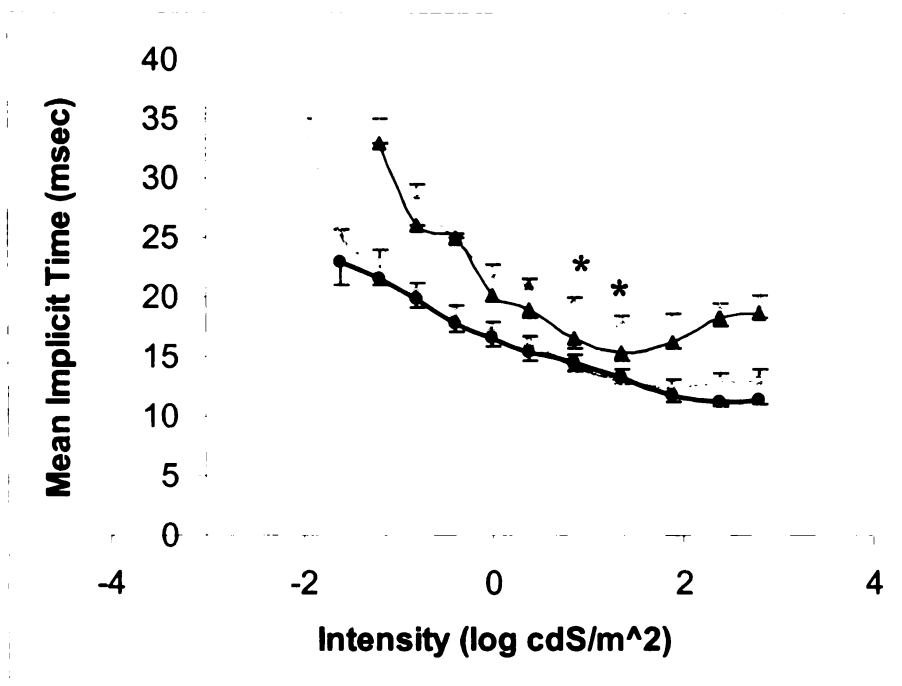
**Figure 3.11.** Mean light-adapted circadian a-wave amplitudes. Gray tracings indicate daytime amplitudes and black tracings indicate nighttime amplitudes. Heavy tracings with circles are control chicks and those with triangles are affected chicks. Error bars display standard error of the mean.



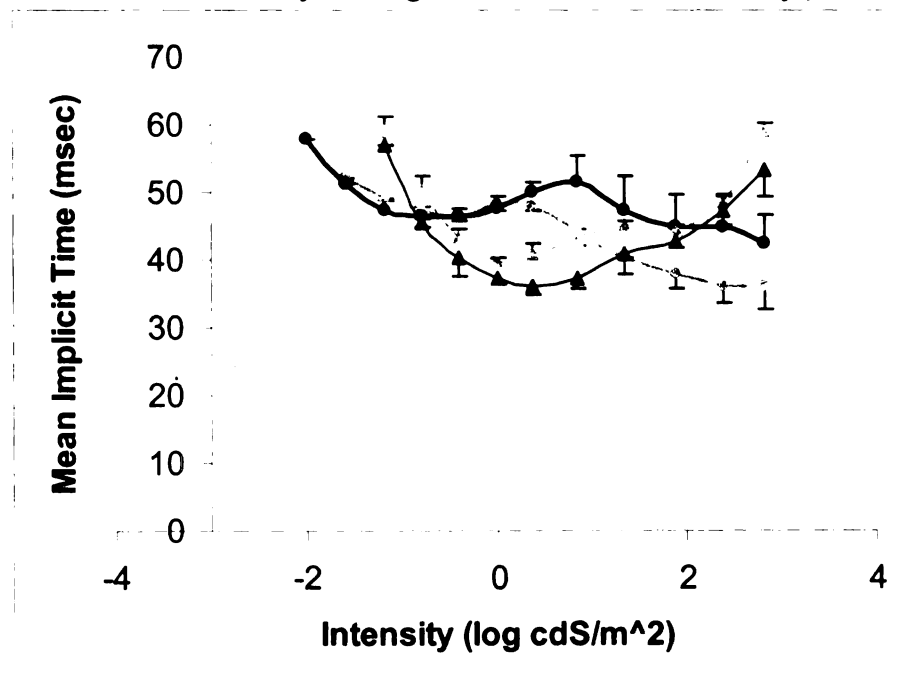
**Figure 3.12.** Mean light-adapted circadian b-wave amplitudes. Gray tracings indicate daytime amplitudes and black tracings indicate nighttime amplitudes. Heavy tracings with circles are control chicks and those with triangles are affected chicks. Error bars display standard error of the mean.

Figure 3.13 displays the mean dark-adapted a-wave implicit times of both control and affected birds at night and during the day. The affected birds' a-wave implicit times were longer than those of the control birds at all intensities, which was previously reported (Montiani-Ferreira et al., 2007). Notice that for both groups, the higher the intensity, the shorter the implicit time. There were only two intensities at which there was a significant difference between day and night a-wave implicit time for the affected birds ( $P < 0.05$ ). There were no other significant differences between day and night for the groups.

Figure 3.14 shows dark-adapted b-wave implicit times of both control and affected birds at night and during the day. Figure 3.15 shows light-adapted a-wave implicit times of both control and affected birds at night and during the day. Figure 3.16 shows light-adapted b-wave implicit times of both control and affected birds at night and during the day. There were several intensities for which the affected birds had significant differences in b-wave implicit times between day and night, but for the most part, there were no significant differences between day and night.



**Figure 3.13.** Mean dark-adapted circadian a-wave implicit times. Gray tracings indicate daytime amplitudes and black tracings indicate nighttime amplitudes. Heavy tracings with circles are control chicks and those with triangles are affected chicks. Error bars display standard error of the mean. (\* indicates a significant difference between day and night for the affected birds only.)



**Figure 3.14.** Mean dark-adapted circadian b-wave implicit times. Gray tracings indicate daytime amplitudes and black tracings indicate nighttime amplitudes. Heavy tracings with circles are control chicks and those with triangles are affected chicks. Error bars display standard error of the mean. (\* indicates a significant difference between day and night for the affected birds only.)



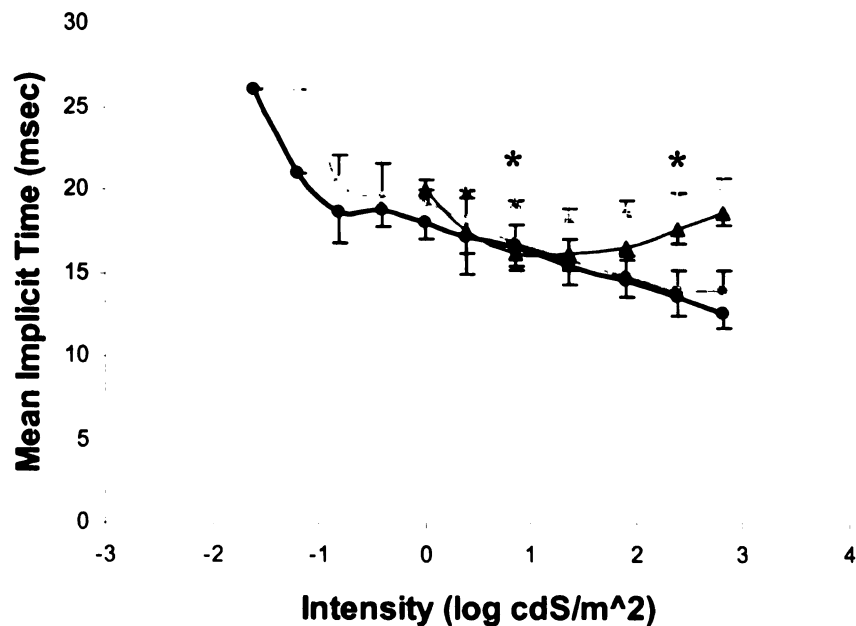


**Figure 3.15.** Mean light-adapted circadian a-wave implicit times. Gray tracings indicate daytime amplitudes and black tracings indicate nighttime amplitudes. Heavy tracings with circles are control chicks and those with triangles are affected chicks. Error bars display standard error of the mean. (\* indicates a significant difference between day and night for the affected birds.)

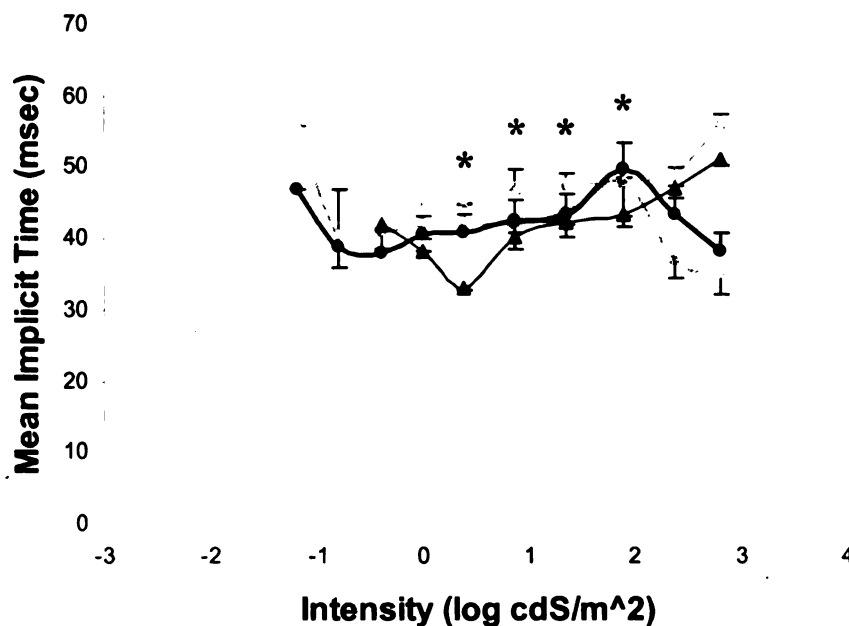


**Figure 3.16.** Mean light-adapted circadian b-wave implicit times. Gray tracings indicate daytime amplitudes and black tracings indicate nighttime amplitudes. Heavy tracings with circles are control chicks and those with triangles are affected chicks. Error bars display standard error of the mean. (\* indicates a significant difference between day and night for the affected birds.)

### 3.4. Discussion

The long flash ERG of both the control and the affected birds contain the expected components (a-, b- and d-waves); however, the affected birds had greatly (and significantly) reduced amplitudes compared to the controls. The brightest intensity that the long flash Ganzfeld stimulator is capable of producing is  $180 \text{ cd/m}^2$ , which is not bright enough to elicit the “supernormal b-wave” seen in the brighter short flash intensities. Although the amplitudes were lower in the affected birds, the long flash does indeed contain both an ON and an OFF response meaning that those responses were intact in the *rge* birds.

As was found previously, APB eliminated the b-wave in both the dark-adapted and light-adapted ERGs of control chicks, thus the a-wave was prolonged and enhanced (Montiani-Ferreira, 2004). APB, a glutamatergic receptor agonist that acts on metabotropic glutamate receptors, has been shown to isolate the OFF-hyperpolarizing responses by maintaining the ON bipolar cells in a hyperpolarized state, thus removing the majority of the b-wave of the ERG (Slaughter and Miller, 1981; Stockton and Slaughter, 1989; Xu et al., 2003; Sharma et al., 2005). The results of the long flash are similar in that the b-wave was eliminated.

The subtraction waveform revealed that the ON bipolar cells contribute to each of the basic ERG components (a-, b- and d-waves). It is interesting that the ON bipolar cells appear to make up part of the d-wave considering the d-wave is usually considered to be the OFF response. The APB-sensitive portion of the d-wave appears to be quick to rise and quick to decline, which would appear to shape the d-wave by shortening the implicit time and beginning a return to baseline. This finding regarding the d-wave suggests that

ON bipolar cells play some sort of role in the d-wave. Ueno et al (2006) found that both ON bipolar cells and cone photoreceptors contribute to the d-wave of the electroretinogram, which may help to explain the finding that the APB-sensitive ON bipolar cells appears to contribute to the chicken d-wave.

APB did not eliminate the *rge* b-wave, which is similar to a previous attempt (Montiani-Ferreira, 2004). This lack of response of the *rge* b-wave suggests that it either does not originate from ON bipolar cells or that the *rge* ON bipolar cells are incapable of responding to APB the way normal ones are. The long flash results show that there is some reduction in b-wave. The quick return to baseline after the a-wave in the post-injection APB long flash could potentially be considered solely the response of the photoreceptors; however, when the post-APB long flash is compared to the post-aspartate long flash (Figures 3.4 B and 3.8 B), the isolated photoreceptor response after aspartate returns to baseline much slower than that of APB. This suggests that the return to baseline after the a-wave in the post-APB long flash is composed of inner retinal contributions (such as ON or OFF bipolar cells).

The post-APB d-wave is slightly larger than the pre-injection d-wave. Therefore, it appears that the ON bipolar cells in the *rge* chicks contribute partially to the b-wave and compete with the positive-going d-wave (OFF response). Unlike in the control birds in which the ON bipolar cells appear to contribute positively to the d-wave, the *rge* birds' ON bipolar cells appear to contribute only negatively to the OFF response.

The post-APB injection results may help to explain the *rge* chicks' lack of oscillatory potentials (OPs). OPs are thought to originate from negative feedback from

amacrine cells to second order neurons. If the input from ON bipolar cells to amacrine cells is disrupted in *rge* birds it might prevent the development of OPs.

PDA, a glutamatergic receptor antagonist, isolates the response of the photoreceptors and ON-depolarizing bipolar cells by blocking transmission from photoreceptors to OFF bipolar cells and horizontal cells and transmission from bipolar cells to third order neurons (Slaughter and Miller, 1983; Stockton and Slaughter, 1989). The results of the PDA injection in control chicks is similar to that previously reported in primates and other species (Sieving et al., 1994; Xu et al., 2003) in which a negative component is removed, thus reducing the a-wave amplitude and increasing the b-wave amplitude. The long flash results are similar to the short flash results in that the a-wave is eliminated and the b-wave amplitude is increased. The d-wave is almost completely eliminated by PDA, which is expected since it blocks the transmission from photoreceptors to OFF bipolar cells.

The post-PDA injection long flash waveform is roughly similar in shape to that which is eliminated by APB (i.e. the subtraction – compare Figure 3.6 and 3.4), which would be anticipated because APB eliminates the ON response (leaving the OFF response) and PDA eliminates the OFF response (leaving the ON response). Similarly, the post-APB long flash waveform (i.e. the OFF response) is roughly similar in shape to that which is eliminated by PDA (i.e. the OFF response).

Previous attempts to dissect the *rge* ERG with PDA by Montiani-Ferreira revealed it had no effect on the waveform; however, a lower concentration (5 mM) was used, whereas in this study, 7mM was used. The difference in concentrations may help to explain the difference in effects of PDA on the ERG waveform. PDA had almost an

opposite effect on the *rge* ERG waveform compared to controls as it increased the implicit time of the a-wave and greatly reduced the b-wave amplitude. Similarly the long flash a-, b- and d-waves were decreased in amplitude and had increased implicit times. These results suggest that the PDA sensitive components of the *rge* ERG may be biphasic; there is an initial negative component that contributes to the a-wave generation followed by a slower positive component that contributes a positive component to the b-wave. And ultimately, this suggests that unlike the control birds, the OFF pathway in the *rge* birds contributes a great deal to the ERG waveform.

Aspartate blocks all post-receptoral responses, thus revealing the PIII response or the fast component of the a-wave, which originates from the photoreceptors (Cervetto and MacNichol, Jr., 1972; Murakami et al., 1975). This was found to be true for both the control and the affected chicks in this study in that the b-wave was completely eliminated, leaving only the PIII response. The larger post-injection a-wave amplitude in dark-adapted compared to light-adapted ERG waveforms suggest that cones are not as capable of responding to light stimulation as rods are in the *rge* chicken.

Evidence suggests that inactive transducin is loosely associated with the rod outer segment disc membrane (and thus rhodopsin which is a transmembrane receptor) (Phillips et al., 1992; Herrmann et al., 2006). If transducin in cones is similarly located, then GNB3 might play an important role of physically positioning the  $\alpha$  subunit where it can interact with activated rhodopsin. Therefore if the mutant GNB3 does not bind with the  $\alpha$  subunit adequately, it might not be available to interact with metarhodopsin II. This would suggest that cones would have a decreased efficiency of photoactivation. This possibility is supported by the *rge* aspartate results.

Aspartate had similar effects on the both the control and affected chicks' long flash ERGs in that it eliminated the b-wave and in doing so revealed the PIII response. At lights off, a d-wave appeared, but it had a larger implicit time and was wider than the pre-injection d-wave, suggesting that the chicken d-wave originates from both pre- and post-receptoral sources as suggested in primates (Ueno et al., 2006). What remained after the aspartate injection is solely from the photoreceptors; at lights on, the photoreceptors slowly hyperpolarize and at lights off, they slowly depolarize.

The control chicks' dark-adapted b-wave amplitudes were significantly different between night and day when all intensities were compared together; however, none of the individual intensities were significant when compared between night and day. The *rge* chicks did not have any statistically significant differences between day and night a- or b-wave amplitudes. Only a few intensities had significant differences in implicit times for a- and b-waves in the affected chicks, suggesting that neither group had an obvious or robust circadian rhythm to their ERG responses in these experiments. This was an unexpected result as ERGs in normal birds have been shown to have a circadian rhythm in previous studies (Schaeffel et al., 1991; Manglapus et al., 1998; Wu et al., 2000). It may be possible that a larger number of birds need to be used to demonstrate significant differences between day and night.

Several of the previously reported circadian studies use much different ERG protocols, making our results difficult to compare with theirs. For instance, Wu et al did not dark adapt the birds before day-time ERGs, so the ERG responses would be mostly cone responses, whereas at night, the responses would be mostly rod responses. Manglapus et al kept the quail used in the study dark adapted for 50 hours over which

time they recorded ERGs. This would confuse the results as well because not only would the quails' circadian rhythms begin to disintegrate over the 50 hours of darkness, but the day-time ERGs would initially be a mixed rod/cone response but as the retina lost its circadian rhythm and became dark adapted, the cones would no longer be as responsive.

## CHAPTER 4:

### CONCLUSION & FUTURE STUDIES

#### 4.1. Conclusion

GNB3 was reported to be the causative gene and mutation of the *rge* chick phenotype by another research group (Tummala et al., 2006) during the research for this project. The GNB3 Asp153 deletion was confirmed in our *rge* chicks and is found in a highly conserved region of the gene. Although it is difficult to absolutely prove that GNB3 is the gene and the Asp153 deletion is the mutation (and only mutation) responsible for *rge* phenotype and not just a rare polymorphism that happens to be in linkage disequilibrium with the disease status, the finding by Tummala et al (2006) that there was a 70% decrease in GNB3 immunoreactivity in the retina supports the idea that GNB3 is responsible. The examination of the electroretinographic changes can be partially explained by the known functions of GNB3, but there remain some unexplained changes in the *rge* ERG.

GNB3 has been shown to be part of cone-transducin, which is the guanine nucleotide binding protein involved in phototransduction in cones coupled to phosphodiesterase (Peng et al., 1992). Thus GNB3 plays an important role in regulating the response of the cone photoreceptors to light stimulation. When the mutation (aspartic acid residue deletion present in *rge* birds) was modeled with GNB1, it was shown to eliminate  $\beta$  sheets in propellers 1 and 5 of the GNB protein and was predicted to create an unstable protein susceptible to premature proteolysis (Tummala et al., 2006). By causing this amount of tertiary protein misfolding, this mutation is likely to interfere with



the  $\beta\gamma$  complex's ability to bind to the  $\alpha$  subunit, which in turn is likely to interfere with the heterotrimer's ability to interact with the 11-*cis* retinal/cone opsin and the facilitation of the  $\alpha$  subunit activation (Phillips et al., 1992; Yarfitz et al., 1994; Herrmann et al., 2006). If the  $\beta\gamma$  complex were unable to bind to interact with either metarhodopsin II (Rho\*) or with the  $\alpha$  subunit, it may affect the cone cell's ability to respond to light stimulation. Additionally, according to Tummala et al, there is a 70% reduction in GNB3 immunoreactivity in the *rge* retina, which would further contribute to disrupting phototransduction. These predicted consequences could potentially cause a reduction in cone sensitivity and perhaps slowed termination of the phototransduction cascade.

In rods, it has been shown that one responsibility of the  $\beta\gamma$  complex is to anchor the  $\alpha$  subunit to the disc membrane in close proximity to activated rhodopsin (Phillips et al., 1992; Herrmann et al., 2006). Because of the similarities between rods and cone, it could be assumed that the  $\beta\gamma$  dimer in cones has similar responsibilities to that of rods. Therefore, the mutation likely alters the  $\beta\gamma$  complex's ability to bind to the  $\alpha$  subunit and anchor it close to opsin in the cone photoreceptors. Because of this, phototransduction could be less efficient in the *rge* birds because the  $\alpha$  subunit is not available to activated opsin and photons of light would go "unnoticed" by the photoreceptor because visual transduction is not taking place properly. These "oblivious" cone photoreceptors may explain why the cones in *rge* chickens appear to be less sensitive. The cone responses that are still present may be explained by a much less efficient phototransduction pathway that is nonetheless still able to produce responses in affected cells.

The results of the aspartate injection on the *rge* ERG support the reduced cone function hypothesis because the remaining PIII response exposed after aspartate

administration is smaller than that of the mixed rod:cone response (Figure 3.7) suggesting that *rge* cones do not function as well as *rge* rods. This finding suggests that the *rge* chicken's cone photoreceptors have reduced sensitivity compared to rods. This may be due to both a reduction in GNB3 protein and to an altered function of the remaining mutant GNB3 protein.

The phototransduction cascade is terminated by the inherent GTP hydrolyzing activity of the transducin  $\alpha$  subunit; following GTP hydrolysis, the bound PDE  $\gamma$  subunit is released and is available to inhibit the active  $\alpha/\beta$  PDE complex. The finding that *Drosophila* mutants with G $\beta$  mutations have slowed deactivation of phototransduction, as well as reduced sensitivity (Dolph et al., 1994), suggest that the  $\beta\gamma$  complex plays a role in transducin deactivation (Sagoo and Lagnado, 1997).

In addition to its role in cone phototransduction, GNB3 has been found to be associated with dendrites of both rod and cone ON bipolar cells and the alpha subunit of a heterotrimeric G-protein ( $G_o$ ) in the outer plexiform layer (Huang et al., 2003). The metabotropic glutamate receptor (mGluR6) is also associated with this exact retinal location (dendritic tips of ON bipolar cells in the outer plexiform layer) and has also been shown to interact with  $G_o\alpha$  (Nomura et al., 1994; Vardi and Morigiwa, 1997; Weng et al., 1997; Vardi et al., 2000) suggesting that GNB3 may be associated with the signal transduction resulting from the activation of mGluR6.

mGluR6 is stimulated by glutamate release from the photoreceptors that occurs when they are depolarized, which is the resting (dark) state of photoreceptors. The stimulation from glutamate release causes closure of cation channels in the ON bipolar cell dendrite. When the photoreceptor is stimulated by light, it becomes hyperpolarized.

This reduces the rate of photoreceptor glutamate release and thus reduces the tonic stimulation of mGluR6 that occurs in the dark, leading to opening of the cation channels in the ON bipolar cell dendrites and depolarization of the cell.  $G_o$  is thought to link mGluR6 to an effector that closes the ON bipolar cell channel (Nawy and Jahr, 1990). The finding that mice deficient in the  $G_o\alpha$  subunit lack the b-wave of the electroretinogram showed that the light response of ON bipolar cells requires  $G_o$  (Dhingra et al., 2000; Dhingra et al., 2002). It is known that mGluR6 couples the reduced glutamate release by photoreceptor cells in response to light, to the depolarization of ON-bipolar cells, via an as-yet unidentified cation channel (Nawy, 1999). This could potentially mean that the mutated GNB3 in the *rge* chicken disrupts the normal response of the ON bipolar cells by disallowing the normal interactions of mGluR6 with the  $G_o\alpha$  subunit of the heterotrimeric G protein. And ultimately, this could mean that the ON bipolar cells are unable to depolarize (as efficiently) in response to a decrease in glutamate from the hyperpolarizing photoreceptors, which may result in a lower amplitude ON response from the bipolar cells.

This hypothesis of altered ON bipolar cell response is supported by the results of the APB injection. APB selectively stimulates the mGluR6 glutamate receptor located solely in ON bipolar cells thus maintaining it in the hyperpolarized state; therefore, it typically eliminates the b-wave (Slaughter and Miller, 1981). As predicted, APB eliminated the b-wave of the control chicken ERG; however, it had almost no effect on the *rge* ERG (Figures 3.3 and 3.4). These results suggest that the *rge* b-wave does not originate from the ON bipolar cells or that they are unable to respond the way normal ones do.

The bulk of the b-wave of other species has been shown to originate from the ON bipolar cells; however, other retinal cells are also known to contribute to the b-wave as well. The b-wave is currently accepted to be the summation of opposing inputs from both ON and OFF pathways with modification of the waveform by contributions from third order retinal neurons (Sieving et al., 1994; Kapousta-Bruneau, 2000; Dong and Hare, 2000; Dong and Hare, 2002). The ON bipolar cells do not appear to make a major contribution to the *rge* b-wave based on the lack of response to APB. Another possibility is that it originates from the OFF pathway and third order neurons.

The PDA injection provides further insight into the *rge* phenotype. PDA is known to block the photoreceptor to OFF bipolar cell (cone pathway only) as well as photoreceptor to horizontal cells and bipolar cells to third order neuron connections. In the normal chick, it unmasks a positive component (assumed to be the ON bipolar cell contribution) thus greatly reducing the a-wave amplitude and eliminating the photopic hill effect. PDA had the opposite effect in the *rge* birds in that it increased the a-wave implicit time and decreased the b-wave amplitude (Figures 3.5 and 3.6). These results suggest that the *rge* waveform may have two different PDA sensitive components; one that contributes to the a-wave generation and one that later contributes to the b-wave.

It is possible that the lack of functional GNB3 protein in the *rge* retina has caused the retinal cells to create connections to different cells. This phenomenon has been reported in the CNGA3 knock-out mice, which lack functional cones. In this model, the cone bipolar cells create ectopic connections with rod photoreceptors (Haverkamp et al., 2006). Therefore, it is possible that the altered cone and ON bipolar cell function in the

*rge* chicken causes other retinal cells to create new connections, which may help to explain the abnormal pharmacological dissection findings.

Although the focus thus far has been on altered cone function, previous work with the *rge* chicken suggested that rod mediated vision is also affected. The *rge* chicks have elevated scotopic (dark adapted or rod-mediated) ERG response threshold (require brighter light stimuli to elicit a response) compared to controls, lower a-wave amplitudes, reduced visual acuity in dim light, and mislocalization and disorganization of opsin-positive rod OSs (Montiani-Ferreira and Petersen-Jones, 2003; Montiani-Ferreira et al., 2005; Montiani-Ferreira et al., 2007). Because rod photoreceptors utilize GNB1 in their visual transduction cycle (and not GNB3), they should function normally; however, since they synapse with (rod) ON bipolar cells, which have also been shown to contain G<sub>o</sub> $\alpha$  and GNB3 immunoreactivity, their signal would be abnormal, which may appear to manifest as defective rod function.

Oscillatory potentials (Figure 1.8) are thought to be the result of inhibitory feedback from amacrine cells to second order neurons. If ON bipolar cells' signal was affected in the *rge* chicken, the amacrine cells might not receive the appropriate signal, thus preventing oscillatory potentials from occurring. Chicks with induced form-deprivation myopia lack oscillatory potentials as well as have reduced a- and b-wave amplitudes (Fujikado et al., 1997). This suggests that the lack of OPs in *rge* chicks could be secondary to changes resulting from altered visual processing in the retina.

The gross globe alterations that develop in the *rge* chicks include increased radial globe diameter, corneal radius, vitreous chamber depth and globe weight (Figure 1.10). These changes develop after alterations in visual processing are apparent, suggesting that

the globe changes are a result of the vision abnormalities, and are not a cause of abnormal vision in the *rge* chicks. These morphological globe changes can be induced in normal chicks by constantly exposing them to light (Li et al., 1995). If the GNB3 mutation causes the ON bipolar cells to be constantly depolarized by causing reduced signal transduction resulting from mGluR6 stimulation by photoreceptor glutamate, the ON bipolar cells would act as though they are constantly light exposed. This may help to explain the globe enlargement as chicks that are constantly light exposed also develop secondary globe enlargement (Li et al., 1995).

In addition to altered cone photoreceptor, rod and cone ON bipolar cell function, the GNB3 immunohistochemistry suggests that it is expressed in more proximal cells in the retina such as amacrine cells and ganglion cells. If it is actually expressed in these cells, it would cause additional, as yet unspecified abnormalities in visual processing in the *rge* chicks.

At this point, the origin of the *rge* b-wave, particularly the supernormal b-wave, is still not known and requires further study.

As of yet, the *rge* chicken is the only reported retinopathy model involving GNB3. Two studies have been done thus far to examine patients (both human and canine) with inherited retinal diseases for mutations in the GNB3 gene, and neither study found any abnormalities in the individuals studied (Akhmedov et al., 1996; Akhmedov et al., 1997; Gao et al., 1998).

## 4.2. Future Studies

The research presented here furthered the knowledge of the *rge* chick phenotype, but it has lead to many more questions that are yet unanswered.

Additional electroretinography could be performed to further evaluate the abnormalities of the *rge* ERG. Additional circadian ERGs could be done, as the control chicks should display some sort of electroretinographic circadian rhythm. Additional drugs that could be used include NMDA (N-methyl-d-aspartate; blocks the response of third order neurons including amacrine and ganglion cells), DNQX and CNQX (6,7-dinitroquinoxaline-2,3-dione and 6-cyano-7-nitroquinoxaline-2,3-dione; antagonists of KA/QQ receptors in AII amacrine cells and ganglion cells), TTX (tetrodotoxin; blocks voltage gated sodium channels found in amacrine and ganglion cells), and various combinations of bicuculline (GABA<sub>A</sub> antagonist), 3-APMPA (3-aminopropyl(methyl)phosphinic acid hydrochloride; GABA<sub>C</sub> antagonist) and strychnine (glycine receptor antagonist), which block feedback from inner retinal neurons to bipolar cells.

Additional electroretinography that would provide valuable information would specifically examine photoreceptor (especially cone) kinetics. One way to do this is to use a paired flash in which the cones' ability to recover from a bright flash would be examined. Another method involves a detailed analysis of the PIII response using two separate techniques: a-wave modeling and aspartate injections.

Because the specific function of GNB3 in the ON bipolar cells is not known, single cell recordings from *rge* ON bipolar cells would provide additional information as to whether and how the GNB3 mutation affects ON bipolar cell function.

The preliminary immunohistochemistry using anti-GNB3 antibodies in the retina suggested that GNB3 is found in both outer and inner segments of the retina; however, the antibody that was used produced a significant amount of background staining suggesting that it is not very specific to chicken GNB3. As was previously mentioned, the peptide sequence against which that particular antibody was raised to is only 73% similar to chicken GNB3. Additionally, the peptide sequence is found to match closely with collagen, which most likely contributed to the background staining.

Additional immunohistochemistry could be performed with frozen sections and fluorescent antibodies to avoid the problems the natural pigment of the outer retina causes. A different antibody to GNB3 from Abcam Inc. (Cambridge, MA) was raised to a different amino acid sequence from human GNB3, to which chicken GNB3 is 91% similar, is available. To definitely look at specificity for the antibody to chicken GNB3, a western blot could be done. This antibody may provide more specific staining, although it hasn't yet been tested in chicken retina. Double labeling with other primary antibodies is feasible with fluorescent immunohistochemistry. Additional primary antibodies that may help to further localize GNB3 in the chicken retina include PKC $\alpha$  (rod ON bipolar cells), G $\alpha$  (ON bipolar cells), mGluR6 (ON bipolar cells) and calbindin (cones and horizontal cells).

Additional immunohistochemistry could be performed to study, in detail, the synapses between photoreceptors and second order neurons using a battery of antibodies that have already been tested in chicks (Wahlin & Adler 2006). Some of these antibodies include anti-piccolo (located in the pre-synaptic active zone), anti-syntaxin 3 (SNARE protein) and NR2A (NMDA receptor).



In addition to more immunohistochemistry, the expression of GNB3 could also be examined. It is reportedly widely expressed throughout the body (Levine et al., 1990). mRNA could be collected from the following tissues: cardiac muscle, skeletal muscle, liver, kidney, brain, lens, aorta, small intestine and lung. Reverse transcriptase PCR could be done to look for GNB3 expression in these tissues.

Although no abnormalities except those of the retina were detected in *rge* chicks, a polymorphism in GNB3 in humans (C825T) has been implicated in a large number of serious metabolic diseases including hypertension, diabetes, obesity and functional gastrointestinal disorders (Siffert, 2000; Holtmann et al., 2004). Therefore, the expression of GNB3 in tissues other than the retina in chicken could allow further study of the effects of this GNB3 mutation in other tissues and organs. Previous histopathology of *rge* liver, muscle and heart revealed no abnormalities, but perhaps a more detailed study of these and additional organs will be warranted based on the tissue expression of GNB3. In addition to expression in these tissues, it would also be interesting to measure *rge* chickens' blood pressure and heart rate to evaluate for any signs of hypertension or other cardiovascular abnormalities.

## Reference List

(2004) Sequence and comparative analysis of the chicken genome provide unique perspectives on vertebrate evolution. *Nature* 432:695-716.

Acland GM, Aguirre GD, Bennett J, Aleman TS, Cideciyan AV, Bennicelli J, Dejneka NS, Pearce-Kelling SE, Maguire AM, Palczewski K, Hauswirth WW, Jacobson SG (2005) Long-term restoration of rod and cone vision by single dose rAAV-mediated gene transfer to the retina in a canine model of childhood blindness. *Mol Ther* 12:1072-1082.

Akhmedov NB, Piriev NI, Acland G, Aguirre G, Farber DB (1996) Analysis of cone transducin  $\beta 3$  subunit cDNA as a candidate for cone degeneration in the CD dog. *Invest Ophthalmol Vis Sci (Suppl)* 37:4557.

Akhmedov NB, Piriev NI, Ray K, Acland GM, Aguirre GD, Farber DB (1997) Structure and analysis of the transducin beta3-subunit gene, a candidate for inherited cone degeneration (cd) in the dog. *Gene* 194:47-56.

Allikmets R, Singh N, Sun H, Shroyer NF, Hutchinson A, Chidambaram A, Gerrard B, Baird L, Stauffer D, Peiffer A, Rattner A, Smallwood P, Li Y, Anderson KL, Lewi RA, Nathans J, Leppert M, Dean M, Lupski JR (1997) A photoreceptor cell-specific ATP-binding transporter gene (ABCR) is mutated in recessive Stargardt macular dystrophy. *Nat Genet* 15:236-246.

Alloway PG, Dolph PJ (1999) A role for the light-dependent phosphorylation of visual arrestin. *Proc Natl Acad Sci U S A* 96:6072-6077.

Asi H, Perlman I (1992) Relationships between the electroretinogram a-wave, b-wave and oscillatory potentials and their application to clinical diagnosis. *Doc Ophthalmol* 79:125-139.

Awatramani G, Wang J, Slaughter MM (2001) Amacrine and ganglion cell contributions to the electroretinogram in amphibian retina. *Vis Neurosci* 18:147-156.

Beltran WA, Hammond P, Acland GM, Aguirre GD (2006) A Frameshift Mutation in RPGR Exon ORF15 Causes Photoreceptor Degeneration and Inner Retina Remodeling in a Model of X-Linked Retinitis Pigmentosa. *Invest Ophthalmol Vis Sci* 47:1669-1681.



Bernard M, Iuvone PM, Cassone VM, Roseboom PH, Coon SL, Klein DC (1997) Avian melatonin synthesis: photic and circadian regulation of serotonin N-acetyltransferase mRNA in the chicken pineal gland and retina. *J Neurochem* 68:213-224.

Birch DG, Berson EL, Sandberg MA (1984) Diurnal rhythm in the human rod ERG. *Invest Ophthalmol Vis Sci* 25:236-238.

Boissy RE, Smyth JR, Jr., Fite KV (1983) Progressive cytologic changes during the development of delayed feather amelanosis and associated choroidal defects in the DAM chicken line. A vitiligo model. *Am J Pathol* 111:197-212.

Bowmaker JK, Heath LA, Wilkie SE, Hunt DM (1997) Visual pigments and oil droplets from six classes of photoreceptor in the retinas of birds. *Vision Res* 37:2183-2194.

Bowne SJ, Sullivan LS, Blanton SH, Cepko CL, Blackshaw S, Birch DG, Hughbanks-Wheaton D, Heckenlively JR, Daiger SP (2002) Mutations in the inosine monophosphate dehydrogenase 1 gene (IMPDH1) cause the RP10 form of autosomal dominant retinitis pigmentosa. *Hum Mol Genet* 11:559-568.

Bresnick GH, Palta M (1987) Oscillatory potential amplitudes. Relation to severity of diabetic retinopathy. *Arch Ophthalmol* 105:929-933.

Brown KT (1968) The electroretinogram: its components and their origins. *Vision Res* 8:633-677.

Burt DW, Morrice DR, Lester DH, Robertson GW, Mohamed MD, Simmons I, Downey LM, Thaung C, Bridges LR, Paton IR, Gentle M, Smith J, Hocking PM, Inglehearn CF (2003) Analysis of the rdd locus in chicken: a model for human retinitis pigmentosa. *Mol Vis* 9:164-170.

Carroll K, Gomez C, Shapiro L (2004) Tubby proteins: the plot thickens. *Nat Rev Mol Cell Biol* 5:55-63.

Cervetto L, MacNichol EF, Jr. (1972) Inactivation of horizontal cells in turtle retina by glutamate and aspartate. *Science* 178:767-768.

Curtis PE, Baker JR, Curtis R, Johnston A (1987) Impaired vision in chickens associated with retinal defects. *Vet Rec* 120:113-114.

Curtis R, Baker JR, Curtis PE, Johnston AR (1988) An inherited retinopathy in commercial breeding chickens. *Avian Path* 17:87-89.

Czepita D. (2002) Myopia – epidemiology, pathogenesis, present and coming possibilities of treatment. *Clinical Practice Review* 3:294-300.

Dhingra A, Jiang M, Wang TL, Lyubarsky A, Savchenko A, Bar-Yehuda T, Sterling P, Birnbaumer L, Vardi N (2002) Light response of retinal ON bipolar cells requires a specific splice variant of Galpha(o). *J Neurosci* 22:4878-4884.

Dhingra A, Lyubarsky A, Jiang M, Pugh EN, Jr., Birnbaumer L, Sterling P, Vardi N (2000) The light response of ON bipolar neurons requires G[alpha]o. *J Neurosci* 20:9053-9058.

Dolph PJ, Man-Son-Hing H, Yarfitz S, Colley NJ, Deer JR, Spencer M, Hurley JB, Zuker CS (1994) An eye-specific G beta subunit essential for termination of the phototransduction cascade. *Nature* 370:59-61.

Dong CJ, Hare WA (2000) Contribution to the kinetics and amplitude of the electroretinogram b-wave by third-order retinal neurons in the rabbit retina. *Vision Res* 40:579-589.

Dong CJ, Hare WA (2002) GABA<sub>C</sub> feedback pathway modulates the amplitude and kinetics of ERG b-wave in a mammalian retina in vivo. *Vision Res* 42:1081-1087.

Dowling JE, Werblin FS (1969) Organization of retina of the mudpuppy, *Necturus maculosus*. I. Synaptic structure. *J Neurophysiol* 32:315-338.

Einthoven W, Jolly WA (1908) The form and magnitude of the electrical response of the eye to stimulation by light at various intensities. *Quarterly Journal of Experimental Physiology* 1:373-416.

Emeis D, Kuhn H, Reichert J, Hofmann KP (1982) Complex formation between metarhodopsin II and GTP-binding protein in bovine photoreceptor membranes leads to a shift of the photoproduct equilibrium. *FEBS Lett* 143:29-34.

Fager LY, Fager RS (1981) Chicken blue and chicken violet, short wavelength sensitive visual pigments. *Vision Res* 21:581-586.

Famiglietti EV, Jr., Kolb H (1976) Structural basis for ON-and OFF-center responses in retinal ganglion cells. *Science* 194:193-195.

Fite KV, Bengston L, Doran P (1985) Retinal pigment epithelial correlates of avian retinal degeneration: electron microscopic analysis. *J Comp Neurol* 231:310-322.

Frost-Larsen K, Larsen HW, Simonsen SE (1980) Oscillatory potential and nyctometry in insulin-dependent diabetics. *Acta Ophthalmol (Copenh)* 58:879-888.

Fujikado T, Kawasaki Y, Suzuki A, Ohmi G, Tano Y (1997) Retinal function with lens-induced myopia compared with form-deprivation myopia in chicks. *Graefes Arch Clin Exp Ophthalmol* 235:320-324.

Gao J, Cheon K, Nusinowitz S, Liu Q, Bei D, Atkins K, Azimi A, Daiger SP, Farber DB, Heckenlively JR, Pierce EA, Sullivan LS, Zuo J (2002) Progressive photoreceptor degeneration, outer segment dysplasia, and rhodopsin mislocalization in mice with targeted disruption of the retinitis pigmentosa-1 (Rpl) gene. *Proc Natl Acad Sci U S A* 99:5698-5703.

Gao YQ, Danciger M, Akhmedov NB, Zhao DY, Heckenlively JR, Fishman GA, Weleber RG, Jacobson SG, Farber DB (1998) Exon screening of the genes encoding the beta- and gamma-subunits of cone transducin in patients with inherited retinal disease. *Mol Vis* 4:16.

Gloriam DE, Schioth HB, Fredriksson R (2005) Nine new human Rhodopsin family G-protein coupled receptors: identification, sequence characterisation and evolutionary relationship. *Biochim Biophys Acta* 1722:235-246.

Gouras P (1971) The function of the midget cell system in primate color vision. *Vision Res Suppl* 3:397-410.

Gouras P, Eggers HM, MacKay CJ (1983) Cone dystrophy, nyctalopia, and supernormal rod responses. A new retinal degeneration. *Arch Ophthalmol* 101:718-724.

Granit R (1933) The components of the retinal action potential and their relation to the discharge in the optic nerve. *J Physiol* 77:207-240.

Gurevich L, Slaughter MM (1993) Comparison of the waveforms of the ON bipolar neuron and the b-wave of the electroretinogram. *Vision Res* 33:2431-2435.

Haider NB, Jacobson SG, Cideciyan AV, Swiderski R, Streb LM, Searby C, Beck G, Hockey R, Hanna DB, Gorman S, Duhl D, Carmi R, Bennett J, Weleber RG, Fishman GA, Wright AF, Stone EM, Sheffield VC (2000) Mutation of a nuclear receptor gene, NR2E3, causes enhanced S cone syndrome, a disorder of retinal cell fate. *Nat Genet* 24:127-131.

Haider NB, Naggert JK, Nishina PM (2001) Excess cone cell proliferation due to lack of a functional NR2E3 causes retinal dysplasia and degeneration in rd7/rd7 mice. *Hum Mol Genet* 10:1619-1626.

Hamm HE, Gilchrist A (1996) Heterotrimeric G proteins. *Curr Opin Cell Biol* 8:189-196.

Harari-Steinberg O, Chamovitz DA (2004) The COP9 signalosome: mediating between kinase signaling and protein degradation. *Curr Protein Pept Sci* 5:185-189.

Haverkamp S, Michalakis S, Claes E, Seeliger MW, Humphries P, Biel M, Feigenspan A (2006) Synaptic plasticity in CNGA3(-/-) mice: cone bipolar cells react on the missing cone input and form ectopic synapses with rods. *J Neurosci* 26:5248-5255.

Heikenwalder MF, Koritschoner NP, Pajer P, Chaboissier MC, Kurz SM, Briegel KJ, Bartunek P, Zenke M (2001) Molecular cloning, expression and regulation of the avian tubby-like protein 1 (tulp1) gene. *Gene* 273:131-139.

Helms JB (1995) Role of heterotrimeric GTP binding proteins in vesicular protein transport: indications for both classical and alternative G protein cycles. *FEBS Lett* 369:84-88.

Herrmann R, Heck M, Henklein P, Hofmann KP, Ernst OP (2006) Signal transfer from GPCRs to G proteins: Role of the Galpha N-terminal region in rhodopsin - transducin coupling. *J Biol Chem*.

Hintsch G, Zurlinden A, Meskenaite V, Steuble M, Fink-Widmer K, Kinter J, Sonderegger P (2002) The calsynenins--a family of postsynaptic membrane proteins with distinct neuronal expression patterns. *Mol Cell Neurosci* 21:393-409.

Hirata A, Negi A (1998) Lacquer crack lesions in experimental chick myopia. *Graefes Arch Clin Exp Ophthalmol* 236:138-145.

Hodos W, Kuenzel WJ (1984) Retinal-image degradation produces ocular enlargement in chicks. *Invest Ophthalmol Vis Sci* 25:652-659.

Hoffman LM, Jensen CC, Kloeker S, Wang CL, Yoshigi M, Beckerle MC (2006) Genetic ablation of zyxin causes Mena/VASP mislocalization, increased motility, and deficits in actin remodeling. *J Cell Biol* 172:771-782.

Holtmann G, Liebrechts T, Siffert W (2004) Molecular basis of functional gastrointestinal disorders. *Best Pract Res Clin Gastroenterol* 18:633-640.

Hood DC, Cideciyan AV, Roman AJ, Jacobson SG (1995) Enhanced S cone syndrome: evidence for an abnormally large number of S cones. *Vision Res* 35:1473-1481.

Huang L, Max M, Margolskee RF, Su H, Masland RH, Euler T (2003) G protein subunit G gamma 13 is coexpressed with G alpha o, G beta 3, and G beta 4 in retinal ON bipolar cells. *J Comp Neurol* 455:1-10.

Ikeda A, Nishina PM, Naggert JK (2002) The tubby-like proteins, a family with roles in neuronal development and function. *J Cell Sci* 115:9-14.

Ikeuchi T, Koide R, Onodera O, Tanaka H, Oyake M, Takano H, Tsuji S (1995) Dentatorubral-pallidoluysian atrophy (DRPLA). Molecular basis for wide clinical features of DRPLA. *Clin Neurosci* 3:23-27.

Inglehearn CF, Morrice DR, Lester DH, Robertson GW, Mohamed MD, Simmons I, Downey LM, Thaung C, Bridges LR, Paton IR, Smith J, Petersen-Jones S, Hocking PM, Burt DW (2003) Genetic, ophthalmic, morphometric and histopathological analysis of the Retinopathy Globe Enlarged (rge) chicken. *Mol Vis* 9:295-300.

Isono K, Fujimura Y, Shinga J, Yamaki M, Wang J, Takihara Y, Murahashi Y, Takada Y, Mizutani-Koseki Y, Koseki H (2005) Mammalian polyhomeotic homologues Phc2 and Phc1 act in synergy to mediate polycomb repression of Hox genes. *Mol Cell Biol* 25:6694-6706.

Jacobson SG, Marmor MF, Kemp CM, Knighton RW (1990) SWS (blue) cone hypersensitivity in a newly identified retinal degeneration. *Invest Ophthalmol Vis Sci* 31:827-838.



Jay DG (2000) The clutch hypothesis revisited: ascribing the roles of actin-associated proteins in filopodial protrusion in the nerve growth cone. *J Neurobiol* 44:114-125.

Kapousta-Bruneau NV (2000) Opposite effects of GABA(A) and GABA(C) receptor antagonists on the b-wave of ERG recorded from the isolated rat retina. *Vision Res* 40:1653-1665.

Kizawa J, Machida S, Kobayashi T, Gotoh Y, Kurosaka D (2006) Changes of oscillatory potentials and photopic negative response in patients with early diabetic retinopathy. *Jpn J Ophthalmol* 50:367-373.

Klein RM, Curtin BJ (1975) Lacquer crack lesions in pathologic myopia. *Am J Ophthalmol* 79:386-392.

Klein RM, Green S (1988) The development of lacquer cracks in pathologic myopia. *Am J Ophthalmol* 106:282-285.

Kofuji P, Davidson N, Lester HA (1995) Evidence that neuronal G-protein-gated inwardly rectifying K<sup>+</sup> channels are activated by G beta gamma subunits and function as heteromultimers. *Proc Natl Acad Sci U S A* 92:6542-6546.

Krapivinsky G, Krapivinsky L, Wickman K, Clapham DE (1995) G beta gamma binds directly to the G protein-gated K<sup>+</sup> channel, IKACH. *J Biol Chem* 270:29059-29062.

Lahiri D, Bailey CF (1993) A comparison of phagocytosis by the retinal pigment epithelium in normal and delayed amelanotic chickens. *Exp Eye Res* 56:625-634.

LaVail MM (1976) Rod outer segment disc shedding in relation to cyclic lighting. *Exp Eye Res* 23:277-280.

Lei B, Perlman I (1999) The contributions of voltage- and time-dependent potassium conductances to the electroretinogram in rabbits. *Vis Neurosci* 16:743-754.

Levine MA, Smallwood PM, Moen PT, Jr., Helman LJ, Ahn TG (1990) Molecular cloning of beta 3 subunit, a third form of the G protein beta-subunit polypeptide. *Proc Natl Acad Sci U S A* 87:2329-2333.

Li L, Dowling JE (1998) Zebrafish visual sensitivity is regulated by a circadian clock. *Vis Neurosci* 15:851-857.

Li T, Troilo D, Glasser A, Howland HC (1995) Constant light produces severe corneal flattening and hyperopia in chickens. *Vision Res* 35:1203-1209.

Linn DM, Solessio E, Perlman I, Lasater EM (1998) The role of potassium conductance in the generation of light responses in Muller cells of the turtle retina. *Vis Neurosci* 15:449-458.

Lu J, Zoran MJ, Cassone VM (1995) Daily and circadian variation in the electroretinogram of the domestic fowl: effects of melatonin. *J Comp Physiol [A]* 177:299-306.

Lyons BL, Smith RS, Hurd RE, Hawes NL, Burzenski LM, Nusinowitz S, Hasham MG, Chang B, Shultz LD (2006) Deficiency of SHP-1 protein-tyrosine phosphatase in "viable motheaten" mice results in retinal degeneration. *Invest Ophthalmol Vis Sci* 47:1201-1209.

Magrys A, Anekonda T, Ren G, Adamus G (2007) The Role of Anti-alpha-Enolase Autoantibodies in Pathogenicity of Autoimmune-Mediated Retinopathy. *J Clin Immunol* 27:181-192.

Manglapus MK, Iuvone PM, Underwood H, Pierce ME, Barlow RB (1999) Dopamine mediates circadian rhythms of rod-cone dominance in the Japanese quail retina. *J Neurosci* 19:4132-4141.

Manglapus MK, Uchiyama H, Buelow NF, Barlow RB (1998) Circadian rhythms of rod-cone dominance in the Japanese quail retina. *J Neurosci* 18:4775-4784.

Mann F, Harris WA, Holt CE (2004) New views on retinal axon development: a navigation guide. *Int J Dev Biol* 48:957-964.

McGoogan JM, Cassone VM (1999) Circadian regulation of chick electroretinogram: effects of pinealectomy and exogenous melatonin. *Am J Physiol* 277:R1418-R1427.

McGoogan JM, Wu WQ, Cassone VM (2000) Inter-ocular interference and circadian regulation of the chick electroretinogram. *Vision Res* 40:2869-2879.

Meyer DB (1977) Handbook of Sensory Physiology. Berlin: Springer.

Molday RS (1998) Photoreceptor membrane proteins, phototransduction, and retinal degenerative diseases. The Friedenwald Lecture. Invest Ophthalmol Vis Sci 39:2491-2513.

Montiani-Ferreira F (2004) Retinopathy, Globe Enlarged. PhD Thesis. Comparative Medicine and Integrative Biology, Michigan State University.

Montiani-Ferreira F, Fischer A, Cernuda-Cernuda R, DeGrip WJ, Sherry D, Cho SS, Evans MG, Hocking PM, Petersen-Jones SM (2005) Detailed histopathologic characterization of the retinopathy, globe enlarged (rge) chick phenotype. Mol Vis 11:11-27.

Montiani-Ferreira F, Kiupel M, Petersen-Jones SM (2004) Spontaneous lacquer crack lesions in the retinopathy, globe enlarged (rge) chick. J Comp Pathol 131:105-111.

Montiani-Ferreira F, Petersen-Jones SM (2003) Characterization of electroretinographic abnormalities in the retinopathy, globe enlarged (RGE) chick. Invest Ophthalmol Vis Sci [ARVO Abstract] 44:4534.

Montiani-Ferreira F, Shaw G, Geller AG, Petersen-Jones SM (2007) Electroretinographic features of the retinopathy, globe enlarged (rge) chick phenotype. Mol Vis 13:553-565.

Montiani-Ferreira F, Li T, Kiupel M, Howland H, Hocking P, Curtis R, Petersen-Jones S (2003) Clinical features of the retinopathy, globe enlarged (rge) chick phenotype. Vision Res 43:2009-2018.

Murakami M, Otsuka T, Shimazaki H (1975) Effects of aspartate and glutamate on the bipolar cells in the carp retina. Vision Res 15:456-458.

Narfström K, Katz ML, Bragadottir R, Seeliger M, Boulanger A, Redmond TM, Caro L, Lai CM, Rakoczy PE (2003) Functional and structural recovery of the retina after gene therapy in the RPE65 null mutation dog. Invest Ophthalmol Vis Sci 44:1663-1672.

Narfström K, Wrigstad A, Nilsson SEG (1989) The briard dog: a new animal model of congenital stationary night blindness. Br J Ophthalmol 73:750-756.

Nawy S (1999) The metabotropic receptor mGluR6 may signal through G(o), but not phosphodiesterase, in retinal bipolar cells. *J Neurosci* 19:2938-2944.

Nawy S, Jahr CE (1990) Suppression by glutamate of cGMP-activated conductance in retinal bipolar cells. *Nature* 346:269-271.

Neer EJ (1995) Heterotrimeric G proteins: organizers of transmembrane signals. *Cell* 80:249-257.

Nelson R, Famiglietti EV, Jr., Kolb H (1978) Intracellular staining reveals different levels of stratification for on- and off-center ganglion cells in cat retina. *J Neurophysiol* 41:472-483.

Newman EA (1989) Potassium conductance block by barium in amphibian Muller cells. *Brain Res* 498:308-314.

Nishimura DY, Fath M, Mullins RF, Searby C, Andrews M, Davis R, Andorf JL, Mykityn K, Swiderski RE, Yang B, Carmi R, Stone EM, Sheffield VC (2004) Bbs2-null mice have neurosensory deficits, a defect in social dominance, and retinopathy associated with mislocalization of rhodopsin. *Proc Natl Acad Sci U S A* 101:16588-16593.

Nomura A, Shigemoto R, Nakamura Y, Okamoto N, Mizuno N, Nakanishi S (1994) Developmentally regulated postsynaptic localization of a metabotropic glutamate receptor in rat rod bipolar cells. *Cell* 77:361-369.

Oakley B (1977) Potassium and the photoreceptor-dependent pigment epithelial hyperpolarization. *J Gen Physiol* 70:405-425.

Oakley B, Green DG (1976) Correlation of light-induced changes in retinal extracellular potassium concentration with c-wave of the electroretinogram. *J Neurophysiol* 39:1117-1133.

Ogden TE (1973) The oscillatory waves of the primate electroretinogram. *Vision Res* 13:1059-1074.

Palczewski K, Subbaraya I, Gorczyca WA, Helekar BS, Ruiz CC, Ohguro H, Huang J, Zhao X, Crabb JW, Johnson RS, . (1994) Molecular cloning and characterization of retinal photoreceptor guanylyl cyclase-activating protein. *Neuron* 13:395-404.

Pang J, Cheng M, Haire SE, Barker E, Planelles V, Blanks JC (2006) Efficiency of lentiviral transduction during development in normal and rd mice. *Mol Vis* 12:756-767.

Peng YW, Robishaw JD, Levine MA, Yau KW (1992) Retinal rods and cones have distinct G protein beta and gamma subunits. *Proc Natl Acad Sci U S A* 89:10882-10886.

Penn RD, Hagins WA (1969) Signal transmission along retinal rods and the origin of the electroretinographic a-wave. *Nature* 223:201-204.

Pepperberg DR, Brown PK, Lurie M, Dowling JE (1978) Visual pigment and photoreceptor sensitivity in the isolated skate retina. *J Gen Physiol* 71:369-396.

Peters JL, Cassone VM (2005) Melatonin regulates circadian electroretinogram rhythms in a dose- and time-dependent fashion. *J Pineal Res* 38:209-215.

Phillips WJ, Wong SC, Cerione RA (1992) Rhodopsin/transducin interactions. II. Influence of the transducin-beta gamma subunit complex on the coupling of the transducin-alpha subunit to rhodopsin. *J Biol Chem* 267:17040-17046.

Piast M, Kustrzeba-Wojcicka I, Matusiewicz M, Banas T (2005) Molecular evolution of enolase. *Acta Biochim Pol* 52:507-513.

Pittler SJ, Baehr W (1991) Identification of a nonsense mutation in the rod photoreceptor cGMP phosphodiesterase  $\beta$ -subunit gene of the rd mouse. *Proc Natl Acad Sci U S A* 88:8322-8326.

Pollock BJ, Wilson MA, Randall CJ, Clayton RM (1982) Preliminary observations of a new blind chick mutant (beg). In: *Problems of normal and genetically abnormal retinas* (Clayton RM, Reading HW, Haywood J, Wright A, eds), pp 241-247. London: Academic Press.

Randall CJ, McLachlan I (1979) Retinopathy in commercial layers. *Vet Rec* 105:41-42.

Randall CJ, Wilson MA, Pollock BJ, Clayton RM, Ross AS, Bard JB, McLachlan I (1983) Partial retinal dysplasia and subsequent degeneration in a mutant strain of domestic fowl (rdd). *Exp Eye Res* 37:337-347.

Raviola E, Raviola G (1982) Structure of the synaptic membranes in the inner plexiform layer of the retina: a freeze-fracture study in monkeys and rabbits. *J Comp Neurol* 209:233-248.

Reichelt W, Pannicke T (1993) Voltage-dependent K<sup>+</sup> currents in guinea pig Muller (glia) cells show different sensitivities to blockade by Ba<sup>2+</sup>. *Neurosci Lett* 155:15-18.

Robson JG, Frishman LJ (1996) Photoreceptor and bipolar cell contributions to the cat electroretinogram: a kinetic model for the early part of the flash response. *J Opt Soc Am A Opt Image Sci Vis* 13:613-622.

Rohrer B, Lohr HR, Humphries P, Redmond TM, Seeliger MW, Crouch RK (2005) Cone Opsin Mislocalization in Rpe65<sup>-/-</sup> Mice: A Defect That Can Be Corrected by 11-cis Retinal. *Invest Ophthalmol Vis Sci* 46:3876-3882.

Sagoo MS, Lagnado L (1997) G-protein deactivation is rate-limiting for shut-off of the phototransduction cascade. *Nature* 389:392-395.

Schaeffel F, Rohrer B, Lemmer T, Zrenner E (1991) Diurnal control of rod function in the chicken. *Vis Neurosci* 6:641-653.

Schwechheimer C (2004) The COP9 signalosome (CSN): an evolutionary conserved proteolysis regulator in eukaryotic development. *Biochim Biophys Acta* 1695:45-54.

Semple-Rowland SL, Lee NR, Van Hooser JP, Palczewski K, Baehr W (1998) A null mutation in the photoreceptor guanylate cyclase gene causes the retinal degeneration chicken phenotype. *Proc Natl Acad Sci U S A* 95:1271-1276.

Sharma S, Ball SL, Peachey NS (2005) Pharmacological studies of the mouse cone electroretinogram. *Vis Neurosci* 22:631-636.

Sherry DM, Wang MM, Frishman LJ (2003) Differential distribution of vesicle associated membrane protein isoforms in the mouse retina. *Mol Vis* 9:673-688.

Sherry DM, Yang H, Standifer KM (2001) Vesicle-associated membrane protein isoforms in the tiger salamander retina. *J Comp Neurol* 431:424-436.

Sieving PA, Murayama K, Naarendorp F (1994) Push-pull model of the primate photopic electroretinogram: a role for hyperpolarizing neurons in shaping the b-wave. *Vis Neurosci* 11:519-532.

Siffert W (2000) G protein beta 3 subunit 825T allele, hypertension, obesity, and diabetic nephropathy. *Nephrol Dial Transplant* 15:1298-1306.

Sillman AJ, Ito H, Tomita T (1969) Studies on the mass receptor potential of the isolated frog retina. II. On the basis of the ionic mechanism. *Vision Res* 9:1443-1451.

Simonsen SE (1980) The value of the oscillatory potential in selecting juvenile diabetics at risk of developing proliferative retinopathy. *Acta Ophthalmol (Copenh)* 58:865-878.

Slaughter MM, Miller RF (1981) 2-amino-4-phosphonobutyric acid: a new pharmacological tool for retina research. *Science* 211:182-185.

Slaughter MM, Miller RF (1983) An excitatory amino acid antagonist blocks cone input to sign-conserving second-order retinal neurons. *Science* 219:1230-1232.

Smith RL, Nishimura Y, Raviola G (1985) Interreceptor junction in the double cone of the chicken retina. *J Submicrosc Cytol* 17:183-186.

Sondek J, Bohm A, Lambright DG, Hamm HE, Sigler PB (1996) Crystal structure of a G-protein beta gamma dimer at 2.1 Å resolution. *Nature* 379:369-374.

Steinberg RH, Schmidt R, Brown KT (1970) Intracellular responses to light from cat pigment epithelium: origin of the electroretinogram c-wave. *Nature* 227:728-730.

Stockton RA, Slaughter MM (1989) B-wave of the electroretinogram. A reflection of ON bipolar cell activity. *J Gen Physiol* 93:101-122.

Takahashi JS, Hamm H, Menaker M (1980) Circadian rhythms of melatonin release from individual superfused chicken pineal glands in vitro. *Proc Natl Acad Sci U S A* 77:2319-2322.

Tummala H, Ali M, Getty P, Hocking PM, Burt DW, Inglehearn CF, Lester DH (2006) Mutation in the guanine nucleotide-binding protein  $\beta$ -3 causes retinal degeneration and

embryonic mortality in chickens. *Investigative Ophthalmology & Visual Science* 47:4714-4718.

Ueno S, Kondo M, Ueno M, Miyata K, Terasaki H, Miyake Y (2006) Contribution of retinal neurons to d-wave of primate photopic electroretinograms. *Vision Res* 46:658-664.

Ulshafer RJ, Allen C, Dawson WW, Wolf ED (1984) Hereditary retinal degeneration in the Rhode Island Red chicken. I. Histology and ERG. *Exp Eye Res* 39:125-135.

Ulshafer RJ, Allen CB (1985) Hereditary retinal degeneration in the Rhode Island Red chicken: ultrastructural analysis. *Exp Eye Res* 40:865-877.

Vardi N, Duvoisin R, Wu G, Sterling P (2000) Localization of mGluR6 to dendrites of ON bipolar cells in primate retina. *J Comp Neurol* 423:402-412.

Vardi N, Morigiwa K (1997) ON cone bipolar cells in rat express the metabotropic receptor mGluR6. *Vis Neurosci* 14:789-794.

Venkataraman V, Duda T, Vardi N, Koch KW, Sharma RK (2003) Calcium-modulated guanylate cyclase transduction machinery in the photoreceptor--bipolar synaptic region. *Biochem* 42:5640-5648.

Veske A, Nilsson SE, Narfström K, Gal A (1999) Retinal dystrophy of swedish Briard/Briard-beagle dogs is due to a 4-bp deletion in RPE65. *Genomics* 57:57-61.

Vuong TM, Chabre M (1991) Deactivation kinetics of the transduction cascade of vision. *Proc Natl Acad Sci U S A* 88:9813-9817.

Wachtmeister L, Dowling JE (1978) The oscillatory potentials of the mudpuppy retina. *Invest Ophthalmol Vis Sci* 17:1176-1188.

Weber BHF, Vogt G, Pruett RC, Stohr H, Felbor U (1994) Mutations in the tissue inhibitor of metalloproteinases-3 (TIMP3) in patients with Sorsby's fundus dystrophy. *Nat Genet* 8:352-356.

Weng K, Lu C, Daggett LP, Kuhn R, Flor PJ, Johnson EC, Robinson PR (1997) Functional coupling of a human retinal metabotropic glutamate receptor (hmGluR6) to



bovine rod transducin and rat Go in an in vitro reconstitution system. J Biol Chem 272:33100-33104.

Werblin F (1991) Synaptic connections, receptive fields, and patterns of activity in the tiger salamander retina. A simulation of patterns of activity formed at each cellular level from photoreceptors to ganglion cells [the Friedenwald lecture]. Invest Ophthalmol Vis Sci 32:459-483.

Wilson MA PBCRRCJ (1982) Early development of a new RP-like mutant in the chick. In: Problems of normal and genetically abnormal retinas. (Clayton RM RHHJWA, ed), pp 233-239. London: Academic Press.

Wu WQ, McGoogan JM, Cassone VM (2000) Circadian regulation of visually evoked potentials in the domestic pigeon, *Columba livia*. J Biol Rhythms 15:317-328.

Xu L, Ball SL, Alexander KR, Peachey NS (2003) Pharmacological analysis of the rat cone electroretinogram. Vis Neurosci 20:297-306.

Xu X, Karwoski CJ (1994) Current source density analysis of retinal field potentials. II. Pharmacological analysis of the b-wave and M-wave. J Neurophysiol 72:96-105.

Yang H, Standifer KM, Sherry DM (2002) Synaptic protein expression by regenerating adult photoreceptors. J Comp Neurol 443:275-288.

Yarfitz SL, Running Deer JL, Froelick G, Colley NJ, Hurley JB (1994) In situ assay of light-stimulated G protein activity in *Drosophila* photoreceptor G protein beta mutants. J Biol Chem 269:30340-30344.

Yen L, Fager RS (1984) Chromatographic resolution of the rod pigment from the four cone pigments of the chicken retina. Vision Res 24:1555-1562.

Yoshizawa T & Fukada Y (1993) Preparation and characterization of chicken rod and cone pigments. In: Methods in neurosciences (Hargrave.P.A., ed), pp 161-179. San Diego: Academic Press.

Young RW (1978) The daily rhythm of shedding and degradation of rod and cone outer segment membranes in the chick retina. Invest Ophthalmol Vis Sci 17:105-116.

Yu J, He S, Friedman JS, Akimoto M, Ghosh D, Mears AJ, Hicks D, Swaroop A (2004) Altered expression of genes of the Bmp/Smad and Wnt/calcium signaling pathways in the cone-only Nrl<sup>-/-</sup> mouse retina, revealed by gene profiling using custom cDNA microarrays. *J Biol Chem* 279:42211-42220.

Zawilska JB, Wawrocka M (1993) Chick retina and pineal gland differentially respond to constant light and darkness: in vivo studies on serotonin N-acetyltransferase (NAT) activity and melatonin content. *Neurosci Lett* 153:21-24.

MICHIGAN STATE UNIVERSITY LIBRARIES



3 1293 02956 1564